



Cite this: *Chem. Soc. Rev.*, 2021, 50, 5668

## Applications of bioluminescence in biotechnology and beyond†

Aisha J. Syed \*‡ and James C. Anderson

Bioluminescence is the fascinating natural phenomenon by which living creatures produce light. Bioluminescence occurs when the oxidation of a small-molecule luciferin is catalysed by an enzyme luciferase to form an excited-state species that emits light. There are over 30 known bioluminescent systems but the luciferin–luciferase pairs of only 11 systems have been characterised to-date, whilst other novel systems are currently under investigation. The different luciferin–luciferase pairs have different light emission wavelengths and hence are suitable for various applications. The last decade or so has seen great advances in protein engineering, synthetic chemistry, and physics which have allowed luciferins and luciferases to reach previously uncharted applications. The bioluminescence reaction is now routinely used for gene assays, the detection of protein–protein interactions, high-throughput screening (HTS) in drug discovery, hygiene control, analysis of pollution in ecosystems and *in vivo* imaging in small mammals. Moving away from sensing and imaging, the more recent highlights of the applications of bioluminescence in biomedicine include the bioluminescence-induced photo-uncaging of small-molecules, bioluminescence based photodynamic therapy (PDT) and the use of bioluminescence to control neurons. There has also been an increase in blue-sky research such as the engineering of various light emitting plants. This has led to lots of exciting multidisciplinary science across various disciplines. This review focuses on the past, present, and future applications of bioluminescence. We aim to make this review accessible to all chemists to understand how these applications were developed and what they rely upon, in simple understandable terms for a graduate chemist.

Received 30th November 2020

DOI: 10.1039/d0cs01492c

[rsc.li/chem-soc-rev](http://rsc.li/chem-soc-rev)

Department of Chemistry, University College London, 20 Gordon Street, London, WC1H 0AJ, UK. E-mail: [Aisha\\_asrar@hotmail.com](mailto:Aisha_asrar@hotmail.com)

† Electronic supplementary information (ESI) available. See DOI: 10.1039/d0cs01492c

‡ Present address: School of Chemistry, University of Leeds, Woodhouse Lane, LS2 9JT, Leeds, UK.



**Aisha J. Syed**

*Aisha J. Syed received her BSc in Chemistry from the University of Birmingham in 2015. She then studied for a PhD in Organic Chemistry and Chemical Biology at University College London with Prof. Jim Anderson on the synthesis and bioluminescence properties of infraluciferins which she received in 2019. She is currently a Research Fellow in the labs of Prof. Andrew Wilson and Prof Adam Nelson at the University of Leeds. Her research*

*interests include using synthesis and related chemical tools for visualising and manipulating biological processes including molecular imaging and protein–protein interactions.*



**James C. Anderson**

*Jim Anderson studied at Imperial College, receiving his PhD in 1990 working with Professor S. V. Ley FRS. After postdoctoral study with Professor D. A. Evans at Harvard University, he started his independent career at the University of Sheffield in 1993. He moved to the University of Nottingham in 1999 and to his current position at University College London in 2009. His work has been mainly concerned with asymmetric reaction methodology and total synthesis. At UCL these have been applied to the rational design of red shifted luciferins, which has led to the development of infraluciferin.*



# 1. Introduction

Bioluminescence is the fascinating natural phenomenon by which living creatures produce and emit light. In nature this has been evolutionarily conserved primarily in marine organisms, some species of bacteria, fungi and terrestrial insects for various purposes such as to hunt prey, ward-off predators, and attract mates.<sup>1–3</sup> Since 1667 when one of the earliest scientific records of the study of bioluminescence was made by Robert Boyle, many researchers have contributed to our understanding of the mechanisms that govern bioluminescence and how this natural phenomenon can be tailored for targeted use as a powerful tool in biotechnology for the visualisation, imaging, and control of biochemical processes.<sup>4</sup>

Naturally occurring light originates from two main kinds of systems – bioluminescent systems which comprise of distinct luciferase enzymes and luciferin moieties, and photoproteins in which the light-emitting chromophore is part of the protein itself and light emission is triggered by changes in the protein's environment. The discovery of the mechanisms underpinning photoproteins such as the green fluorescent protein (GFP), aequorin, kaede and pholasin and their subsequent applications have been previously reviewed and will not be discussed in this review.<sup>5–8</sup>

Whilst there are more than 40 known bioluminescent systems, the structures of the luciferin and luciferase have only been elucidated for 11 of them. The quest for the mechanistic characterisation of luciferin and luciferase pairs is an active area of research as is the search for new pairs.<sup>9–11</sup> The bioluminescent reaction generally requires a luciferase enzyme, its luciferin substrate and an oxidant which is often molecular oxygen. Some systems require energy in the form of ATP or NADH as well. One of the earliest luciferin structures to be elucidated were those of D-luciferin found in fireflies, reported in the mid 1900s.<sup>12</sup> About twenty years later the luciferin coelenterazine and its luciferase were discovered from the deep-sea shrimp *Oplophorus gracilirostris*.<sup>13</sup>

Since then, due to the low toxicity, high quantum yield and high sensitivity of both of these reactions, these molecules and their luciferase enzyme partners have found wide use as *in vitro* reporters of analytes and metabolites – for example the firefly luciferase (FLuc) and D-luciferin system are widely used in biochemical assays to determine ATP levels. The last decade or so has seen luciferins and luciferases to reach previously uncharted applications fuelled by great advances in protein engineering, synthetic chemistry, physics and light capture technology. We will first cover some of the basic qualities and characteristics of the most widely used natural luciferin/luciferase pairs, with a brief mention of their uses as well as their shortcomings that make them less than ideal candidates for certain applications. This then leads up to the developments in synthetic luciferins and engineered luciferases and their improved properties and uses. The applications of bioluminescence are then extensively discussed including ATP sensing, hygiene control in the fish and milk industries, mapping pollution in ecosystems using bioluminescence based assays, culture and

heritage in the form of art work preservation, the sensing of pH, metal ions, membrane potential, drug molecules, other metabolites, gene assays, the detection of protein–protein interactions, high-throughput screening in drug discovery and *in vivo* imaging of tumours as well as infections. Apart from sensing applications, the discussion will then move to how new applications are now trying to make use of the light from bioluminescence for various purposes such as to effect healing in the form of bioluminescence based photodynamic therapy (PDT)<sup>14</sup> or using the light for bioluminescence-induced photocaging of small molecules,<sup>15,16</sup> and the use of bioluminescence to control neurons.<sup>17</sup> Exciting recent blue-sky research is also discussed such as the engineering of a light emitting plants of various types.<sup>18</sup> We aim to make this review accessible to all chemists to understand how these applications were developed and what they rely upon, in simple understandable terms for a graduate chemist. Hence, a stepwise journey across the various applications of bioluminescence has been taken, and how protein-engineering, synthetic chemistry and chemical biology tools have fed into the development of novel, state-of-the-art applications.

Whilst bioluminescence has found utility in various fields including medicine, biology, physics and engineering and led to exciting multidisciplinary science across all of them, we also discuss the current limitations in the state of the art, as well as prospects and future directions for the research community for the future development of applications of the luciferin–luciferase reaction from a chemical biology tool to something more widely used in industry, daily life or in a clinic.

## 2. Natural luciferin, their luciferases and mechanisms

The structures of D-luciferin and coelenterazine, and their respective luciferases were some of the earliest luciferin–luciferase pairs to be elucidated and their enzymes synthetically expressed.<sup>12,19–25</sup> Hence, these bioluminescence systems are used in the vast majority of applications of bioluminescence by virtue of our greater understanding of their mechanisms of action and ease in preparing the reagents needed for their assays.

In this section the mechanisms of bioluminescence with respect to D-luciferin, coelenterazine and bacterial luciferin have been looked at in greater detail as these luciferins and their respective luciferases have found the most utility in various applications. The remaining eight known luciferin–luciferase pairs have been included and discussed briefly towards the end of the section, as their understanding and inclusion would help foster future applications.

### 2.1 D-Luciferin

Although each bioluminescent insect species has a distinct luciferase enzyme, they all share the same substrate D-luciferin which is found in around 40 different species of fireflies, click-beetles and the rail-road worms.<sup>12,26–33</sup> In the bioluminescence reaction, the 62 kDa insect luciferase (Fluc)<sup>19</sup> catalyses the



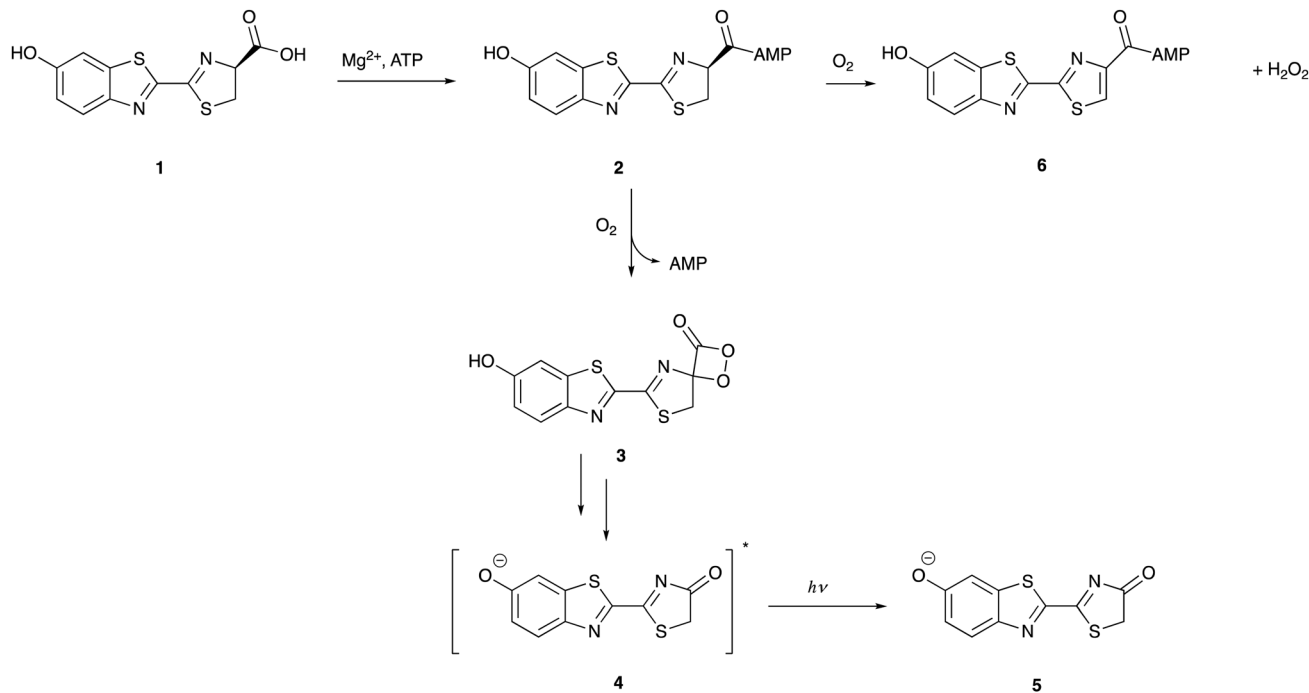


Fig. 1 The mechanism of firefly bioluminescence.

oxidation of D-luciferin **1** in two distinct steps – the activation of the carboxyl group of **1** through adenylation, followed by the oxidation of the luciferyl-adenylate **2** to form oxyluciferin **4** as an excited state anionic species through a dioxetanone intermediate **3** (Fig. 1).<sup>34–36</sup> The excited state oxyluciferin species **4** relaxes to its ground state **5** by giving off a photon of light. Around 20% of luciferyl adenylate undergoes a dark-side oxidation to form  $H_2O_2$  and dehydro-luciferyl-adenylate **6** which is a strong inhibitor of luciferase ( $K_i = 3.8 \pm 0.7$  nM),<sup>37</sup> and this limits the quantum yield of the bioluminescence reaction.<sup>38</sup> Protonated **5**, oxyluciferin itself is also an inhibitor of the luciferase enzyme ( $K_i = 500 \pm 30$  nM).<sup>37</sup> Due to the dark-side reaction and other energy losses, firefly luciferase catalyses light emission from D-luciferin with a maximum quantum yield of 41% at pH = 8.5.<sup>39</sup>

The activation of D-luciferin by ATP prior to oxidation is a unique feature of D-luciferin bioluminescence that is not shared by other luciferins such as coelenterazine. This feature bestows a variety of unique benefits upon the D-luciferin/firefly luciferase system that are not enjoyed by other bioluminescent systems. For example, as D-luciferin requires activation in the form of adenylation, it is less susceptible to auto-oxidation and more stable in solution, leading to less background chemiluminescence.<sup>40</sup> ATP is widely known as the ‘energy currency’ of a cell and found in varying amounts in virtually all eukaryotic and prokaryotic cells.<sup>41</sup> As the D-luciferin/Fluc assay produces ATP dependent light output, this assay has been widely adapted to measure ATP concentration in the double digit nanomolar region in various systems for both quality control and hygiene, often to determine the extent of bacterial contamination.<sup>42,43</sup> It is also used to monitor both ATP-forming reactions<sup>44–47</sup> and ATP-degrading reactions.<sup>48–50</sup> With the advent

of more sensitive luminometers and improved assay techniques, ATP levels as low as attomole levels – corresponding to a single bacterial cell – can be routinely detected now using commercially available ATP bioluminescence reagents and kits.<sup>42</sup> More details on these assays are discussed in Section 4.1.

It is known that D-luciferin has greater aqueous solubility<sup>51</sup> and lower toxicity than coelenterazine.<sup>52</sup> Moreover D-luciferin has the most impressive quantum yield amongst all known luciferin/luciferase systems ( $41.0 \pm 7.4\%$  compared to 15–30% for most luciferase/luciferin pairs)<sup>39,53</sup> and the longest emission wavelength amongst them ( $\lambda_{max} = 558$  nm<sup>39</sup>), it is more ideal for imaging applications where blood is involved. Haemoglobin and tissues absorb light most strongly of wavelength  $< 500$  nm.<sup>54</sup> Mammalian cells and other biological entities of interest such as bacteria, fungi, protozoa and viruses can be genetically encoded with the luciferase gene of interest<sup>55,56</sup> and introduced in to a small mammal for proliferation, tracking and imaging. From naturally occurring luciferins and luciferases, D-luciferin and the firefly luciferase from the North American firefly, *Photinus pyralis* are the most common pair used for *in vivo* imaging (Table 1).<sup>57</sup>

D-Luciferin is commercially available in its carboxylic acid form (CAS Number: 2591-17-5) as well as its sodium salt

Table 1 Properties of firefly luciferase (Fluc) from the American firefly *Photinus Pyralis*

	PpyLuc
Wavelength	558 nm
Optimum pH	7.8
Optimum temperature	28 °C
Quantum yield <sup>39</sup>	41 ± 7% at pH 8.5



(CAS Number: 103404-75-7). It can also be readily prepared in up to >50 mg scale batches using multi-step organic synthesis – preparations up to 50 mg scale have been reported although it can be envisaged that larger batches of >200 mg could be readily prepared too.<sup>58,59</sup> The plasmids and vectors used to express firefly luciferase are also readily available.

Although the light from D-luciferin bioluminescence is red-shifted compared to that from other naturally occurring luciferins, it is still strongly absorbed by blood and tissue. Near infra-red light (650–900 nm) has better penetration through blood and tissue.<sup>60</sup> Whilst there is a portion of light in the broad emission spectrum of D-luciferin within this desirable range of wavelengths, more red-shifted light would allow more sensitive imaging.<sup>54</sup>

There are other factors as well that make D-luciferin a less than ideal candidate for bioluminescence imaging. For example, D-luciferin has modest cell permeability<sup>61</sup> and hence has to be dosed in large amounts for *in vivo* experiments.<sup>62</sup> Studies in which the <sup>14</sup>C-labelled radioactive D-luciferin substrate has been used have also demonstrated the inhomogeneous bio-distribution of the substrate in rodents.<sup>63</sup> Moreover, there is poor uptake of the probe in some organs of interest such as the brain.<sup>64</sup> Whilst D-luciferin is capable of emitting light of different wavelengths on interaction with various mutants of Fluc,<sup>65</sup> the range of wavelengths emitted does not render it suitable for *in vivo* multi-parametric imaging particularly in deep tissue imaging because the most red-shifted  $\lambda_{\text{max}}$  obtained by D-luciferin and Fluc mutants is 620 nm.<sup>66,67</sup> The light at this wavelength suffers from absorption, attenuation and scatter in tissues making spectral unmixing from different luciferases more challenging.<sup>68</sup> Some of these set-backs have been overcome with the design, synthesis and testing of novel D-luciferin analogues, which have led to brighter, red-shifted emission in some cases.<sup>69</sup> Details on these can be found in Section 3.1.

There has also been a strong case for engineering the firefly luciferase enzyme to obtain better properties more suited for various applications. For example, in order to detect a variable ATP concentration, it is essential that the luciferase concentration remains constant during the duration of the measurement and luciferase is not inactivated by other factors such as pH, temperature, the concentration of metal ions, detergents and other soluble proteins such as bovine serum albumin, in the assay mixture. The optimum pH for wild-type luciferase activity is pH 7.8.<sup>70,71</sup> A workable pH of 6–8 can be used for analytical applications using the wildtype enzyme.<sup>46</sup> However, the colour of emission from some wild-type firefly luciferases such as *P. pyralis* and *H. parvula* changes from yellow-green to red when the pH is lowered below optimum.<sup>72–74</sup> The reason for this has been proposed to be the disruption of a key hydrogen-bonding network involving key water molecules and amino acid residues in the enzyme's active site around the oxyluciferin emitter. It is believed that disruption at lower pH enhances the delocalisation of the phenolate negative charge that increases red shifted emission.<sup>75</sup> This rendered these wild-type luciferases not as useful for comparative bio-analytical applications where often photons of a specific wavelength of light are being quantified.

Moreover, most wild-type luciferases are thermolabile at even room temperature, whilst work on mammalian cells often requires temperatures of around 37 °C.<sup>76</sup> Indeed, wild-type luciferase has a half-life of only 3–4 h in mammalian cells due to both thermal inactivation and proteolysis.<sup>77</sup> Consequently, there has been significant work done in protein engineering to create mutant firefly luciferases of greater pH stability, thermostability and proteolytic stability. Indeed, a small change in the sequence of the enzyme can lead to changes significant changes in the emission and properties of the enzyme. For example, the mutant S286N of the Japanese Firefly Luciferase has red-shifted emission at  $\lambda_{\text{max}} = 605$  nm compared to the wild-type at  $\lambda_{\text{max}} = 560$  nm (Fig. 2A and B). This is because Ser 286 is involved in a key hydrogen-bonding network that is disrupted when it is mutated to an asparagine residue. Moreover, this also causes a change in the conformation of Ile 288 close to the emitter making the hydrophobic pocket more flexible (Fig. 2C and D). For further details on engineered Fluc enzymes please see Section 3.1.

## 2.2 Coelenterazine

Coelenterazine is found in several marine creatures including copepods and the deep-water shrimp, and is the other most commonly used luciferin.<sup>13,78</sup> Coelenterazine is the substrate for around 15 different naturally occurring luciferases.<sup>24,25,79–84</sup> From these, the luciferases from *Renilla* luciferase (Rluc), *Gaussia* luciferase (Gluc) and *Metridia longa* luciferase (Mluc) were one of the earliest to be cloned and have found most utility in biotechnological applications. The bioluminescent reaction of coelenterazine also involves an enzymatically catalysed oxidation. Coelenterazine 7 is converted to an excited state coelenteramide oxyluciferin **10** through a dioxetanone intermediate **9**. The excited state oxyluciferin relaxes to its ground state to emit a photon of blue light of wavelength 454–493 nm, dependent upon the enzyme (Fig. 3). This bioluminescent reaction is not dependent on ATP.

Coelenterazine is commercially available (CAS Number: 55779-48-1) and can be synthesised in up to >200 mg scale batches using multi-step synthesis.<sup>85</sup> However, coelenterazine is a larger molecule than D-luciferin, has poor water solubility, greater toxicity and is also susceptible to auto-oxidation leading to chemiluminescence in solution as it does not need activation in the form of adenylation.<sup>40</sup> Moreover, coelenterazine has also been reported to be transported into cells through other mechanisms. For example, the multidrug resistance P-glycoprotein (MDR1 Pgp) was reported to mediate the transport of coelenterazine into cell lines. This led to greater amounts of coelenterazine being transported into cancer cells expressing greater quantities of MDR1 Pgp. This could lead to an inaccurate representation of tumours in small mammal *in vivo* imaging *i.e.* tumours that do not express MDR1 Pgp would not be detected.<sup>86</sup> Coelenterazine gives out blue light which is strongly absorbed by blood and tissue, making it a poor candidate for *in vivo* imaging when used alone without the red-shifting effects of BRET.<sup>54</sup> To overcome these short-comings, several synthetic coelenterazine analogues have been prepared, of which some are



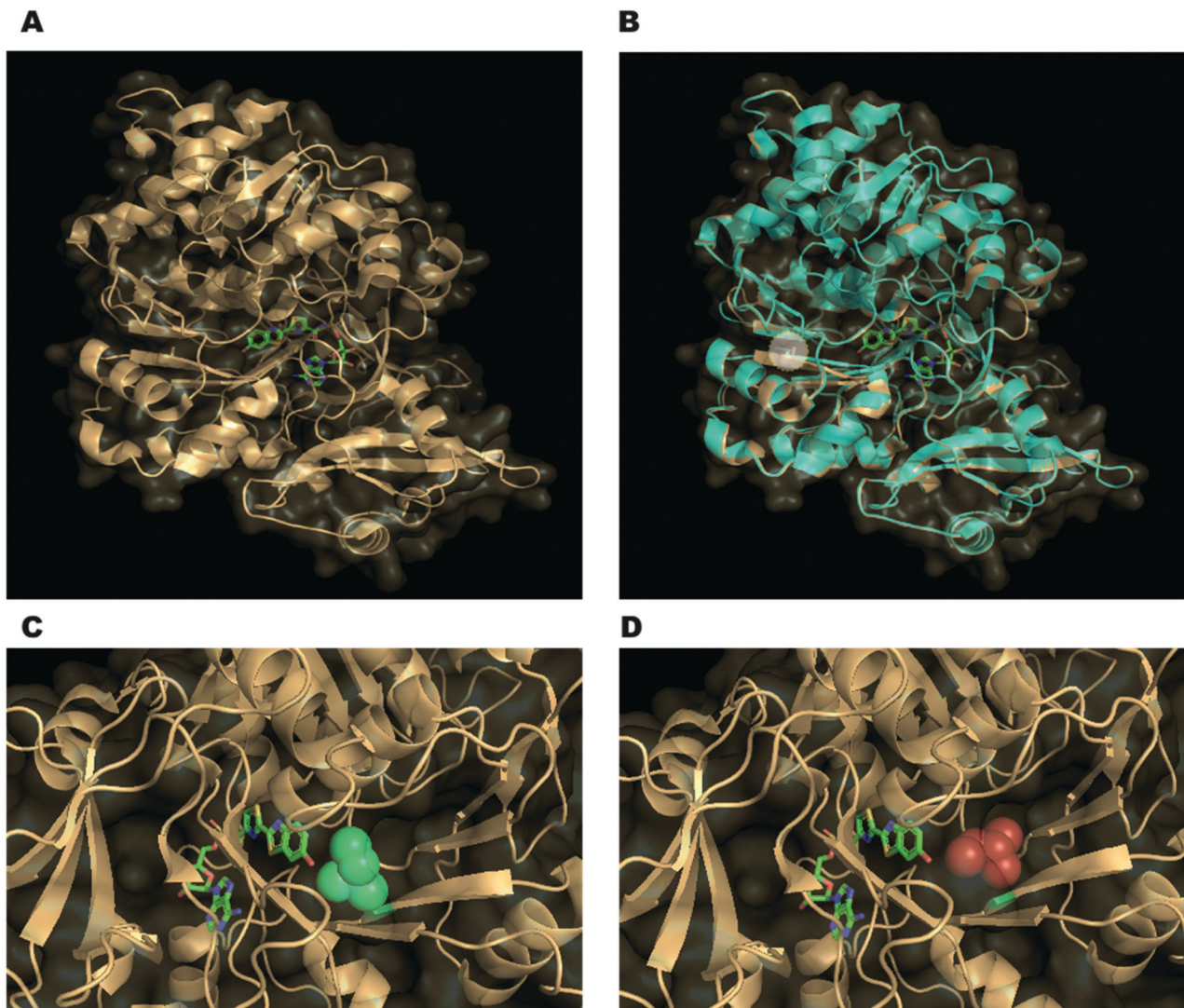


**Fig. 2** (A) The co-crystal structure of the Japanese firefly luciferase (*Luciola cruciata*) with a high-energy intermediate analogue, 5'-O-[N-(dehydro-luciferyl)-sulfamoyl]adenosine (DLSA) – PDB code: 2D1S. (B) Overlay of complex of *Luciola cruciata* luciferase with DLSA (PDB code: 2D1S – coloured in light orange) with mutant S286N complexed with DLSA (PDB code: 2D1T – coloured in cyan). The side-chains of the residues of the key mutation are shown as sticks and highlighted in the white circle. (C) The conformation of Ile 288 (green spheres) in wild-type *Luciola cruciata*. (D) The changed conformation of Ile 288 in the S286N mutant (red spheres), leading to a more flexible hydrophobic pocket.

commercially available. Details of these analogues are presented in Section 3.2.

In terms of size, both *Rluc* (~34 kDa), *Gluc* and *Mluc* (both ~20 kDa) are smaller than *Fluc* (~62 kDa). This makes them more suitable for applications involving small vectors and/or proteins. In the sea pansy, *Renilla reformis* the luciferase *Rluc* is closely associated with a green fluorescent protein (GFP) and the blue light emitted by the luciferase is coupled through resonance energy transfer to the fluorophore of the GFP allowing it to form an excited-state species which emits a photon of green light ( $\lambda_{\max}$  510 nm).<sup>87</sup> This principle of resonance energy transfer led to the development of bioluminescence resonance energy transfer (BRET) and several associated applications where the BRET light emission has been used as a measure for the spatial proximity of two proteins.<sup>88</sup>

Most coelenterazine utilising luciferases possess several disulphide bonds in the protein structure which often help in protein-folding and confer these enzymes with greater thermal stability than firefly luciferases. However, these disulfide bonds also make the enzymes sensitive to any reducing agents in buffer solutions as it is vital for the cysteine residues to be in the correct oxidation state for native protein folding. Moreover, the optimum conditions for activity of these luciferases often mimic their natural marine environment. So, most of these luciferases are halophilic reflecting the saltiness of seawater and some forms – for example the *Mluc2* isoform of *Metridia longa* luciferase – is psychrophilic *i.e.* has a very low optimum temperature reflecting the low temperatures at the bottom of the ocean (Table 2).<sup>89</sup> Copepod luciferases *Gluc* and *Mluc* are the only known luciferases that are naturally secreted from



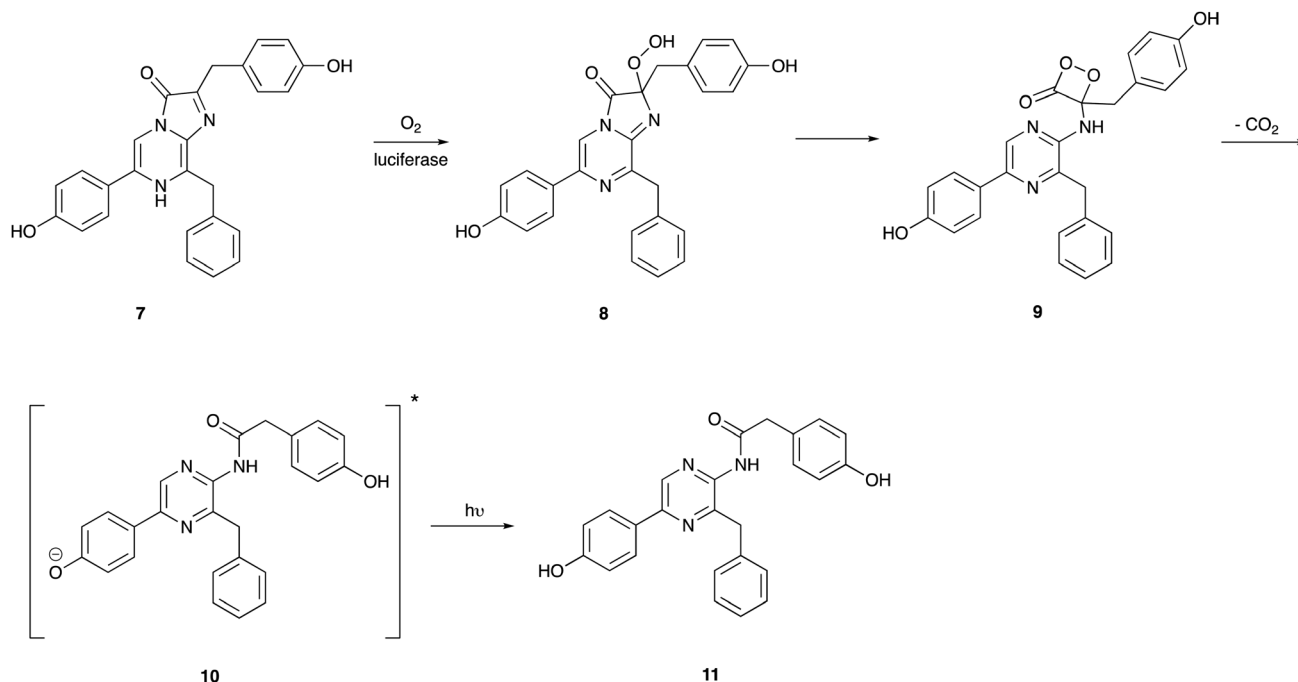


Fig. 3 The mechanism of coelenterazine bioluminescence.

Table 2 Properties of common marine luciferases

	Rluc <sup>91</sup>	Gluc <sup>92</sup>	Mluc2 <sup>89</sup>
Wavelength	480 nm	485 nm	488 nm
Optimum pH	7.4	7.5–8.4	7.5–8.4
Optimum temperature	32 °C <sup>91</sup>	15–20 °C <sup>92</sup>	5 °C <sup>89</sup>
Optimum [NaCl]	0.5 M	1.6 M	1.0–1.5 M
Quantum yield	5.3 ± 0.1% <sup>93</sup>	Not determined	Not determined

eukaryotic cells.<sup>90</sup> These unique properties make them potentially useful for a unique set of applications such as high throughput studies as cell-lysis is not required.

### 2.3 Bacterial luciferin

Besides firefly bioluminescence and coelenterazine based marine bioluminescence, bacterial bioluminescence has also received considerable attention in terms of applications over the past half century or so.<sup>57,94,95</sup> All known bioluminescent bacteria are Gram-negative, facultative anaerobic<sup>94</sup> and most are symbiotic and found in their host organisms such as the Hawaiian Bobtail squid (*Aliivibrio fischeri*)<sup>96</sup> or terrestrial roundworms (*Photobacterium luminescens*).<sup>97</sup> Although some are free-living species such as *Vibrio harveyi*<sup>98</sup> and *Alteromonas hanedai*.<sup>99</sup> Although bioluminescent bacteria belong to various species and genre, the biochemical machinery of bacterial light emission is globally conserved between species. In bacteria, all the enzymes required for bioluminescence are completely genetically encoded for in the *luxCDABEG* operon.<sup>100</sup> An operon is a functioning unit of DNA containing a cluster of genes under the control of a single promoter.<sup>101</sup> A promoter is a sequence of DNA to which proteins bind that initiate transcription of a single RNA from the DNA downstream of it.<sup>102</sup> The *luxA* and *luxB* genes encode for the

40 kDa  $\alpha$  subunit and 37 kDa  $\beta$  subunit of the bacterial luciferase respectively. The *luxC*, *luxD* and *luxE* genes encode enzymes involved in the synthesis of the aldehyde co-factor, and *luxG* encodes for flavin reductase which participates in flavin mononucleotide (FMN) turnover.<sup>94,103</sup>

The mechanism of bacterial bioluminescence is well understood (Fig. 4).<sup>104</sup> Flavin mononucleotide (FMN) reductase reduces oxidised FMN **12** to form reduced FMN **13** which reacts with molecular oxygen to form an FMN-hydroperoxide species **14**, possibly through a single electron transfer (SET) process as suggested for adenylated *D*-luciferin and oxygen.<sup>35,105,106</sup> In the absence of long-chain aldehyde **15**, intermediate **14** is fairly stable and was characterised by UV-vis absorption and NMR spectroscopy.<sup>107,108</sup> It has been proposed that the long-chain aldehyde **15** adds to **14** to form the FMN-4*a*-peroxyhemiacetal species **16** which collapses to form the carboxylic acid **17** and FMN-4*a*-hydroxide **18** in an excited state.<sup>106</sup> The exact mechanism of formation of the excited-state species is still under debate. A few different mechanisms have been proposed for the breakdown of FMN-4*a*-peroxyhemiacetal species **16**, including the proposed formation of a dioxirane intermediate<sup>109</sup> or a flavin-mediated intra-molecular electron transfer mechanism initiating the collapse of **16**. There is greater computational<sup>110</sup> and experimental data<sup>111</sup> to support the intra-molecular flavin-mediated electron transfer from the 5-N of the isoalloxazine ring to the distal oxygen atom of FMN-4*a*-peroxyhemiacetal species **16**. Light emission occurs when the flavin mononucleotide species FMN-4*a*-hydroxide **18** relaxes to its ground state **19** and emits a photon of bluish-green light ( $\lambda_{\text{max}}$  490 nm) (Table 3). The long-chain aldehyde is oxidised to the corresponding carboxylic acid as part of the cycle.

In essence, the entire light emission machinery including luciferase production, luciferin biosynthesis and recycling



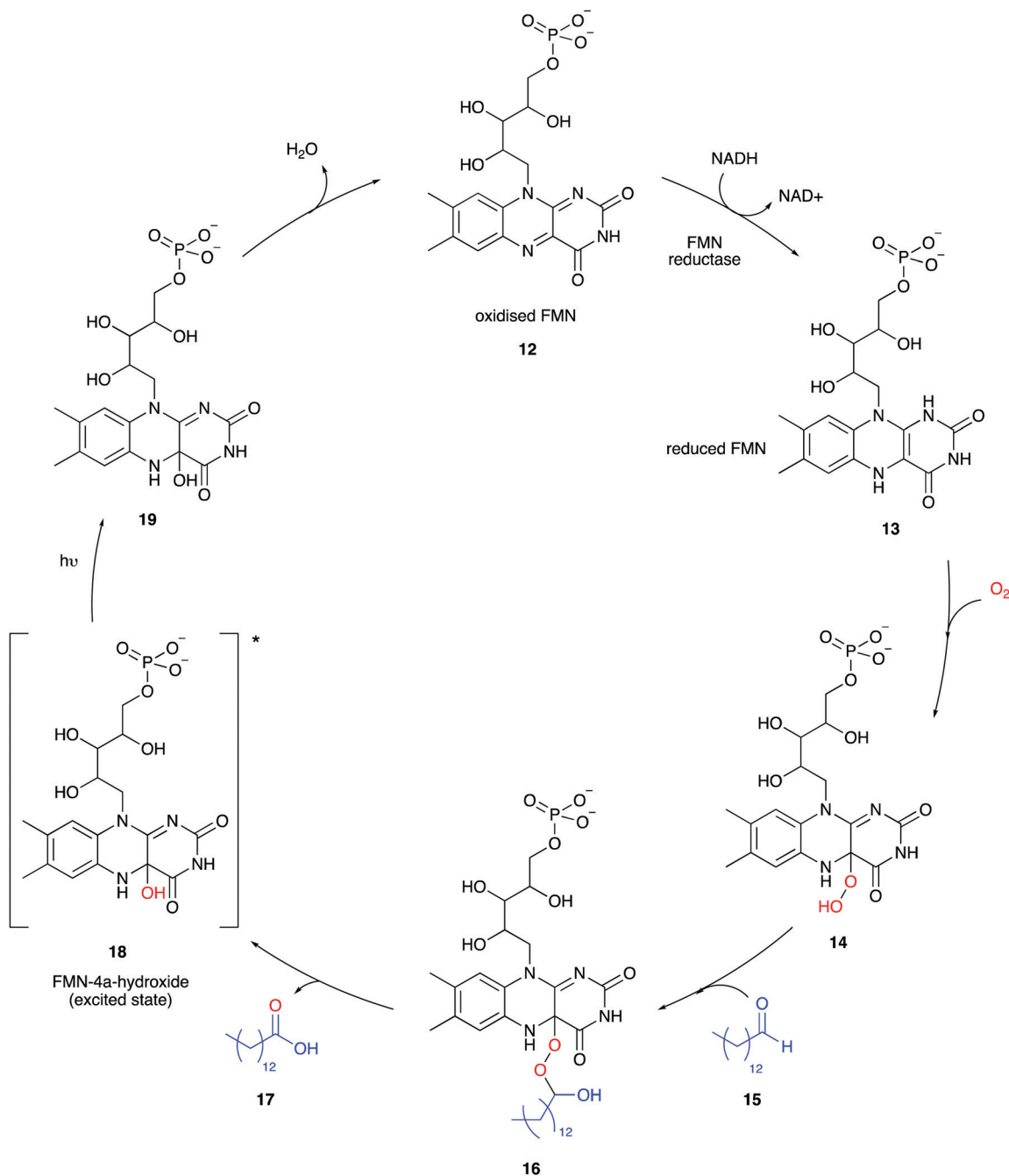


Fig. 4 The mechanism of bacterial bioluminescence.

Table 3 Properties of the bacterial bioluminescent system

	Bacterial luciferase
Wavelength	490 nm <sup>122</sup>
Optimum pH	6.8 <sup>122</sup>
Optimum temperature	23 °C <sup>123</sup>
Quantum yield	30% <sup>124</sup>

machinery is genetically encoded for together in a single operon, so transgenic auto-luminescence is possible. Exogenous administration of luciferin is not required in any imaging applications,

unlike what is observed in firefly bioluminescence imaging and coelenterazine bioluminescence imaging. This is of great value in synthetic biology, especially as the administration of expensive and unstable luciferins in some hosts such as plants is difficult.<sup>112,113</sup> However, considerable work and optimisation of the genetic make-up was required to make bacterial operons useful in eukaryotic cells and machinery. Although in early studies only *luxA* and *luxB* were expressed in plant cells such as tobacco and carrots to form functional luciferase in them, autoluminescent tobacco plants were later designed using the operons from *Photobacterium leighognathi lux* operon.<sup>114,115</sup> Although previously,



Table 4 Summary of the key properties of the remaining luciferin–luciferase pairs

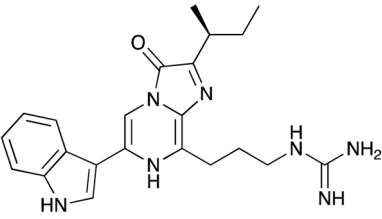
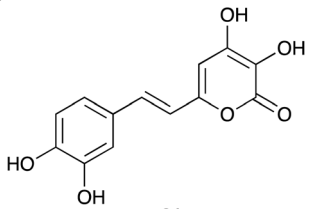
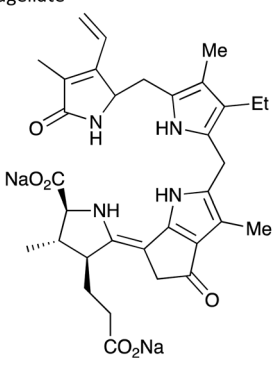
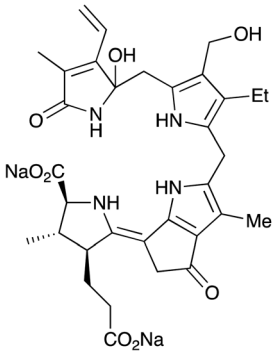
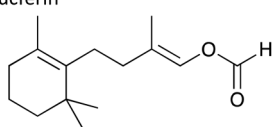
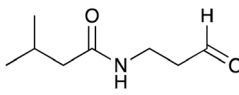
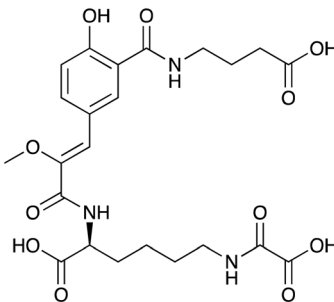
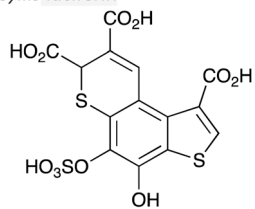
Luciferin	Luciferase size	Wavelength ( $\lambda_{\text{max}}$ )	Required components	Key facts
<p><i>Cypridina</i> luciferin</p>  <p><b>20</b></p>	~ 61 kDa <sup>22</sup>	452 nm <sup>22</sup>	Luciferin, luciferase and O <sub>2</sub>	<ul style="list-style-type: none"> <li>• Bioluminescence mechanism is very similar to that of coelenterazine</li> <li>• It is a secreted luciferase</li> <li>• Several applications exist which will be discussed in depth in later sections.</li> <li>• Quantum yield = 28%<sup>125</sup></li> </ul>
<p>Fungal luciferin</p>  <p><b>21</b></p>	~ 29 kDa <sup>126</sup>	520 nm <sup>126</sup>	Luciferin, <sup>127</sup> luciferase and O <sub>2</sub>	<ul style="list-style-type: none"> <li>• The only eukaryotic auto-luminescent system.</li> <li>• So far used to create GM glowing plants.<sup>128</sup></li> <li>• Quantum yield not determined.</li> </ul>
<p>Dinoflagellate</p>  <p><b>22</b></p>	~ 135 kDa <sup>129</sup> 3 distinct domains that are each catalytically active	476 nm <sup>129</sup>	Luciferin, <sup>130</sup> luciferase and O <sub>2</sub> at pH 6.3	<ul style="list-style-type: none"> <li>• No chemical synthesis of the luciferin reported to-date</li> <li>• Fewer than half a dozen known applications of the luciferase exist. Examples include use as a reporter enzyme for <i>in vitro</i> gene expression,<sup>131</sup> measuring quantities of cell-surface expressed membrane proteins,<sup>132</sup> and pregnancy-specific glycoproteins in HeLa cells to investigate cell senescence.<sup>133</sup></li> <li>• Quantum yield not determined.</li> </ul>
<p>Krill luciferin</p>  <p><b>23</b></p>	~ 600 kDa <sup>134</sup>	468 nm <sup>135</sup>	Luciferin, <sup>138</sup> luciferase and O <sub>2</sub>	<ul style="list-style-type: none"> <li>• No chemical synthesis of the luciferin reported to-date and a pure sample of luciferin not isolated either – structure elucidated through crude luciferin sample and oxyluciferin sample</li> <li>• Cross-reactivity is observed between krill luciferin and dinoflagellate luciferase and dinoflagellate luciferin and krill luciferase<sup>136</sup></li> <li>• No known applications to-date</li> <li>• Quantum yield not determined.</li> </ul>
<p><i>Latia</i> luciferin<sup>a</sup></p>  <p><b>24</b></p>	~ 173 kDa <sup>137</sup>	536 nm <sup>138</sup>	Luciferin, <sup>130</sup> luciferase, purple protein and O <sub>2</sub>	<ul style="list-style-type: none"> <li>• The structure of the light-emitting species is still unknown<sup>a</sup></li> <li>• Synthetic analogues of the luciferin have been reported that are less active in bioluminescent emission<sup>139–141</sup></li> <li>• Quantum yield = 17%<sup>142</sup></li> </ul>



Table 4 (continued)

Luciferin	Luciferase size	Wavelength ( $\lambda_{\max}$ )	Required components	Key facts
<p><i>Diplocardia</i> luciferin<sup>a</sup></p>  <p>25</p>	~ 300 kDa <sup>143</sup> copper dependent	500–530 nm <sup>144</sup>	Luciferin, <sup>144</sup> luciferase and H <sub>2</sub> O <sub>2</sub>	<ul style="list-style-type: none"> <li>• Used in analytical tools to detect H<sub>2</sub>O<sub>2</sub> levels and peroxidase activity.<sup>145</sup></li> <li>• A major limitation on its use is that the luciferase has not been cloned so needs to be sourced directly from the earthworms themselves.<sup>146</sup></li> <li>• Quantum yield = 3%<sup>a</sup><sup>146</sup></li> <li>• A major limitation on its use is that the luciferase has not been cloned so needs to be sourced directly from the earthworms themselves.<sup>146</sup></li> <li>• Quantum yield not determined.</li> </ul>
<p><i>Fridericia</i> luciferin</p>  <p>26</p>	~ 35 kDa <sup>147</sup>	478 nm <sup>147</sup>	Luciferin, <sup>148,149</sup> luciferase, Mg <sup>2+</sup> ions, O <sub>2</sub> and ATP	<ul style="list-style-type: none"> <li>• Luciferin structure was reported in late 2019.<sup>11</sup></li> <li>• Quantum yield not determined.</li> <li>• No known applications to-date.</li> </ul>
<p><i>Odontosyllis</i> luciferin</p>  <p>27</p>	~ 35 kDa <sup>150</sup>	510 nm <sup>150</sup>	Luciferin, luciferase and O <sub>2</sub>	<ul style="list-style-type: none"> <li>• Luciferin structure was reported in late 2019.<sup>11</sup></li> <li>• Quantum yield not determined.</li> <li>• No known applications to-date.</li> </ul>

<sup>a</sup> This is the proposed structure for the luciferin although other proposals suggest that the light emitting species could be a flavin moiety as is the case in the bacterial bioluminescent system.

the bacterial *lux* operon had been used to produce a weakly autoluminescent human cell line (*HEK293* cells), more recently codon-optimised *lux* sequences have been developed that produce bright, autonomous bioluminescence in mammalian cells.<sup>116,117</sup> Further details of the codon-optimisation and enzyme engineering involved are presented in Section 3.3.

Bioluminescent bacteria are often used as biosensors in ecotoxicological studies as these can often be tuned to detect concentrations of a variety of different organic (alcohol, carboxylic acids, aromatic compounds) and inorganic substances (heavy metal ions).<sup>118–120</sup> Moreover, bioluminescent bacteria are also being used to create unique glowing artwork and proposals have been suggested to use them in indoor aquariums as part of aesthetic architecture in skyscrapers.<sup>121</sup>

As both bacterial luciferase and luciferin are encoded for in the *lux* operon, this has led to limited mutations in the native luciferase structure and no mutations to the luciferin, although shorter-chain aldehydes are also tolerated and as expected result in no change in wavelength of the light emitted.<sup>105</sup>

#### 2.4 Other known luciferins

There are over 30 known bioluminescent systems but the luciferin–luciferase pairs of only 11 systems have been

characterised to-date with a handful of systems only partially characterised.<sup>10</sup> Of these D-luciferin, coelenterazine and the bacterial bioluminescent systems have found most utility in biotechnological applications, by virtue of a more comprehensive understanding of them. The table below (Table 4) details succinctly the other known bioluminescence systems and some of their applications.

The discovery and characterisation of yet-unknown luciferins and luciferases is an area of active research and recent highlights include reports on the luciferin–luciferase systems of the New Zealand glow-worm *Arachnocampa luminosa* and the diptera *Orfelia fultoni* from the United States.<sup>151,152</sup> Both systems emit blue light and although structures of the luciferins have been proposed based on NMR spectroscopy, mass spectrometry and isotopic labelling studies although, the proposed structures need to be validated through chemical synthesis.

### 3. Designer luciferins and their luciferases

Advances in synthetic chemistry and protein engineering have been crucial to take the known natural luciferin and luciferase systems to uncharted territories and use them for a wide



range of applications. Significant work has been done in both fields to prepare optimum luciferin–luciferase pairs that give access to previously inaccessible applications through bioluminescence imaging (BLI). Although significant research has been done in accessing ‘caged’ luciferins and ‘tagged’ luciferins as well as ‘split’ luciferases and ‘tagged’ luciferases – this particular portion of the review will focus on the basic structural modifications of both luciferins and luciferases that have bestowed them with beneficial properties, whereas as ‘tagged’ and ‘caged’ luciferins and ‘split’ luciferases will be discussed where relevant and have been discussed in greater detail in Sections 4.5 and 4.7. This section will focus on some of the key developments in the area of novel luciferins and luciferases.

### 3.1 Novel D-luciferin analogues and luciferase mutants

As the D-luciferin/Fluc assay is the most red-shifted and bright natural luciferin to date, it has emerged as the assay of choice for *in vivo* imaging in small mammals. However, it does have some drawbacks that limits quantitative deep-tissue imaging in small mammals (Section 2.1). In order to address these, the quest for bright, non-toxic, red-shifted luciferin analogues that have optimum biochemical properties such as solubility, biodistribution and the ability to be useful in quantitative, multi-parametric imaging continues.

The chemical synthetic routes towards luciferin analogues were succinctly compiled by Podsiadly *et al.* in 2019.<sup>69</sup> Herein, we briefly highlight synthetic luciferin analogues, particularly those that have found use in applications, or have useful and interesting properties such as brightness that could potentially make them useful in applications. As the primary use of red-shifted D-luciferin analogues is in *in vivo* applications, we particularly highlight analogues that emit in the near infra-red region (>650 nm), and of those analogues, specifically those that have been successfully tested *in vivo* (Table 5). It is important to note that although the Fluc/D-luciferin combination emits at  $\lambda_{\text{max}} = 558$  nm *in vitro*, there is a spectral red-shift observed in *in vivo* imaging, with  $\lambda_{\text{max}} \sim 610$  nm due to attenuation through tissue.<sup>153</sup>

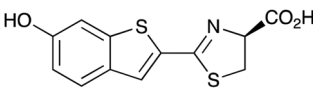
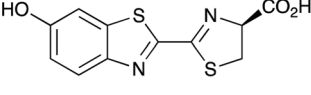
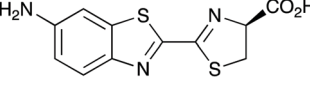
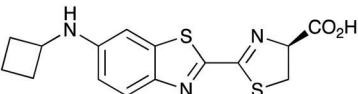
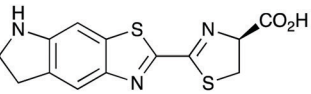
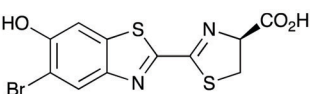
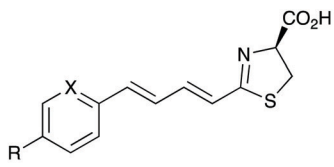
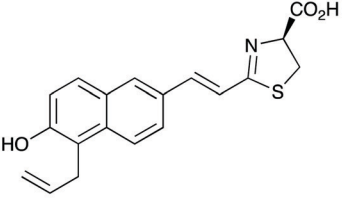
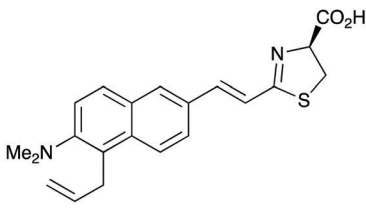
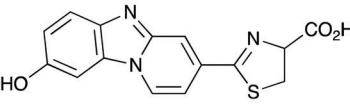
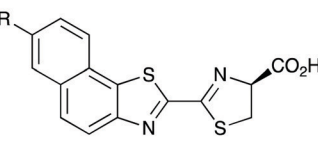
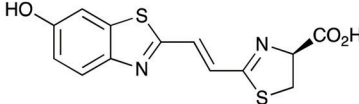
Of all the synthetic luciferin analogues reported to-date, BtLH<sub>2</sub> **28** was reported to have the highest bioluminescence quantum yield (70%) relative to that of D-luciferin **1** with wild-type Fluc. Although BtLH<sub>2</sub> **28**, had a bioluminescence  $\lambda_{\text{max}}$  of 523 nm which was around 20 nm blue-shifted, it was also reported to have a longer-lasting and sustained bioluminescence signal compared to that of D-luciferin.<sup>154</sup> This could possibly make it a better candidate for applications that require blue-shifted and longer-lasting light emission. One of the earliest reported synthetic luciferins was the aminoluciferin **29** by White *et al.* This synthetic luciferin was red-shifted ( $\lambda_{\text{max}} = 594$  nm) compared to D-luciferin ( $\lambda_{\text{max}} = 558$  nm) but only about 10% as bright *in vitro*.<sup>61,155</sup> Since then, several other synthetic aminoluciferin analogues were reported, and although all of them are dimmer than D-luciferin **1**, with the wild-type Fluc, some have useful properties for *in vivo* imaging. For example, aminoluciferin analogues **30** and **31** have emission around  $\lambda_{\text{max}} \sim 600$  nm.

Both analogues **30** and **31** was reported to have better penetration than D-luciferin through the blood–brain barrier in mice.<sup>156,157</sup> Moreover, analogue **31** CycLuc1 was reported to have brighter bioluminescence output from cells at lower substrate concentrations than D-luciferin **1**, indicating that it had better cell-permeability than D-luciferin **1**.<sup>62</sup> Both analogues **30** and **31** are commercially available. The Prescher group reported a brominated luciferin analogue, that was red-shifted ( $\lambda_{\text{max}} = 625$  nm) and had an appreciable relative bioluminescence quantum yield of 46% compared to D-luciferin **1** at 100  $\mu\text{M}$  substrate concentration and 1  $\mu\text{g}$  of Fluc.<sup>158</sup> At these concentrations they reported aminoluciferin **29** to be 61% as bright as D-luciferin **1**.

A handful of synthetic luciferin analogues truly emit in the nrIR region (>650 nm). The analogues **32–34** were reported by Maki *et al.* and have been successfully taken on to *in vivo* detection of tumours in mice.<sup>159–161</sup> In particular, the hydrochloride salt of Akalumine **32** was used with the engineered firefly luciferase *Akaluc* in single-cell bioluminescence imaging (BLI) of deep-tissue in the lungs of live, freely-moving mice and to image small numbers of neurones in the brains of live marmosets.<sup>64</sup> The analogues Akalumine **32** and Sempei **34** are now commercially available from Merck. The analogues **34** and **36** were also reported by Maki *et al.* as significantly dimmer substrates than Akalumine **32** but whose emission was  $\sim 700$  nm.<sup>162</sup> Anderson *et al.* reported the analogue iLH<sub>2</sub> **38** as a significantly red-shifted luciferin that showed enhanced tumour burden in deep-seated tumours such as liver metastasis in mice due to less scattering and greater penetration of the near-infrared (nrIR) light.<sup>66</sup> The luciferin iLH<sub>2</sub> **38** was designed to emit different colours of light with different Fluc mutants through retention of the phenol group which is deemed necessary to modulate the colour emission of D-luciferin analogues. This ability of iLH<sub>2</sub> **38** to emit different colours of light with different Fluc mutants made it unique, and it was proposed that iLH<sub>2</sub> **38** was a suitable analogue for multiparametric imaging and tomography. Recently, the suitability of iLH<sub>2</sub> **38** also demonstrated in a report by Anderson and co-workers in which racemic iLH<sub>2</sub> **38** together with stabilised colour mutants of firefly luciferase (Fluc<sub>green</sub>  $\sim 680$  nm and Fluc<sub>red</sub>  $\sim 720$  nm) were shown to be a suitable system for nrIR dual *in vivo* bioluminescence imaging in mouse models where they simultaneously monitored both tumour burden and CAR T cell therapy within a systemically induced mouse tumour model.<sup>68</sup> The Anderson lab also reported the analogue PBIiLH<sub>2</sub> **37** as a racemic compound, which was prepared as a conformationally restrained infra-luciferin analogue.<sup>163</sup> Although PBIiLH<sub>2</sub> **37** was only tested in *in vitro* assays and found to be less bright than racemic iLH<sub>2</sub> **38**, it did demonstrate an increased bimodal emission with increasing pH. A primary bioluminescence peak at 608 nm was observed with Fluc x11 and a secondary peak at 714 nm of increasing intensity. This emission pattern could potentially be used to monitor pH, although the work does not build on this possibility.<sup>164</sup> In 2018, Mezzanote *et al.* reported the most red-shifted luciferin analogue **40** and sister compound **39** with mutant CBR2opt luciferases without the use of resonance transfer.<sup>165</sup> Both analogues **39** and **40** were tested



Table 5 A selection of synthetic D-luciferin analogues that have useful properties organised in increasing wavelength

$\lambda_{\max} < 550$ nm	Natural substrate	$\lambda_{\max} \sim 550$ –600 nm
 <b>28 BtLH<sub>2</sub></b> $(\lambda_{\max} \sim 523$ nm)  	 <b>1 D-LH<sub>2</sub></b> $(\lambda_{\max} \sim 558$ nm) CAS Number = 103404-75-7   	 <b>29 Aminoluciferin</b> $(\lambda_{\max} \sim 594$ nm) CAS Number = 161055-47-6   
 <b>30 cybLuc</b> $(\lambda_{\max} \sim 600$ nm) CAS Number = 1649470-26-7   	 <b>31 CycLuc1</b> $(\lambda_{\max} \sim 601$ nm) CAS Number = 1247879-16-8   	 <b>32 5'-BrLuc</b> $(\lambda_{\max} \sim 625$ nm)   
 <b>33 Akalumine</b> R = NMe <sub>2</sub> , X = CH $(\lambda_{\max} \sim 675$ nm) CAS Number = 1176235-08-7    	 <b>34</b> R = N-pyrrolidine, X = CH $(\lambda_{\max} \sim 667$ nm)   	 <b>36</b> $(\lambda_{\max} \sim 690$ nm)   
 <b>35 Sempei</b> R = NMe <sub>2</sub> , X = N $(\lambda_{\max} \sim 675)$ CAS Number = 1821155-77-4   	 <b>37</b> $(\lambda_{\max} \sim 705$ nm)   	 <b>38 PBIiLH<sub>2</sub></b> $(\lambda_{\max} \sim 714$ nm with x11) 
 <b>40</b> R = NH <sub>2</sub> $(\lambda_{\max} \sim 730$ nm with CBR2)   	 <b>41</b> R = OH $(\lambda_{\max} \sim 748$ nm with CBR2)  	 <b>39 iLH<sub>2</sub></b> $(\lambda_{\max} \sim 720$ nm with Fluc <sub>red</sub> )   

Key	
	<i>in vitro</i> measurements
	<i>in cellulo</i> measurements (mammalian cells)
	<i>in cellulo</i> measurements (bacterial cells)
	<i>in vivo</i> imaging in mouse models
	<i>in vivo</i> imaging in monkey

in HEK-293 cell lines expressing CBR2opt, and as the analogue **39** gave higher light output than the analogue **40**, the analogue

**39** was tested in *in vivo* mouse studies. The most useful output from this study appeared to be the development of the mutant



luciferase CBR2opt as the  $D$ -luciferin **1** and CBR2opt combination was demonstrated to be the brightest and most useful in all the experiments reported in the work, whilst both analogues **39** and **40** were dimmer than  $D$ -luciferin with CBR2opt.

In the area of luciferase engineering, several firefly and beetle luciferase mutants have been reported with improved properties such as increased stability, increased substrate affinity, and increased brightness over the years and these were comprehensively reviewed in 2016 by Yampolsky *et al.*<sup>10</sup> Some highlights since then include engineered luciferases for improved light output of specific synthetic substrates such as *Akaluc* for Akalumine **32** and *CBR2opt* for the analogue **39**.<sup>165,166</sup> Other highlights include work by Miller *et al.* on mutants that have a significantly higher  $K_m$  for  $D$ -luciferin and ATP than for cyclic amino-luciferins. The rate of reaction when the enzyme is saturated with substrate is the maximum rate of reaction,  $V_{max}$ . For practical purposes,  $K_m$  is the concentration of substrate which permits the enzyme to achieve half  $V_{max}$ . An enzyme with a high  $K_m$  for a particular substrate has a low affinity for that substrate and requires a greater concentration of the substrate to achieve  $V_{max}$ . Hence the mutants developed by Miller *et al.* are more selective for cyclic aminoluciferins than for  $D$ -luciferin and this allowed substrate-selective BLI in mouse-brain.<sup>167</sup> The Prescher group reported an elegant piece of work in which they prepared a library of 159 mutant luciferases by mutations of 23 key residues near the active site of the enzyme.<sup>168</sup> These were then screened against 12 synthetic luciferins to identify orthogonal luciferin–luciferase pairs. Three of the ‘hit’ pairs from this analysis were taken up for *in vivo* mouse studies of mammary carcinoma.<sup>169</sup> Imaging conditions are sensitive to a variety of factors, such as concentration of the imaging agent, the type of cell line used and the type of mouse model and tumour or infection studied. Although a number of synthetic luciferin analogues and mutant luciferases have been reported, there are very few studies reported that compare these against each other to match the best luciferin analogue and its complementary luciferase for a particular application in one study.

### 3.2 Coelenterazine analogues and luciferase mutants

Coelenterazine 7 (CTZ) is utilised by both photoproteins and luciferases. Coelenterazine utilising photoproteins such as aequorin, are often activated by  $Ca^{2+}$  ions and hence these are routinely used to detect intracellular  $Ca^{2+}$  ion concentration in biological studies. These photoproteins and the synthetic coelenterazine analogues with improved properties have been reviewed elsewhere.<sup>8,10</sup>

A host of luciferases including Renilla luciferase (Rluc) from the sea pansy, Gaussia luciferase (Gluc) from the marine copepod and *Oplophorus gracillirostris* luciferase (Oluc), from the deep-sea shrimp use coelenterazine 7 as their substrate.<sup>24,25,79–84</sup>

A number of key developments using protein engineering were carried out on these coelenterazine utilising luciferases, which resulted in useful imaging and visualisation tools. For example, Nagai and co-workers developed the Nano-lantern,

which was the brightest luminescent protein reported at the time in 2012. This was a chimera of Rluc8 (a brighter and more stable Rluc mutant)<sup>93</sup> and a fluorescent protein called Venus which has high BRET efficiency.<sup>170</sup> They then further developed this work by using different fluorescent proteins as BRET acceptors of Rluc8 and other Rluc mutants to develop a suite of Nano-lanterns that emit light of different colours, including the most red-shifted Nano-lantern ReNL ( $\lambda_{max}$  585 nm).<sup>171–173</sup> The Nano-lantern series was shown to have broad applicability in both *in vitro* and *in vivo* imaging, as well as in the detection of  $Ca^{2+}$  ions.

In another ground-breaking development, the catalytically active portion of Oluc was identified and mutated using a combination of both rational mutagenesis and random mutagenesis for enhanced thermal stability and light output by Promega.<sup>174</sup> This small 19 kDa mutant enzyme was called Nanoluc and it was optimised to perform best with the synthetic substrate furimazine (Fz) **42** Table 6.<sup>175</sup> Both Nanoluc and furimazine are now commercially available. However, the Nanoluc-furimazine combination emits blue light ( $\lambda_{max}$  ~ 456 nm) which makes it unsuitable for *in vivo* applications, although the fact that this system has ATP-independent emission has led to possible advantages in some applications over the firefly bioluminescence system.<sup>176</sup>

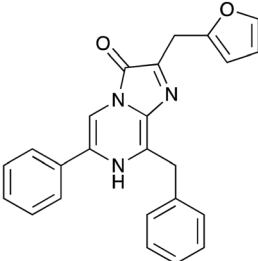
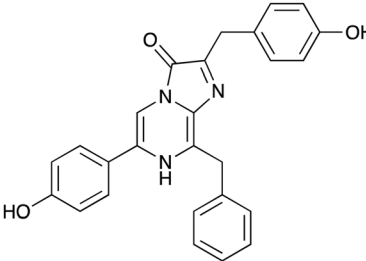
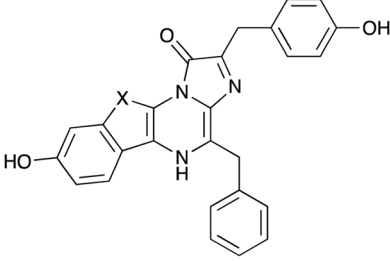
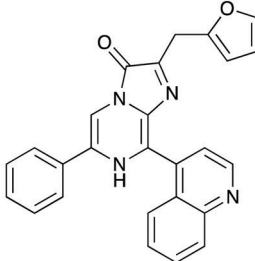
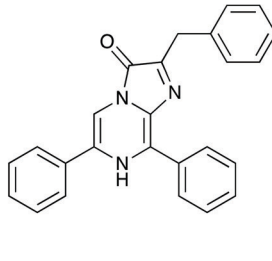
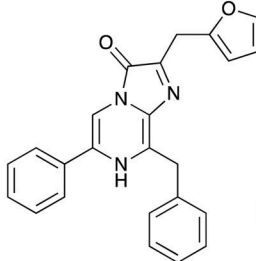
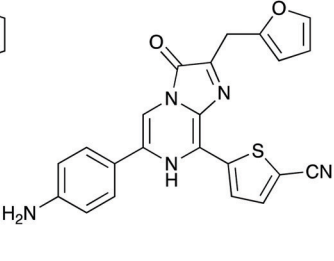
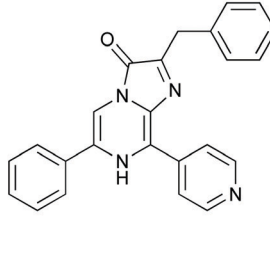
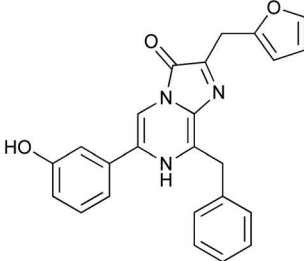
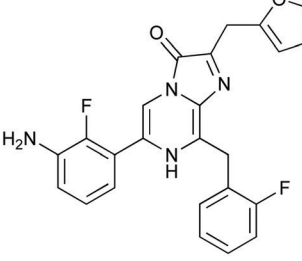
Following the development of Nluc, there were reports of chimeric proteins that use Nluc as the BRET donor together with a fluorescent protein as the BRET acceptor. For example, the LumiFluor series was developed by creating chimeras of Nluc with bright, fluorescent proteins such as eGFP to get emission of around ~460–508 nm or with an orange light emitting GFP variant LSSmOrange for emission ~572 nm.<sup>177</sup> The LumiFluor series was shown to be useful in the *in vivo* imaging of tumours as well. In a complimentary approach to the development of Nano-lanterns, small-molecule fluorophores could also be appended to Nluc through the development of Nluc-Halotag fusion proteins.<sup>178,179</sup> BRET then occurs from the furimazine oxyluciferin to the fluorophore.

A number of coelenterazine analogues including **43** and **44** were reported by Shimomura *et al.* and these were tested against the wild-type luciferases that naturally utilise coelenterazine.<sup>180</sup> The analogue e-CTZ **43** was reported to be ~1.4 times brighter than CTZ 7 with Rluc and had a 7.5 times higher initial peak intensity than CTZ 7. This could potentially be due to the fact that this analogue is a conformationally restrained analogue of CTZ 7. The analogue v-CTZ **45** was reported to be 0.73 times brighter than CTZ 7 with Rluc but had a 6.4 times higher initial peak intensity than CTZ 7. It was also unsurprisingly more red-shifted than CTZ 7, possibly due to extended conjugation of the  $\pi$ -electron system. This led to an emission of  $\lambda_{max}$  ~ 512 nm. Both these analogues have been used with modified and optimised Rluc luciferase systems in the *in vivo* imaging of small mammals and are commercially available.<sup>181,182</sup>

Recently, some furimazine analogues such as **45** and **47** have been reported which have red-shifted emission with Nanoluc in the absence of any resonance transfer fluorophore.<sup>183</sup>



Table 6 Representative examples of synthetic coelenterazine analogues that have useful properties organised in increasing wavelength

$\lambda_{\max} < 460$ nm	Natural substrate	$\lambda_{\max} \sim 460$ –550 nm	
 <b>42 Fz</b> $(\lambda_{\max} \sim 456$ nm with NanoLuc) CAS Number = 1374040-24-0 	 <b>7 CTZ</b> $(\lambda_{\max} \sim 460$ nm with NanoLuc) CAS Number = 50909-86-9 	 <b>43 e-CTZ</b> X = CH <sub>2</sub> CH <sub>2</sub> $(\lambda_{\max} \sim 418/475$ nm with RLuc) CAS Number = 114496-02-5  <b>44 v-CTZ</b> X = CHCH $(\lambda_{\max} \sim 512$ nm with RLuc) CAS Number = 114496-03-6 	
$\lambda_{\max} \sim 550$ –600 nm  <b>45</b> $(\lambda_{\max} \sim 571$ nm with NanoLuc) 	 <b>46 DTZ</b> $(\lambda_{\max} \sim 583$ nm with Antares2) 	 <b>42 Fz</b> $(\lambda_{\max} \sim 589$ nm with Antares) CAS Number = 1374040-24-0 	 <b>47</b> $(\lambda_{\max} \sim 598$ nm with NanoLuc) 
$\lambda_{\max} \sim 600$ –650 nm  <b>48 8-PyDTZ</b> $(\lambda_{\max} \square 600$ nm with LumiScarlet) 	 <b>49 HFz</b> $(\lambda_{\max} \square 650$ nm with Antares) 	 <b>50 FFz</b> $(\lambda_{\max} \square 650$ nm with Antares) 	<div style="border: 1px solid black; padding: 5px;"> <p><b>Key</b></p> <p> <i>in vitro</i> measurements</p> <p> <i>in cellulo</i> measurements</p> <p> <i>in vivo</i> imaging in mouse models</p> </div>

However, these analogues were about  $10^2$ – $10^4$  times dimmer in *in vitro* assays than the Fz-Nanoluc combination. Consequently, Nanoluc was mutated further in attempts towards red-shifted emission. These attempts had limited success, with light emission being red-shifted only up to 509 nm which is still blueish-green light.<sup>184</sup> In an attempt to create bright and red-shifted reporters, Nanoluc was fused with CyOPF1, a bright, engineered, orange-red fluorescent protein that is excitable by

cyan light (497–523 nm), to develop a BRET-based genetically encoded reporter called Antares. The Fz-Antares combination was reported to be the brightest *in vitro* and *in vivo* when compared with D-luciferin-Fluc, Fz-Nanoluc and Fz-Orange Nanoluc combinations.<sup>185</sup>

Building on from this work, Ai *et al.* created another fusion protein Antares2 in which random mutations were introduced in NanoLuc across the gene using error-prone PCR.<sup>184</sup> From this,



they identified a Nanoluc mutant (Nanoluc-D19S/D85N/C164H) with a 5.7-fold enhancement of DTZ bioluminescence and named it teLuc as it gave teal coloured emission ( $\lambda_{\text{max}} \sim 502$  nm). The teLuc fusion with CyOFP1 was named Antares2. This BRET based reporter utilised DTZ **46** rather than Fz **42** and emitted 3.8 times more photons above 600 nm than Antares. Although this analogue is reported to be brighter than D-luciferin **1** and Akalumine **33** *in vitro*, it suffers from poor solubility in aqueous media and poor stability as like all coelenterazine analogues it is prone to auto-oxidation. This makes *in vivo* studies particularly challenging. In order to address these challenges, Ai *et al.* reported a number of pyridyl analogues of DTZ **46** including 8-pyDTZ **48** that had  $\sim 13$  times better aqueous solubility and bioavailability than DTZ **46**.<sup>186</sup> In their work they reported the development of a teLuc mutant called LumiLuc which was through a series of error-prone PCR experiments on teLuc resulting in a total of 12 mutations, The emission from 8-pyDTZ/LumiLuc was  $\sim 5$  times brighter than 8-pyDTZ/teLuc and had emission around  $\lambda_{\text{max}} \sim 525$  nm. LumiLuc was then fused to a fluorescent protein mScarlet-I to form LumiScarlet which was useful in BRET based BLI and had emission around  $\lambda_{\text{max}} \sim 600$  nm. The emission from 8-pyDTZ/LumiScarlet in *in vivo* imaging was reported to be comparable to that by Akalumine/Akaluc.

Two new substrates hydrofurimazine **49** (HFz) and fluorofurimazine **50** (FFz) were also reported recently to address the challenges of solubility and bioavailability in coelenterazine analogues. The analogue HFz **49** exhibited similar brightness to AkaLuc with its substrate Akalumine **33**, whilst a second substrate, FFz **50** with even higher brightness *in vivo*. The FFz-Antares combination was used to track tumour size *in vivo* whilst Akalumine-AkaLuc combination was used to visualise CAR-T cells within the same mice.<sup>187</sup>

### 3.3 Bacterial bioluminescence

Several site-directed mutagenesis studies and some random-mutagenesis studies have been carried out on the bacterial luciferase system. However, most of these mutations have resulted in reduced activity, poorer quantum yield and have primarily served the purpose of improving our understanding of the nature of and the key residues in bacterial luciferase.<sup>188–192</sup> A select few of these studies have resulted in altered properties of the bioluminescent system that could potentially be of use in applications. For example, an E175G mutation to the  $\alpha$ -subunit of *X. luminescens* luciferase using random mutagenesis, resulted in faster kinetics and a faster decline in peak height, which could be useful in certain applications.<sup>193</sup> Moreover, a number of red-shifted, mutant bacterial luciferases from *Vibrio harveyi* were reported.<sup>194</sup> The mutant  $\alpha$ A75G/C106V/V173A was reported to emit at 505 nm whilst the mutant  $\alpha$ A75G/C106V/V173S emitted at 510 nm. However, both these systems were 80–90% dimmer than the wildtype system. Hence, they are too dim to be useful in *in vivo* imaging and would need substantial optimisation to make them more useful.

A breakthrough in this area was reported by Gregor, Hell and co-workers, who engineered the *ilux* operon.<sup>195</sup> Prior to their

work, bacterial bioluminescence resulted in a weakly auto-luminescent mammalian cell line.<sup>116</sup> Hell and co-workers chose the *luxCDABE* operon from *P. luminescens* due to its thermostability and systematically carried out studies to identify the cause of poor luminescence in mammalian cells. This led to codon optimisation and enzyme engineering, including supplementing the FMN reductase in *P. luminescens* with that from *V. campbellii* followed by error-prone PCR to select brighter mutants. The final result *ilux* contains a total of at least 15 mutations and around 8 times brighter than the original construct allowing single-cell imaging of bacterial cells for extended periods of time *in vitro*.<sup>195</sup> This work was then further developed by codon optimisation of *ilux* for mammalian cells, which led to brighter emission by around 3 orders of magnitude compared to previous approaches. The light output was also reported to be comparable to that of a D-luciferin/Fluc system in HeLa cells.

## 4. Applications

### 4.1 ATP sensing

ATP is the energy currency in living cells and found in virtually all prokaryotic and eukaryotic cells. As Mg-ATP is a necessary co-factor in the mechanism of firefly bioluminescence, the firefly luciferase and D-luciferin system has been adapted into a variety of assays for ATP detection with different detection limit levels for ATP. Luciferase reagent preparations and their delivery devices for ATP detection vary from supplier to supplier and are optimised for each system. Each reagent system is a balanced cocktail of enzyme, co-factors, buffer and extractants.<sup>196</sup>

Once the reagents are mixed at 25 °C, there is a 0.25 ms time lag until light emission is observed after which light output peaks at around 300 ms. This is followed by a rapid decay in light output and then finally slow, sustained light emission.<sup>197</sup> This phenomenon is known as 'burst kinetics' and the decay in light output is thought to be due to inactivation of the enzyme or if a significant proportion of the substrates D-luciferin and ATP are consumed per minute in the reaction, when their concentration is low compared to that of the luciferase.<sup>42</sup> Inactivation of the luciferase can occur if the luciferase is bound to surfaces or there is a significant concentration of an inhibitor such as oxyluciferin – the product of the reaction, or contaminants in the D-luciferin preparation such as L-luciferin and dehydroxyluciferin. Inactivation of the enzyme can be counteracted by using a highly pure D-luciferin sample to avoid contaminants, and by the addition of stabilising substances such as bovine serum albumin (BSA), neutral detergents and osmolytes for the protein, so that stable light output is obtained.<sup>198</sup> In most ATP sensing assays, a fixed amount of D-luciferin is added to the assay mixture, which is in excess of ATP levels. At high luciferase concentrations, the peak light output is proportional to the amount of luciferase, as ATP is depleted in a first-order reaction. When luciferase concentration is low, ATP is slowly depleted and so light emission is stable and proportional to the ATP concentration, when the ATP concentration is significantly



below the  $K_m$  of the enzyme *i.e.*  $ATP < 0.1 \text{ mM L}^{-1}$ , as the rate of reaction and hence light output are proportional to the ATP concentration below  $K_m$ .<sup>48</sup> This is useful to monitor ATP forming and ATP degrading reactions including kinetic and end-point assays of enzymes and metabolites.<sup>42,48,199</sup>

Through the careful manipulation of all of these factors, a series of ATP-bioluminescence reagents have been made commercially available as simple-to-use kits which include the luciferin and luciferase preparations. These reagents are of two main types based on the intensity and duration of light-emission. Constant light emitting reagents have moderate sensitivity towards ATP (working range:  $10^{-6}$  to  $10^{-11}$  M ATP). The constant light signal is useful for kinetic studies of enzymes and metabolic studies, or if coupled enzymatic assays are applied. Such assays have been used to determine the amount of ATP in various diseased and healthy cell lines using both lysed human HeLa cells, mouse MEF cells and in worms such as the round worm, as well as intact cells or isolated mitochondria.<sup>200–203</sup> This type of reagent can also be used to determine the activity of enzymes such as the activity of  $H^+$ -ATP synthase from live isolated mitochondria.<sup>204</sup>

The second type of ATP-bioluminescence reagents are high sensitivity light emitting reagents. These have a higher concentration of luciferase and exploit the 'burst kinetics' phenomenon where the peak height is proportional to the amount of ATP in the sample and dependent on the concentration of luciferase. These reagent combinations have higher sensitivity towards ATP (working range:  $10^{-5}$  to  $10^{-12}$  M ATP), although reagents that report even lower detection limits are available in the market. These reagents are often sold packaged with cell lysis reagents, and are suitable for use in luminometers where automatic injection of the reagents is possible such as in

tube luminometers and microplate luminometers (Table S1, ESI†).<sup>48</sup>

It is important to note that different types of cells have varying levels of ATP. For example, bacteria have lower levels of ATP compared to fungi or mammalian cells.<sup>48</sup> It is important to pre-treat the sample effectively, and to use aseptic conditions to ensure that ATP levels from the correct desired source are detected. For example, a clinical urine sample may contain 3 different pools of ATP – extracellular ATP, ATP in mammalian cells, and ATP in bacterial cells and the purpose of an ATP bioluminescence measurement might be to estimate bacterial levels. The level of ATP from all 3 sources can be detected by using an appropriate kit containing ATP-degrading enzyme, neutral detergent, strong extractant, ATP reagent, and ATP standard (Fig. 5 and Table S1, ESI†).<sup>48</sup>

Recently, there have been developments in luciferase engineering that allow ATP bioluminescence technology to reach uncharted territories. For example, Branchini *et al.* reported a red-emitting chimeric firefly luciferase that has a low  $K_m$  for ATP and D-luciferin and would reach half of the maximum rate of the bioluminescence reaction at lower levels of ATP and D-luciferin than the wild-type enzyme making it suitable for *in vivo* imaging in low ATP cellular environments.<sup>205</sup> Moreover Pinton *et al.* reported protocols for the *in cellulo* and *in vivo* the use of chimeric luciferases that ensure the specific cellular localisation of the luciferase in a cell *i.e.* in the mitochondrial matrix and the outer surface of the plasma membrane to determine the ATP concentration in those areas.<sup>206</sup> Viviani and co-workers also reported a blue-shifted luciferase that has the lowest reported  $K_m$  for ATP, highest catalytic efficiency, and thermal stability among beetle luciferases that was suitable for ratiometric ATP, metal and pH biosensing assays.<sup>207</sup>

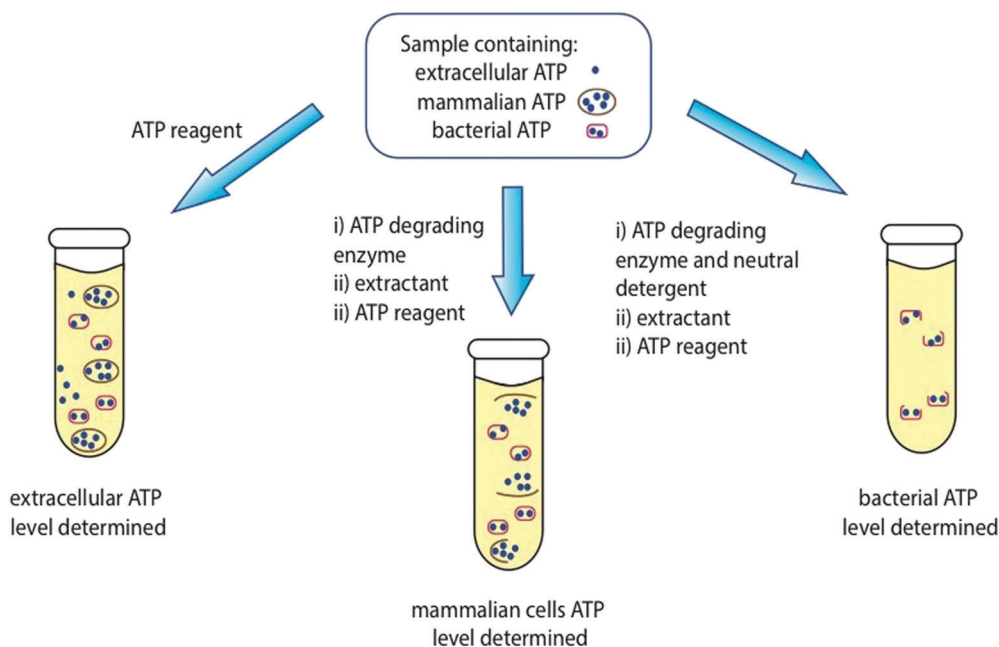


Fig. 5 Determination of ATP levels in a sample containing extracellular ATP, mammalian cell ATP and bacterial ATP. Table S1 in the ESI† contains a list of commercially available ATP reagents and their details.



Metal sensing bioluminescence assays are covered in greater detail in Section 4.3, while pH sensing assays are covered in Section 4.5. There have also been advances in the development of more sensitive and portable luminometers and sensing devices.<sup>208,209</sup> More recently, Roda and co-workers reported a low-cost wax-printed nitrocellulose paper biosensor that immobilised luciferase/luciferin reagents, and whose light signal could be detected and analysed by a smart phone to detect *E. coli* levels in urine samples.<sup>210</sup> This low-cost, readily available technology would be ideal for use in developing countries where access to a luminometer and other specialist kit would be limited.

#### 4.2 Hygiene control

Bioluminescence based sensing technology has been of great use in hygiene control for several decades now. In particular the ATP-bioluminescence assay based on the firefly bioluminescence system is routinely used to monitor the cleanliness of surfaces in healthcare facilities such as hospitals and clinics and in the dairy and meat processing industries.<sup>211,212</sup> This is the technique of choice when the speed and ease of analysis are of vital importance as alternative methods such as culturing or microorganisms usually take days to offer results, whilst techniques based on fluorescence need an external light source for excitation and do not discriminate between living and dead cells.<sup>213</sup> Bacterial bioluminescence is also used in the food industry to monitor the behaviour of *Lux*-tagged bacteria *in situ* in complex food systems, for problem-solving and for the development of modified and improved processing and storage purposes as discussed further below (Fig. 6).<sup>214</sup>

Several studies have been reported on the use of swab taking and ATP bioluminescence as a quick and objective way of monitoring the cleanliness of hospital surfaces, including those of large objects such as tables and benches and small pieces of equipment such as tweezers and other kit. Swabs that are impregnated with buffer are often commercially available as part of ATP-bioluminescence kits. These are used to sample surfaces, and then processed with the ATP-bioluminescence reagent in a portable luminometer. The swabs and portable luminometer are often sold from the same supplier and complement each other. However, this technique is still poorly

standardised at an international level and the difference in kit and reagents used in different studies is one reason why significant differences in ATP levels are reported.<sup>215,216</sup> Despite these limitations over the comparability of results, ATP bioluminescence remains a quick and cost-effective measure for surface cleanliness and hygiene control in hospitals and routinely informs the cleaning practices of housekeeping and healthcare staff.<sup>217</sup> More recently these assays have been used to monitor the cleanliness of not just surfaces but surgical instruments and dentures as well.<sup>218,219</sup>

ATP bioluminescence measurements are routinely used to monitor quality control and hygiene in the food industry.<sup>212</sup> In particular, fish processing plants have used it for decades to determine contamination levels.<sup>220</sup> Recently a study was reported to determine the contamination levels in various fish processing environments *i.e.* different lines of production including different fish types such as trout and cod, different types of meat such as protein-rich loin meat or fat-rich belly meat and different levels of processing such as slaughtered or cooked products, and the results were compared against conventional culture and plating techniques.<sup>221</sup> It was established that it is essential to set up critical limits after a period of validation and calibration that are specific to each processing plant, type of ATP-bioluminescence kit used, specific areas, types of fish and fish meat and different hygiene zones, to obtain more robust, consistent and meaningful results. The dairy industry also benefits greatly from ATP bioluminescence assays as these are used to determine the quality of milk by selectively measuring the ATP from somatic cells and milk spoilage by determining ATP levels from bacteria and other microorganisms both before and after UHT treatment to estimate shelf life.<sup>222</sup>

The *lux* operon which is responsible for bacterial bioluminescence has also found great utility in the food industry.<sup>214</sup> The *lux* genes responsible for bioluminescence can be genetically encoded onto bacteria that are not naturally bioluminescent, and the localisation, population size and environment of these bacteria can be monitored in real time. As all known bioluminescent bacteria are Gram-negative, there were initial challenges in obtaining a good level of light output and gene expression in Gram positive bacteria. However, this was overcome by introducing translational

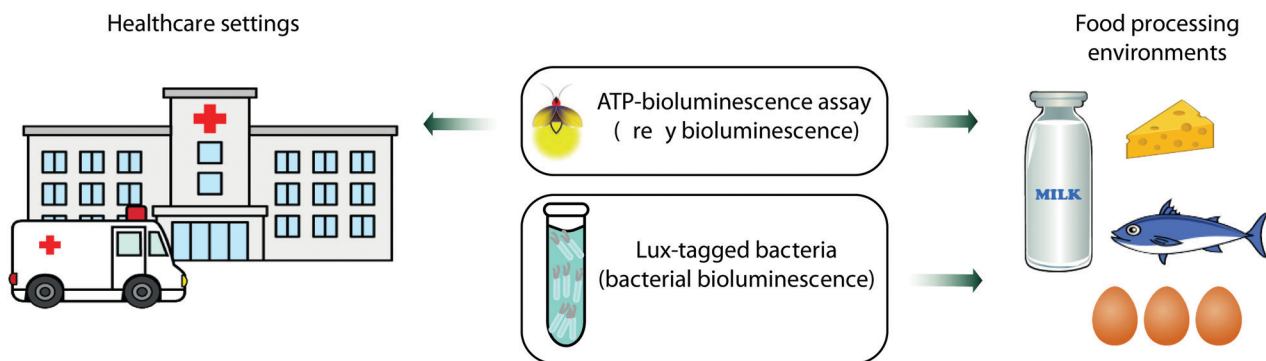


Fig. 6 ATP-bioluminescence assays are used for hygiene control in several settings and industries including healthcare and food processing plants, whereas *Lux*-tagged bacterial bioluminescence is used to develop improved hygiene practices in the food industry.



signals optimized for Gram positive bacteria in front of *luxA*, *luxC* and *luxE* genes.<sup>223,224</sup> To date bioluminescent *E. coli* and *Listeria* have been used to monitor the survival of these bacteria post-processing in yoghurt and cheese.<sup>225</sup> A number of *lux*-tagged bacteria such as *Campylobacter jejuni* and *Salmonella enteritidis* have also been used to determine egg-shell penetration and colonisation.<sup>225,226</sup> *Lux*-tagged bacteria have also been used to monitor the development of bacterial infection in plant seedlings so interventions can be made at the appropriate time.<sup>227</sup> The *lux*-based gene expression system has also been fused to genes of bacterial toxin production such as the promoter of the cereulide toxin gene *ces* in *B. cereus* to determine the ability of various foods to support toxin formation.<sup>228</sup> *Lux*-tagged bacteria have been administered to mice for *in vivo* imaging of the resultant developing bacterial infection – for example *lux*-tagged *L. monocytogenes* were shown to grow and localise in the gallbladder of mice and cause re-infection in the intestines when bile was released.<sup>229</sup> However, as bacterial bioluminescence emits predominantly blue light which is strongly absorbed by blood and tissue, it is important to do *ex vivo* analysis of the organs as well to ensure bacterial colonies are not missed. Another use of *lux*-tagged bacteria has also been to detect biofilms and to develop cleaning methods against them, as well as to test the efficacy of hand sanitisers and disinfectants. As well as monitoring the growth and development of pathogenic bacteria, *lux*-tagged probiotic bacteria can also be monitored in foods that contain them as well as tracking the bacteria using *in vivo* imaging to understand their lifecycle and environment.<sup>230,231</sup>

### 4.3 Mapping pollution in ecosystems

The most widely used bioluminescence sensors in the toxicology monitoring of ecosystems are whole-cell bacterial bioluminescence sensors.<sup>232</sup> Like most bioluminescence-based assays, these sensors provide a quick result to help assess toxicity levels. Other protocols for measuring environmental toxicity often involve exposing test organisms, such as fish, crustaceans, plants or bacteria to environmental samples and to monitor survivorship. The benefit of bioluminescent bacteria is that their light output can be used as a quick measure of survival. Moreover, their bioluminescence is directly linked to their respiratory chain and so any toxin that interferes with their respiratory chain, interferes with the light output.<sup>233</sup> These sensors have been used to monitor a wide variety of contaminants including both heavy metal contaminants and organic compounds such as toluene and naphthalene.

If the *lux* gene is expressed continuously, luciferase and luciferin will be formed continuously and the baseline light intensity would change on addition of the target analyte, depending on how well the bacterial cell survives. Alternatively, the *lux* gene can be controlled in an inducible manner wherein it would be fused to a promoter that is regulated by the compound of interest. In this case, the concentration of the compound can be quantitatively detected by measuring the bioluminescence intensity.<sup>118</sup> Previously bacterial bioluminescence sensors were reported to analyse a variety of analytes including zinc, bioavailable toluene and uranium.<sup>234–236</sup> Some recent examples in the development of bacterial bioluminescence biosensors to detect various analytes of ecotoxicology interest can be seen below (Table 7). Like most assays, careful pre-treatment of the sample to eliminate interference causing agents is essential to get meaningful results.

The other common application of bioluminescence in ecotoxicology and pollutant monitoring is ATP quantification using the firefly bioluminescence ATP assay in both aquatic environments and bioaerosols in the atmosphere. ATP bioluminescence-based sensors have been used to determine the total ATP in water bodies including ocean environments and drinking water up to a detection limit of  $1.1 \times 10^{-11}$  M.<sup>244,245</sup> This would include ATP from not just bacteria but also fungal cells and any parasitic protozoa. ATP bioluminescence-based sensors have also been used to detect the location and density of several air-borne bacteria in both artificially created and natural bioaerosols in indoor environments.<sup>246</sup> The biosensors reported have either used fabricated paper disks immobilised with luciferase/*D*-luciferin or sensors microfluidic chips.<sup>247,248</sup> Air was vented into and bubbled into a bio-sampler bottle containing 20 mL of deionised water to capture any cells found in the air. This solution was then concentrated and heated to lyse the cells. This lysate was then dripped on the fabricated paper disks immobilised with luciferase/*D*-luciferin. The fabricated paper disks with immobilised with luciferase/*D*-luciferin were reported to have up to 10 times longer shelf-life compared to the liquid assay reagents when stored at room temperature.<sup>247</sup> Although this is a quick method to identify air-borne bacteria and their levels in studies where the identity of the bacterium is known *i.e.* artificially created bioaerosols, it is important to calibrate the assay effectively with known samples and use the ATP bioluminescence assay together with another assay to validate the results.<sup>249–251</sup>

### 4.4 Culture and heritage – preservation of art work

The ATP bioluminescence assay from the firefly has also been adapted to take surface measurements of ATP from old artwork

Table 7 Recent examples of the use of bacterial bioluminescence biosensors to detect various analytes in ecotoxicology

Target	Microorganisms	Detection limit	Ref.
Common antibiotics	<i>Bacillus</i> WT and <i>E. coli</i> FhuAT	0.043–324 mg L <sup>-1</sup>	Jonkers <i>et al.</i> <sup>237</sup>
Mercury	<i>P. leiognathi</i>	9.87 mg L <sup>-1</sup>	Kassim <i>et al.</i> <sup>238</sup>
Chlorine	<i>E. coli</i> mutants	1 mg L <sup>-1</sup>	Borisover <i>et al.</i> <sup>239</sup>
PyC <sub>12</sub> Phe (ionic liquid)	<i>Vibrio fischeri</i>	4.17 mg L <sup>-1</sup>	Kahru <i>et al.</i> <sup>240</sup>
Sucralose (sweetener)	<i>E. coli</i> mutants	1 g L <sup>-1</sup>	Harpaz <i>et al.</i> <sup>241</sup>
Terbutryn (herbicide)	<i>Aliivibrio fischeri</i>	81 mg L <sup>-1</sup>	Conrad <i>et al.</i> <sup>242</sup>
Arsenite	<i>E. coli</i>	39.6 mg L <sup>-1</sup>	Ginet <i>et al.</i> <sup>243</sup>



to estimate bacterial, fungal, yeast, algae and lichen levels in antique work for the purposes of cultural and historic preservation.<sup>252</sup> A bioluminescence low-light imaging technique was reported that was used on artwork consisting of paper, stone, fibre and wood.<sup>253,254</sup> All reagents were applied directly to the samples and the conditions were optimised for sample geometry and surface conditions. More recently, the level of the microbial contamination of the seventeenth-century wall paintings in the nave of the old Church of the Holy Ascension (Veliki Krcimir, Serbia) was evaluated using the ATP bioluminescence method, and traditional cultivation-based method, using dip slides that were commercially available.<sup>255</sup> It was established that ATP bioluminescence measurements can be a quick way to determine 'hot spots' of contamination on the art-work, allowing a quick assessment of areas that require greater concern.

#### 4.5 Sensing of pH, metal ions, reactive oxygen species (ROS), enzymes, drug molecules, and membrane potential including *in cellulo* applications

As the light output in bioluminescent reactions is dependent on the conditions of the assay *in vitro* or *in vivo*, it has been modified and adapted to be able sense various parameters such as pH, concentrations of metal ions, glucose, reactive oxygen species, enzymes and drug molecules. These sensing applications can use either modified luciferins such as caged luciferin

structures or modified luciferases that are conjugated with sensing domains in a form of activity-based sensing (ABS) where the optical signal output is dependent on the intrinsic chemical activity of the bio-analyte in question with either the sensing domain of the luciferase or the caged-luciferin.

**Luciferin based sensors.** In the area of luciferin based sensors for specific sensing applications, caged luciferins are the most common and well-known.<sup>256</sup> In a caged-luciferin, one of the key functional groups, is masked in some way and then it is modified or revealed by external conditions that are then detected by bioluminescence. The masked key functional group is often the electron-donating -NHR or OH at the 6-position of the benzothiazole, but in some cases the carboxylic acid in D-luciferin was the group that was masked. These are often designed and used as turn-on probes in which the bioanalyte in question uncages the luciferin and the light output is triggered in the presence of the bioanalyte (Fig. 7). There are fewer examples of caged-coelenterazine probes, probably due to the fact that the auto-oxidation of coelenterazine analogues make them more difficult to manipulate and handle synthetically. The reported caged-CTZ probes usually have the C-3 carbonyl of coelenterazine caged by the analyte of interest. Such probes have been reported to measure  $\beta$ -galactosidase activity,<sup>257</sup> for the detection of thiophenols,<sup>258</sup> and for the targeting and detection of biothiols such as cysteine, glutathione and

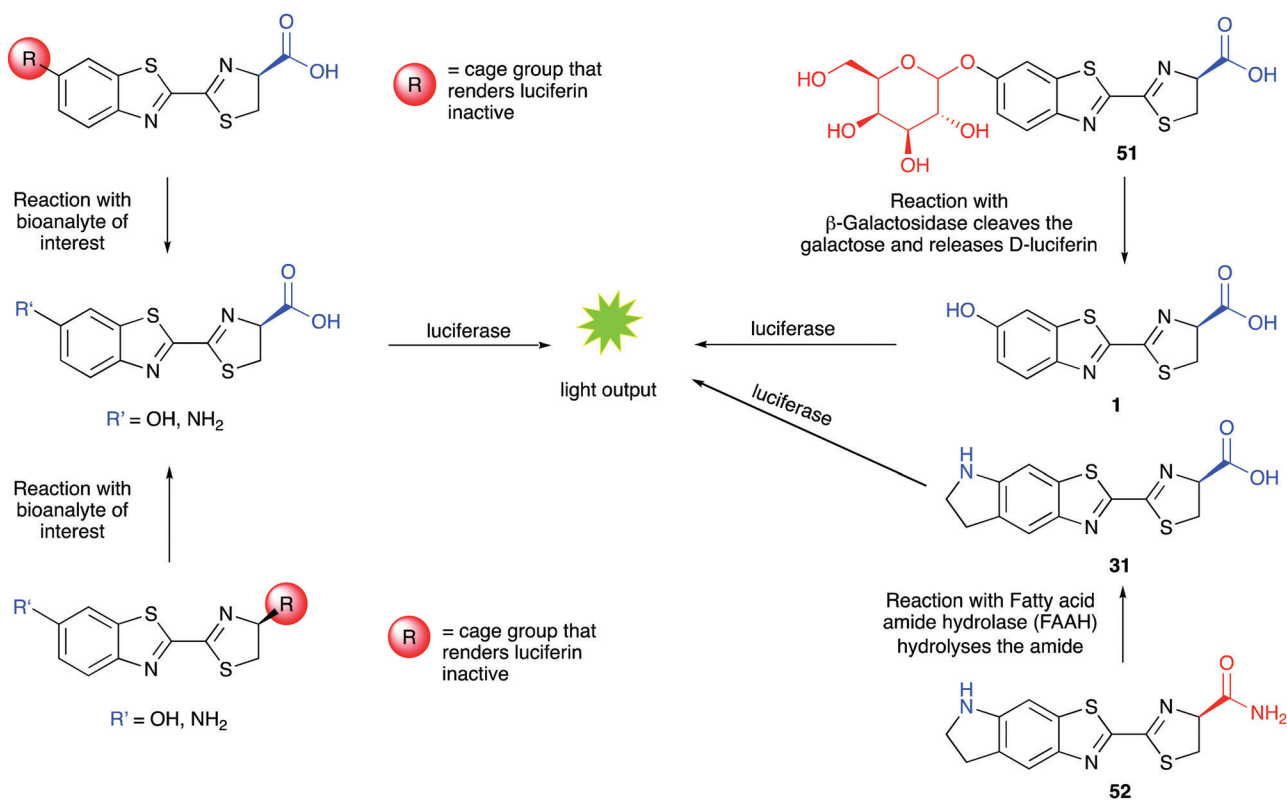


Fig. 7 Caged luciferins – left hand side – a general scheme showing the 2 common sites of caging in red. Uncaging of the luciferin occurs in the presence of the bioanalyte of interest and the uncaged luciferin reacts with luciferase to emit light. A turn-on response is obtained in the presence of the analyte of interest. Right hand side – specific examples of caged-luciferin probes from the literature. Probe **51** was reported to measure  $\beta$ -galactosidase activity<sup>261</sup> and probe **52** was reported to measure the activity of Fatty acid amide hydrolase.<sup>262</sup>



homocysteine.<sup>259</sup> A number of caged-CTZ probes were also included as glycosidase inhibitors in a patent by the Promega corporation.<sup>260</sup>

Caged D-luciferin probes have been used as sensors for enzyme activity,<sup>262–269</sup> small molecule sensors for molecules such as glycans,<sup>270</sup> hydrogen sulphide,<sup>271</sup> hypochlorous acid,<sup>272</sup> carbon monoxide<sup>273,274</sup> and hydrogen peroxide,<sup>275</sup> and sensors for metal ions such as copper,<sup>276</sup> iron,<sup>277,278</sup> and cobalt.<sup>279</sup> The benefit of bioluminescence is that no incident light is needed and so the signal to noise ratio is higher and therefore more accurate. Although a potential drawback of these bioluminescence-based probes compared to similar fluorescent probes is that the bioluminescent probes are administered in much higher concentrations in cell-based assays than fluorescent probes, and this might affect the physiological conditions of the cells. Nonetheless, several caged-luciferins have been successfully used for *in vivo* imaging of mice and there has been an excellent recent review covering the advances in this area.<sup>280</sup> Moreover, the first example of a bioluminescent probe that can measure mitochondrial membrane potential in a non-invasive manner *in vivo* has just been reported to be a caged luciferin probe that called a 'mitochondria-activatable luciferin' (MAL probe) (Fig. 8). The MAL probe is uncaged by a bioorthogonal Staudinger reaction with an organic azide (Azido-TPP1), to release a functional luciferin, which will emit light in the presence of luciferase. The triphenylphosphonium (TPP) groups on both the organic azide and the caged luciferin directs both reagents to the mitochondria. The rate of uncaging and hence rate of formation of active luciferin is proportional to the combined changes in mitochondrial membrane potential and plasma membrane potential.<sup>281</sup>

The other type of luciferin probes that have been reported are designed to use the Bioluminescent Enzyme-Induced Electron Transfer (BioLeT) process to modify the light output generated. Bioluminescent Enzyme-Induced Electron Transfer (BioLeT) is analogous to photoinduced electron transfer (PeT) which has often been incorporated in the design of fluorescent probes.<sup>282,283</sup> The design concept is that the singlet excited-state oxyluciferin species can be quenched by the electron transfer from the highest energy molecular orbital (HOMO) of an electron rich benzene moiety in close proximity. This was first reported in the design of a sensor for nitric oxide (NO), which is very dim in the absence of NO, due to BioLeT, but significantly brighter in the presence of NO, due to the absence of the electron-donating moiety (Fig. 9).<sup>284</sup> This work also reported the successful use of this probe *in vivo* mice models. The authors have also reported another BioLeT probe with turn-on luminescence that detect highly reactive oxygen species.<sup>285</sup>

**Luciferase based sensors.** A smaller number of modified firefly luciferases have also been reported for the ratiometric analysis and detection of pH, metal ions and reactive oxygen species (ROS). Viviani and co-workers reported a technique to estimate the intracellular pH in *E. coli* using mutant firefly luciferases,<sup>164</sup> as well as a mutant firefly luciferase for ratiometric pH sensing and the selective detection of cadmium.<sup>207</sup> A genetically encoded pH sensitive reporter has also been recently reported that consists of a pH-sensitive GFP (*super-ecliptic pHluorin*) that emits at 510 nm, and a pH-stable luciferase Antares that emits at 580 nm. On the addition of furimazine, a ratiometric readout  $R_{580/510}$  was indicative of pH and this system was shown to be functional both *in vitro* and *in vivo* using xenograft murine tumours to detect

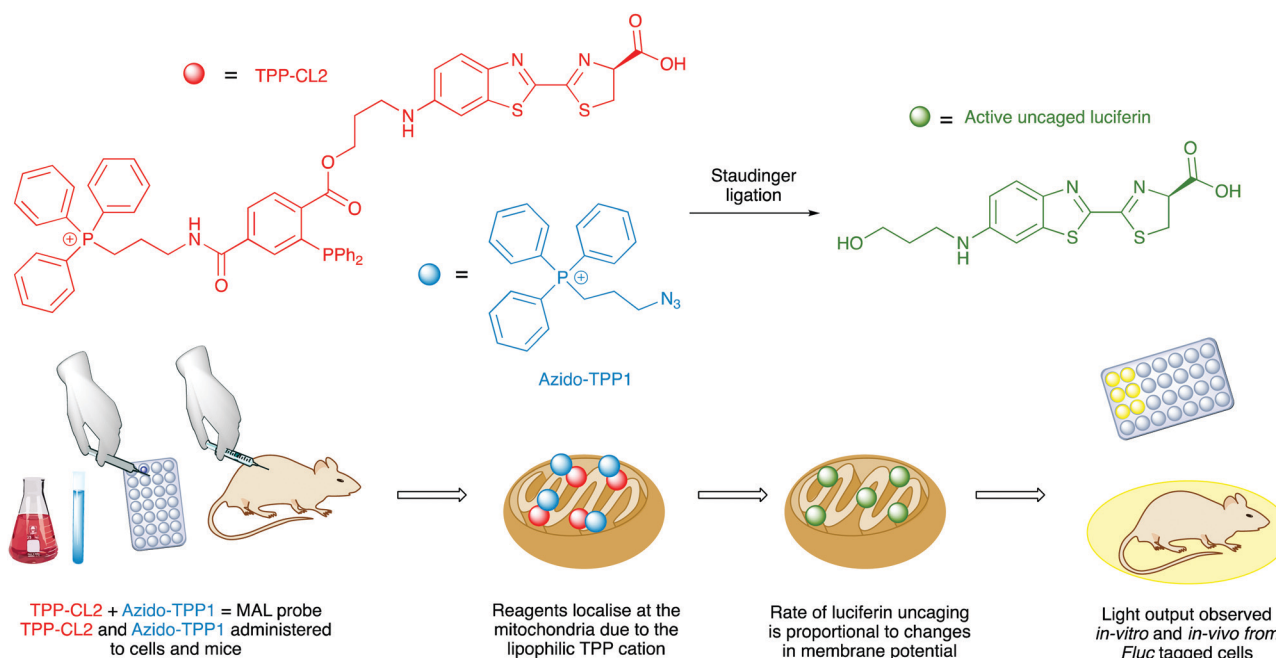


Fig. 8 The design and functioning workflow of the mitochondria-activatable luciferin probe.



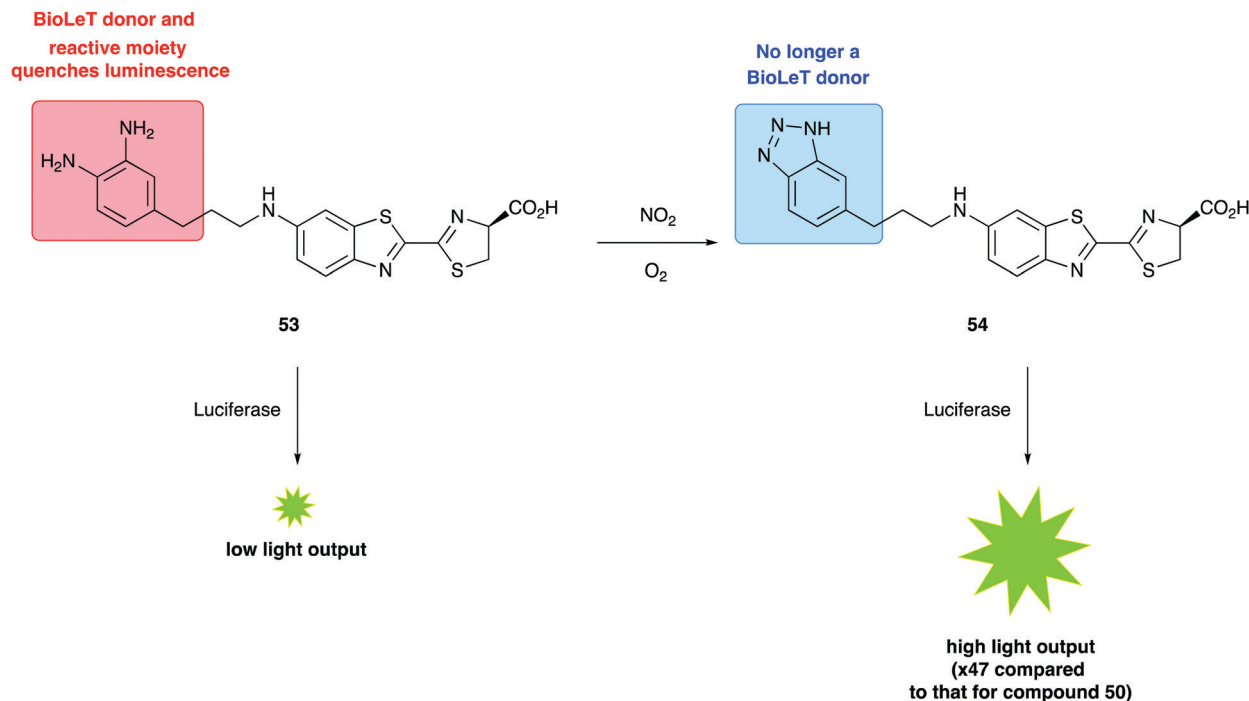


Fig. 9 The use of a BioLeT probe to detect the presence of nitric oxide.<sup>285</sup> The BioLeT donor has a high energy HOMO that is capable of donating an electron to the singlet excited state oxyluciferin.

acidosis.<sup>286</sup> A genetically encoded calcium ion indicator (GECI) was also reported in which Nanoluc was fused on the N terminus of the  $\text{Ca}^{2+}$  sensitive GCaMP6s protein. The blue light from the reaction of Nanoluc with furimazine was used as an excitation source for the fluorescent GCaMP6s protein. In the presence of  $\text{Ca}^{2+}$ , the GCaMP6s was in the correct conformation to receive this blue excitation light and emit yellow-green light as a sign of  $\text{Ca}^{2+}$  ion signalling.<sup>287</sup>

The Nano-lantern developed by Nagai *et al.* (Section 3.2) were also developed further in the same piece of work to detect ATP concentration.<sup>170</sup> A chimeric fusion protein of the Nano-lantern with a subunit of bacterial  $\text{F}_0\text{F}_1$ -ATP synthase led to the development of Nano-lantern (ATP1) which exhibited an increase in light output on the addition of ATP with a  $K_d$  of 0.3 mM. This was then used to visualise ATP formation in chloroplasts.<sup>170</sup> A number of Nano-lantern based GECIs were also developed by genetically engineering the Nano-lantern probe with a calcium-sensing domain from an established fluorescent  $\text{Ca}^{2+}$  sensor to form Nano-lantern ( $\text{Ca}^{2+}$ ) which gave comparable output and sensitivity to the fluorescent, genetically encoded  $\text{Ca}^{2+}$  sensor it was developed from.<sup>170</sup>

Another important class of luciferase-based sensors are the luciferase-based indicators of drugs (LUCIDs) developed by Johnsson and co-workers.<sup>288</sup> These are semisynthetic bioluminescent sensor proteins that consist of three components: a receptor protein for the drug of interest covalently linked to a luciferase (Nluc), which is linked to a self-labelling protein such as SNAP-tag (Fig. 10A). The self-labelling protein was further linked to a synthetic molecule that consists of a fluorophore that can accept BRET from the luciferin–luciferase reaction and

a ligand for the receptor protein. Binding of the protein with the ligand, lead to close proximity of the Nluc with the fluorophore and red-shifted emission due to BRET. In the presence of a drug molecule, this interaction is perturbed and hence a measure of the ratio of blue light/red light leads to a measure of drug concentration. LUCIDs were shown capable of detecting both small-molecule drugs and larger peptidic and macrocyclic drugs as well. The LUCIB and analytes were spotted on filter paper and the light output measured using a digital camera making them useful candidates for point-of-care diagnostics. Later Johnsson and co-workers reported the use of antibodies in place of the receptor protein to make the technology more easily accessible.<sup>289</sup>

A number of BRET-based antibody sensors have also been reported. Merckx and co-workers reported a luminescent antibody sensing (LUMABS) technology to detect antibodies in blood plasma.<sup>290</sup> In these single protein sensors Nluc is connected to a green fluorescent protein mNeonGreen *via* a semiflexible linker and two antibody binding epitopes. A helper domain is found on each protein that keep both them in close contact to allow efficient BRET in the absence of an antibody (Fig. 10B). When an antibody binds to the sensing domain, the close proximity of the two light emitting proteins is disrupted leading to loss of BRET. A measure of this signal allows a ratiometric measure of antibody concentration. Initially this assay was optimised to a 384 well plate and the light output measured using a mobile phone. This technology has been further developed to enable identification of non-peptide epitopes,<sup>291</sup> optimised to use as a microfluidic paper-based analytical device,<sup>292</sup> and optimised further to require very small volumes



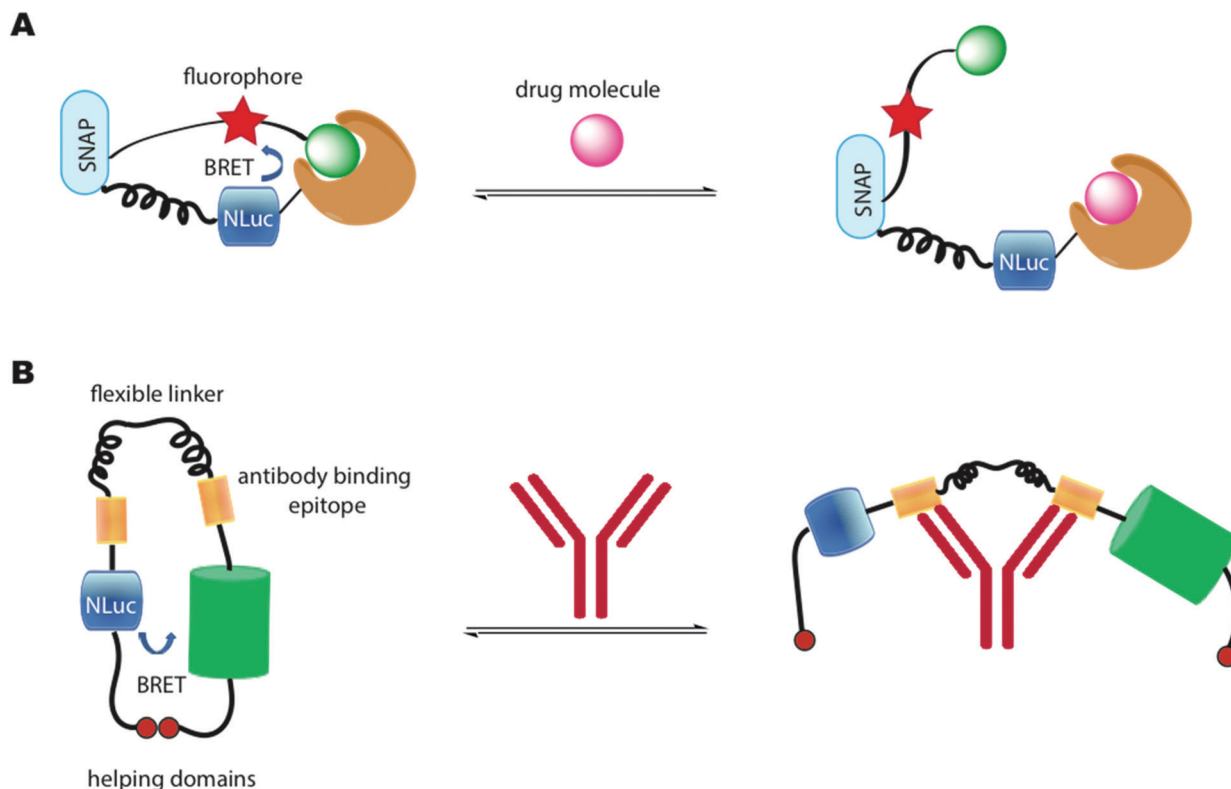


**Fig. 10** (A) LUCID developed by Johnsson and co-workers. BRET between NLuc and the fluorophore is disrupted in the presence of a drug molecule. (B) LUMABS developed by Merck and co-workers. BRET between NLuc and mNeonGreen is disrupted in the presence of an antibody.

of blood ( $\sim 5 \mu\text{L}$ ) by depositing the biological machinery on cotton threads.<sup>293</sup>

As discussed earlier, whole cell bioluminescent bacterial biosensors are widely used to detect heavy metal concentrations such as mercury, zinc and chromium in ecotoxicology studies.<sup>294–296</sup> For more details on this please refer to Section 4.3.

#### 4.6 Gene assays

A number of gene and DNA based assays have been reported that use a bioluminescence-based readout to detect various analyte levels. For example, Christopoulos and co-workers reported some of the earliest work in this area, utilising either Aequorin as the photoprotein,<sup>297</sup> or firefly luciferase.<sup>298</sup> This expression immunoassay used a Fluc coding DNA fragment as a label, and reported the limit of detection of prostate specific antigen (PSA) as low as 1 pM (Fig. 11).<sup>298</sup> The antigen was

isolated on polystyrene plates pre-coated with a suitable capture antibody. The captured antigen was then reacted with a biotinylated antibody. The biotin tag was then able to capture a streptavidin bound Fluc DNA tag. Transcription and translation of the Fluc DNA template resulted in 12–14 Fluc luciferase molecules per DNA tag bound to the plate. On addition of D-luciferin, the light output was proportional to the number of antigens bound. Recently, this limit of detection was improved to 0.007 pM by improving the number of enzyme molecules produced per DNA template by using a highly productive *E. coli* extract-based cell-free protein synthesis system.<sup>299</sup> A DNA hybridization assay based on similar principles, but to detect DNA instead using Fluc bioluminescence was also reported by Christopoulos and co-workers.<sup>300</sup>

One of the most common applications of Fluc and RLuc bioluminescence is their use as reporter genes for the study of

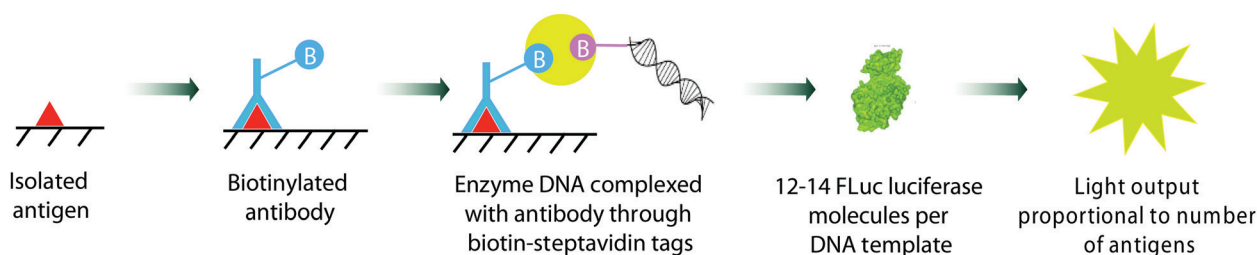


**Fig. 11** The gene expression immunoassay for detection of prostate specific antigen (PSA) reported by Christopoulos *et al.*<sup>264</sup>



gene expression in prokaryotic and eukaryotic cells and systems.<sup>301–304</sup> A notable recent and relevant example is the use of luciferase based assays to determine the infectivity of viruses such as the various coronaviruses in different host cell types.<sup>305,306</sup> Such an assay was also used to establish that SARS-Cov-2 coronavirus and a closely related RaTG13 coronavirus that was found in bats can both successfully infect human cells to produce daughter viruses (Fig. 12).<sup>307</sup> The interaction and binding of the spike glycoprotein in coronaviruses to the cell receptor Angiotensin-converting enzyme 2 (ACE2) in human cells is considered key in the entry of the viruses into human host cells.<sup>308</sup> Plasmids containing the genes for Fluc and the genes for the spike protein from the coronavirus strain of interest were co-transfected into host cells and incubated for 72 h. The pseudoviruses formed after this period were collected and these pseudoviruses would have the desired spike-protein on their surface and the genetic material encoding for Fluc inside of them. These pseudoviruses were then incubated with ACE-2 expressing human cells for 60 h. If the viruses are successfully able to infect the human cells, daughter viruses and Fluc would be produced. On addition of D-luciferin, the light output would be a measure of infectivity.

There has also been a report of the blue light from a Nanoluc-furimazine reaction being used to activate a photoactive LOV protein that in-turn uncages a transcription factor – so in essence the light is used to regulate gene expression, although this assay can also be used as a protein–protein interaction assay.<sup>309</sup> In their assay, protein A is linked to a light-activated LOV protein as well as a transcription factor through a protease cleavage site and protein B is linked to Nanoluc as well as a protease (tobacco etch virus protease TEVp). When proteins A and B come into contact with each other, and blue light is emitted from Nanoluc in the presence of

Furimazine, this light activates the LOV protein, which changes conformation to present the protease cleavage site to the TEVp protease. The protease works on the protease cleavage site and releases the transcription factor, which then heads towards the nucleus for transcription. In the work, the transcription factor induces the transcription of the red fluorescent protein mCherry. The readout of the assay is the result of this transcription and hence the expression and fluorescence of mCherry (Fig. 13). This is one of the few examples of light from the bioluminescent reaction being used to control an effector function.

#### 4.7 Protein–protein interactions (PPIs)

One of the most established uses of bioluminescence-based assays is in the interrogation, analysis and determination of interactions between proteins. The two main types of technology used in this area are the bioluminescence resonance energy transfer assays (BRET) using the NanoBRET technology,<sup>175,310,311</sup> and split-luciferase systems.<sup>181,312</sup>

BRET is based on the concept of Förster resonance energy transfer, which is a non-radiative energy transfer between two luminescent molecules, an excited state donor that transfers its energy to an acceptor which then emits light. The efficiency of the energy transfer is dependent on the distance between the donor and acceptor and their respective dipoles, which means that for efficient energy transfer to occur the molecules must be in close proximity to each other (1–10 nm),<sup>313</sup> and have the correct orientation.<sup>314</sup> In BRET the donor is a photoprotein such as Aequorin or a luciferin molecule such as coelenterazine or furimazine, while the acceptor is often the green fluorescent protein GFP, which emits green light. This circumvents the problems with Förster resonance energy transfer (FRET) with fluorophores, such as the need for an external light source,

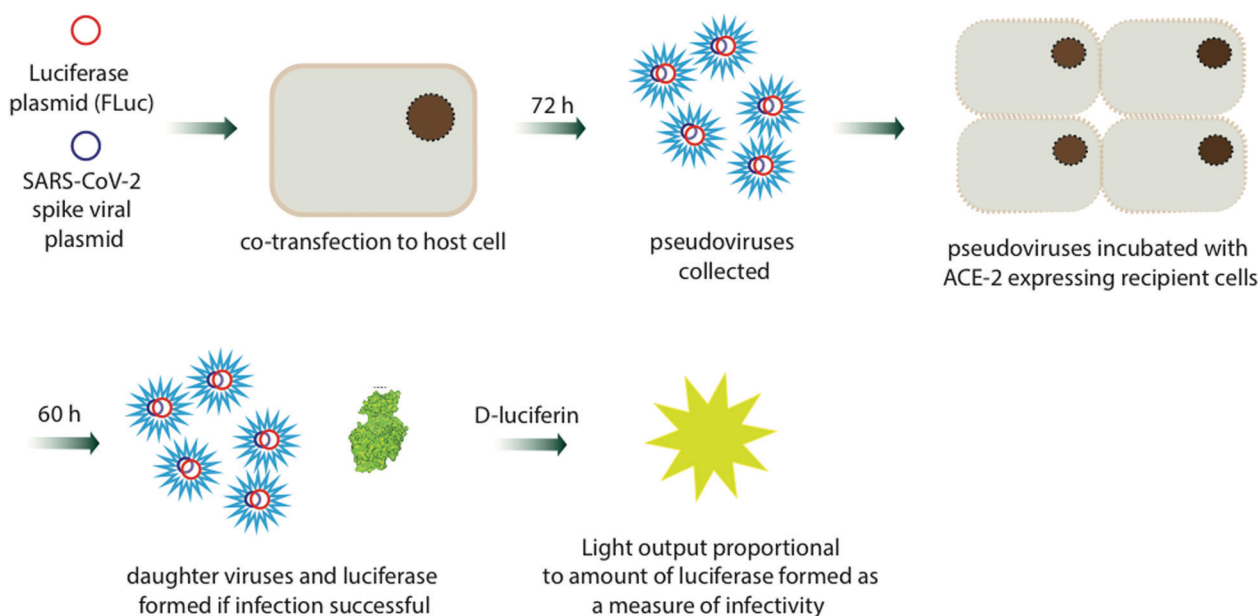
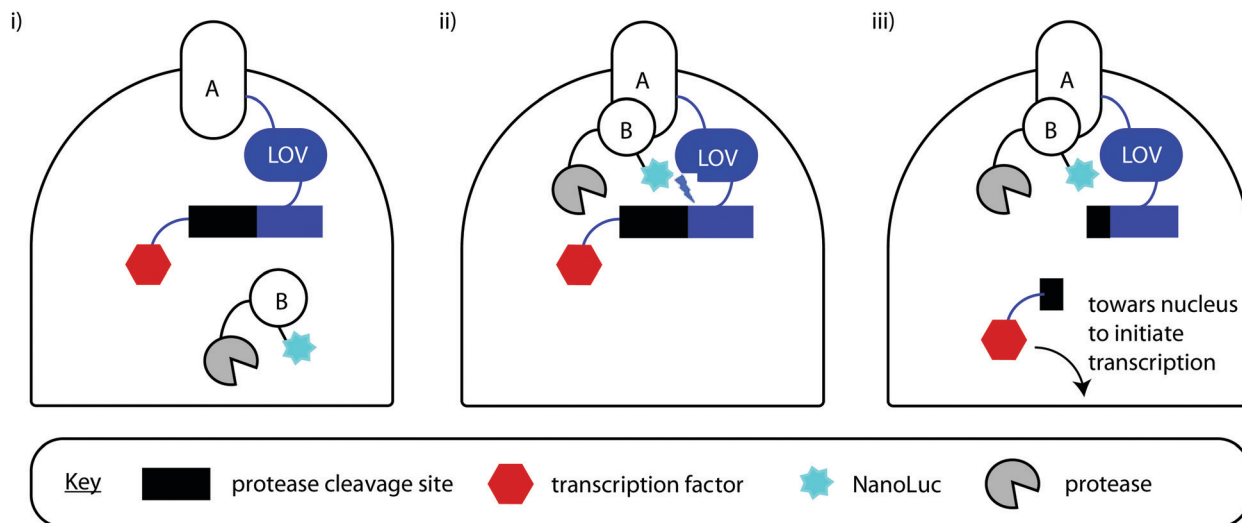


Fig. 12 A Fluc/D-luciferin based assay used to determine the infectivity of coronaviruses in different host cells – image shows process used for SARS-CoV-2 in ref. 273.





**Fig. 13** The use of bioluminescence to control gene expression – (i) When proteins A and B are distant, the LOV protein is deactivated and nothing happens. (ii) When A and B are in close proximity and interacting in the correct orientation AND NanoLuc reacts with furimazine to release light, the LOV protein gets activated and changes conformation to present the protease cleavage site to the protease. (iii) After cleavage the transcription factor is free to move to the nucleus and initiate transcription of the fluorescent protein mCherry.

photobleaching of the donor fluorescent protein, simultaneous excitation of both the donor and acceptor molecules and autofluorescence in cells or animal models (Fig. 14).

Previously, BRET based assays were well established to study various protein–protein interactions of interest such as oncology based targets including p53/hDM2 as well as G-coupled protein receptors both *in vitro* and *in cellulo*.<sup>315,316</sup> More recently the inhibition or stabilisation of other PPIs of interest has also been successfully detected using the NanoBRET technology in which BRET from the bright NanoLuc to an acceptor chromophore allows the determination of the proximity and orientation of two proteins of interest. Examples of such

analysis include the localisation and conformation of viral HCV NS5A protein,<sup>317</sup> analysis of the interaction between the PRAS40 and hippo pathway,<sup>318</sup> analysis of the CD26-ADA-A<sub>2A</sub>R trimeric complex in cells,<sup>319</sup> the use of miniG proteins as probes for GPCRs,<sup>320</sup> and analysis of the interaction between the H2 relaxin protein and the RXFP1 protein.<sup>321</sup> With the development of BRET acceptors that emit red light, NanoBRET technology has also been used to measure protein–ligand interactions *in vivo* mouse models of breast cancer to determine target engagement.<sup>322</sup> For a more detailed review on the developments in NanoBRET technology, please refer to the recently published review on the topic.<sup>311</sup> The vast majority of BRET systems use the

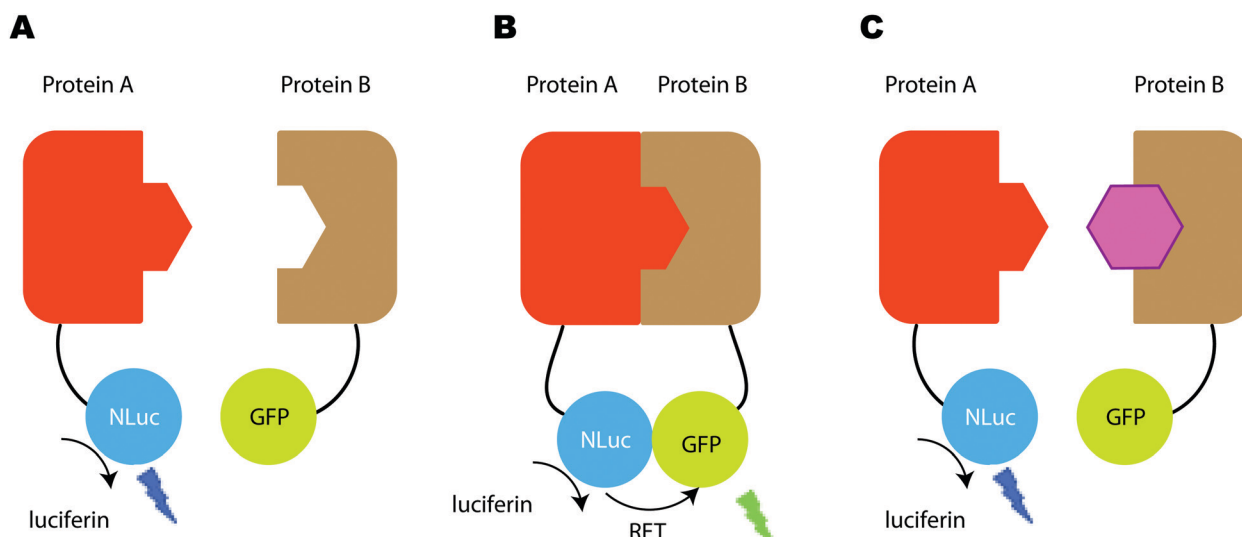


**Fig. 14** (A) When both protein partners are away from each other only blue luminescence is observed due to the NanoLuc reaction with furimazine. (B) When both protein partners are in close proximity, resonance energy transfer from NanoLuc to the acceptor GFP chromophore, results in the emission of yellow-green light from GFP. (C) In the presence of an inhibitor of the protein–protein interaction, both proteins are again at a distance and hence no BRET is observed.



Nanoluc/Furimazine combination as the energy donor as it is significantly brighter than D-luciferin/Fluc and is also much a smaller enzyme than Fluc, which makes tagging it on to proteins of interest easier and more useful as it is unlikely to disturb the protein's natural state. However, this is of limited use for *in vivo* imaging studies. Consequently, some efforts have been made towards red-shifted BRET systems. In this regard, Fluc enzyme mutants such as Ppy RE10 ( $\lambda_{\max}$  617 nm with D-luciferin) has been covalently labelled with nrIR fluorescent dyes such as Alexa-Fluor680. This resulted in BRET emission of  $\lambda_{\max}$  705 nm with an acceptor to donor emission ratio of 34.0 (Fig. 15).<sup>323</sup> Another interesting avenue has been BRET from a luciferase/luciferin combination to an appropriate quantum dot. Quantum dots are nanoparticles (diameters  $\sim$  2–10 nm) composed of a semiconducting material with diameters in the range of 2–10 nm. Due to their high surface-to-volume ratios they demonstrate a number of interesting properties such as fluorescence. For example, NanoLuc was covalently linked to a polymer-coated CdSe/ZnS core-shell quantum dot QD705 that emits at  $\lambda_{\max}$  705 nm. BRET from the Nanoluc/Furimazine reaction to the quantum dot led to red-shifted emission at 705 nm and this was used to image a tumour in mouse.<sup>324</sup> Nonetheless, the toxicity of quantum dots is a cause of concern for many, particularly for *in vivo* applications, leading to research into more biocompatible quantum dots.<sup>325</sup>

As brighter and red-shifted BRET systems are being engineered,<sup>184</sup> and tagging technology is improving as well,<sup>326</sup> it can be reasonably expected that increasing numbers of *in vivo* monitoring of protein-protein interactions and protein-ligand interactions will emerge in the near future.

Split luciferase assays are also widely used to detect and evaluate PPIs.<sup>327</sup> These have been based on various luciferases including the firefly luciferase, click-beetle luciferase, *Gaussia* luciferase and *Renilla* luciferases, which have all been used to sensitively monitor dynamic PPIs with close to real-time kinetics both *in vitro* and *in vivo*.<sup>328,329</sup> The luciferase is split

into 2 portions with one consisting of the N-terminal and the other of the C-terminal domain. Each of these portions is tagged to proteins of interest. On addition of a ligand, the proteins of interest are brought together and both termini of the luciferase come in close proximity to each other, hence reconstituting the luciferase reporter function (Fig. 16).

Before the development of Nanoluc, *Gaussia* luciferase was arguably the most suited for protein-fragment complementation assays (PCA) as it is ATP independent, can be located in the extra-cellular space, is shown to be brighter than Rluc as part of these assays and the N-terminal and C-terminal enzyme fragments are small in size. The first split *Gaussia* luciferase assay was reported by Michnick *et al.* In their work, they interrogated the FRB/FKBP protein-protein interaction, using rapamycin as a ligand to induce complex formation, and FK506 as a competitive inhibitor. The PPI dynamics were visualised both *in vitro* and *in vivo*.<sup>330</sup> Tao *et al.* reported the development of a split Gluc template which was adapted to visualise the protein-protein interaction of three different PPIs namely CaM/M13 with  $\text{Ca}^{2+}$  ions behaving as the ligand and the interactions of the ligand binding domains of (LBD) of representative steroid hormone receptors such as androgen receptor (AR), glucocorticoid receptor (GR), and oestrogen receptor (ER) with various peptide or small-molecule ligands.<sup>331</sup> Others have reported PCAs based on Gluc for visualisation of PPIs both *in vitro* and *in vivo* mouse models.<sup>332</sup> Recently, split Nano luciferase has been used to determine protein-protein interactions in plant cells, wherein the PPI between receptor kinase flagellin-sensitive 2 (FLS2) and plant receptor kinase BAK1 (BRI1-associated receptor kinase 1) was found to be induced by bacterial flg22 peptide through a split Nanoluc system.<sup>333</sup> Split luciferase assays have also been used to study viruses,<sup>334,335</sup> as well as to detect protein-protein aggregation in human cells.<sup>336</sup>

#### 4.8 High-throughput screening

Bioluminescence based assays are routinely used in drug-discovery programmes as part of high-throughput screens particularly against infectious pathogens such as bacteria, viruses or parasites. This is due to the ease in converting the assays to the commonly used 96 well or 384 well plate format and a quick, sensitive and straightforward readout of light output, that is often a measure of living cells. The gene, protein, enzyme or pathogen of interest are genetically encoded together with the luciferase gene and then pathogen replication along with simultaneous luciferase expression can be determined in the presence of luciferin through the light output of the sample both in the presence and absence of drug targets.

For example, Tan and co-workers reported the development of high-throughput screening assay to identify inhibitors of coronaviruses.<sup>337</sup> In particular, they replaced the *ns2* accessory gene in the human coronavirus strain HCoV-OC43 with the gene for *Renilla* luciferase (*Rluc*) to form a functional reporter virus strain rOC43-ns2DelRluc whose pathogenicity was unaltered. This mutant virus strain was then used to infect cells, and Rluc was expressed in the infected cells during viral replication. On addition of coelenterazine, the light output was proportional

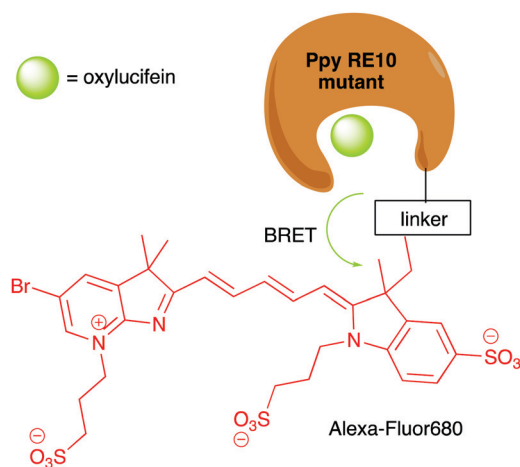


Fig. 15 BRET from the oxyluciferin in the reaction of D-luciferin/PpyRE10 Fluc mutant to the covalently linked Alexa-Fluor680 resulted in emission at 705 nm with an excellent BRET ratio.



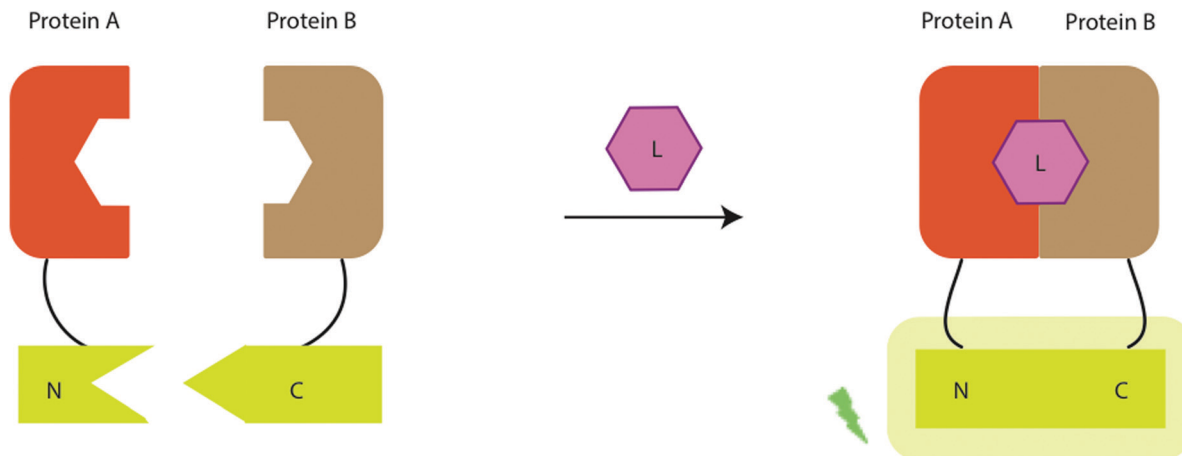


Fig. 16 General principle behind split luciferases – on the addition of a ligand (L), the N and C terminals of the luciferase come together to give functional reporter luciferase and a glow and readout on administering of luciferin.

to the Rluc levels in the cells, which are a measure of viral replication. On addition, of small-molecule compounds that inhibit viral replication, a significant reduction in light-output was observed.<sup>338</sup> This assay could be readily adapted in a 96-well format (Fig. 17).

More recently, similar high-throughput assays have been developed for screening for antibiotics in aquatic samples,<sup>237</sup> screening of antibacterial dental adhesives against mutants of streptococcus,<sup>339</sup> and monitoring and inhibiting kinase activity.<sup>340,341</sup>

Both Fluc and Rluc have been extensively used in high-throughput screening campaigns against large compound libraries in both biochemical assays and cell-based assays. Whilst these assays are extremely useful and still widely used, it is important to note that they have some limitations. For example, both Fluc and Rluc can be inhibited by various small molecules. For example, Fluc in particular suffers from competitive inhibition from compound classes that have similar chemical structures to that of its substrate *D*-luciferin including benzothiazoles, benzimidazoles, benzoxazoles and biaryl oxadiazoles. This can lead to false-positives in inhibitory assays for these compounds. Moreover, some compounds can also lead to increased transcription or translation of the reporter enzyme leading to a false-negative result. A critical discussion on the use of bioluminescence based assays is covered in seminal reviews written by Inglesse and co-workers.<sup>342,343</sup>

#### 4.9 *In vivo* imaging

The exceptional sensitivity and specificity afforded by bioluminescence imaging at the molecular level has rendered it particularly useful for *in vivo* imaging in small mammals.<sup>344</sup> Whilst fluorescent probes suffer from photobleaching and background auto-luminescence and radioactive tracers have a short shelf-life and need a synchrotron source to be produced, bioluminescent probes do not suffer these disadvantages. Moreover, developments in charge couple devices allow the detection of low levels of light output. With the advent of engineered, brighter, substrate specific luciferases and red-shifted, synthetic luciferins, significant

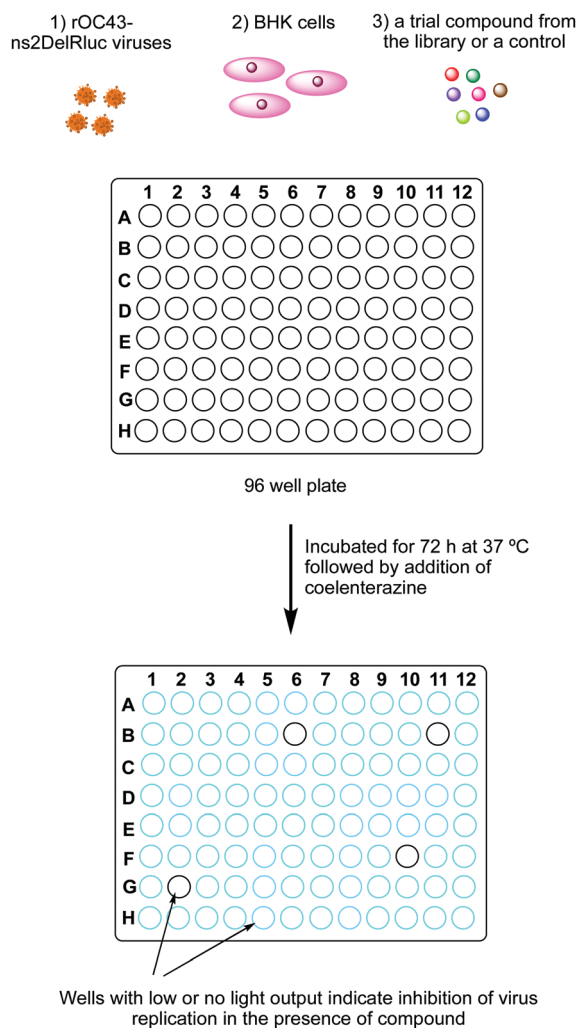


Fig. 17 The high-throughput screening assay for coronavirus inhibitors that uses the coronavirus mutant strain rOC43-ns2DelRluc developed by Tan and co-workers.<sup>302</sup>



advances have been made in *in vivo* imaging, most of which have been discussed in Section 3. Most often, these new, engineered, bioluminescence systems are first trialled and used in the imaging of developing tumours in cell studies and *in vivo* in mice. Although initial studies described the monitoring of tumours and gene expression subcutaneously, more recent work has focused on the imaging of more-deep seated tumours and challenging targets such as imaging in the brain of moving animals with novel red-shifted and bright luciferin–luciferase pairs.<sup>345</sup>

For bioluminescence *in vivo* imaging the cells of interest are genetically modified to include the gene for luciferase production. These cells can then be injected and tracked in the body of the small mammal, when the respective luciferin is added. Whilst, eukaryotic cells are often genetically tagged with Fluc, Rluc or Nluc mutants, bacterial cells are genetically modified to incorporate the *lux* codon responsible for bacterial bioluminescence. The light output is then recorded using a cooled charge-coupled device camera (Fig. 18). This allows the monitoring of *in vivo* processes in real time, without the need to sacrifice the animal.

Bioluminescence imaging has also been effectively used in imaging the development of infectious diseases both *in vitro* and *in vivo*.<sup>347</sup> Genetically modified bioluminescent pathogens, such as bacteria, parasites, viruses and fungi have been designed and monitored both *in vivo* and *in vitro*, in the presence and absence of therapies to test their effectiveness. The bioluminescent light output has been shown to correlate with the infection load.

Some notable examples include the first real time visualisation of the influenza virus in ferrets infected with A/California/04/2009 H1N1 virus (CA/09) encoding Nanoluc (Nluc) luciferase.<sup>348</sup> The replication and development of human coronavirus strain HCoV-OC43 in the central nervous system of live mice was achieved using an Rluc reporter and coelenterazine,<sup>349</sup> while another study reported the entry sites of encephalitis viruses in the central nervous system of mice, using the Fluc/ $\Delta$ -luciferin system.<sup>350</sup> An engineered firefly luciferase was also used with  $\Delta$ -luciferin to monitor the development of a

*Candida albicans* fungal infection real time in mice using *in vivo* imaging.<sup>351</sup>

*In vivo* BLI is also the modality of choice when monitoring the development of parasitic infections that cause neglected tropical diseases such as those from *Toxoplasma gondii*,<sup>352</sup> *Trypanosoma cruzi*,<sup>353,354</sup> and *Leishmania amazonensis*.<sup>355,356</sup> The gene for firefly luciferase can be readily encoded into these parasites and as bioluminescent output from the  $\Delta$ -luciferin/Fluc system is ATP dependent, only living parasites are selectively imaged, which would not necessarily be the case in fluorescence imaging. Moreover, as the imaging technique is non-invasive, the diseased mice can be kept alive and monitored over time whilst being administered different treatments.

Bacterial infections such as *Klebsiella pneumoniae*, *Citrobacter rodentium* and antibiotic resistance to them is also monitored using BLI; however the bacterial *lux* operon is often used for this.<sup>357,358</sup> The bacteria of interest are genetically encoded with the *lux* operon for bacterial bioluminescence and then injected into the mouse. The mouse is then treated with antibiotics and imaged over time to visualise the development of a disease. This technique has often been used to visualise the effectiveness of photodynamic therapy (PDT) on the treatment of bacterial infections such as surgical wounds, burns and lacerations as an alternative to treatment with antibiotics to combat antibiotic resistance. For example, dermal abrasions on mice infected with bioluminescent methicillin-resistant *S. aureus* (MRSA) were monitored while a treatment of PDT using a phthalocyanine derivative and toluidine blue with red light was administered by Hamblin and co-workers.<sup>359</sup>

Although now BLI reporters can emit light up to a wavelength of 750 nm, there is still much to be desired in terms of brightness to achieve desirable outcomes in *in vivo* imaging. Moreover, research into fluorescent probes has demonstrated that light output in the NIR-II window (1000–1700 nm) has significantly better penetration through blood and tissue than light in the NIR-I window.<sup>360</sup> This is the next frontier in bioluminescence *in vivo* imaging.

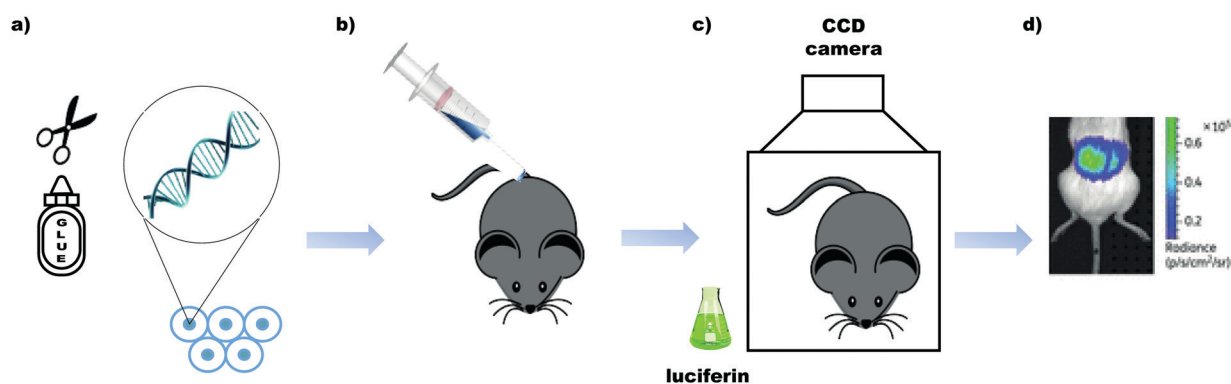


**Fig. 18** The process of *in vivo* imaging – (a) the cells of interest are genetically encoded with genes for expressing the luciferase of interest. (b) The luciferase expressing cells are injected into the mouse and incubated for a set period of time. (c) The respective luciferin is added, and the cells are tracked in real-time *in vivo*. Image acquisition is carried out using a camera with a cooled charged-coupled device. (d) An image of the tracked cells is obtained. This exemplar image is of the fungal cells of *C. albicans*, tagged with Fluc and imaged after the administration of  $\Delta$ -luciferin. Image reused with permission from Oxford University Press on behalf of Brock *et al.*<sup>346</sup>



#### 4.10 Disease therapy using the light from bioluminescence

The light from bioluminescence has been used as a localised and controlled light source for the excitation of photosensitisers in photodynamic therapy. Photodynamic therapy makes use of photosensitiser molecules that are activated by light and generate reactive oxygen species (ROS) radicals, such as singlet oxygen that can destroy protein and tissue. This cytotoxicity can be advantageous in cases where cell death is required as a form of therapy such as in infection or cancer.

Both the Fluc and RLuc systems have been used as genetically encoded sources of light for photosensitisers. For example, Theodossiou *et al.* reported that increased cell death was observed when both the photosensitiser Rose Bengal and  $\Delta$ -luciferin were administered to a Fluc expressing cancer cell line, in the absence of ambient light.<sup>361</sup> This work was contested by a later report that reported that the increase in cell death was insignificant when non-toxic levels of photosensitiser and luciferin were used, and that the quantum yield of the light output from the  $\Delta$ -luciferin/Fluc reaction was the limiting factor.<sup>362</sup> Another study by Lai *et al.* reported RLuc-immobilized quantum dots-655 (QD-RLuc8) for bioluminescence resonance energy transfer (BRET)-mediated PDT using the photosensitiser Foscan<sup>®</sup> to target cancer cells both *in vitro* and *in vivo* in mice.<sup>363</sup> Although the PDT did not completely eradicate the tumour, it significantly delayed tumour growth, and it was proposed that this method of low-light dosage, compared to the use of external light, may cause lower inflammation and unnecessary death of healthy tissue.

Yun and co-workers reported RLuc and rose-bengal conjugates that generate singlet oxygen by bioluminescence resonance energy transfer (BRET). In their work, they used bovine serum albumin (BSA) as a central backbone and conjugated RLuc and rose-bengal to the BSA to achieve the desired distance between RLuc and Rose Bengal which allowed both moieties to be functional, without quenching the emission from either of them (Fig. 19). When coelenterazine was administered to this system, evidence of cytotoxicity and oxidative stress was observed in cells.<sup>14,364</sup> Unsurprisingly, the uptake of the large and bulky conjugate into cells was poor and optimisation is required on that front.

It is to be noted, that an improvement in the light output efficiency of the bioluminescent reaction, as well as the BRET efficiency between the coelenteramide and the photosensitiser would improve the generation of singlet oxygen.

An alternative approach that circumvents the need for cellular uptake of large and bulky biological conjugates could be to use a nanoparticle to bring the luciferase and photosensitiser in close proximity. This approach was taken by Wu *et al.* and in their work they encapsulated Rose-Bengal in biodegradable poly(lactic-co-glycolic acid) (PLGA) nanoparticles, which were then conjugated with Fluc. In the presence of  $\Delta$ -luciferin, effective PDT and cancer cell death was observed both *in vitro* and *in vivo* in mice suffering from cancer of the liver.<sup>365</sup>

Although increasing numbers of studies with PDT activated by BRET from bioluminescence are being reported, the scope of the work is somewhat limited by amongst other factors,

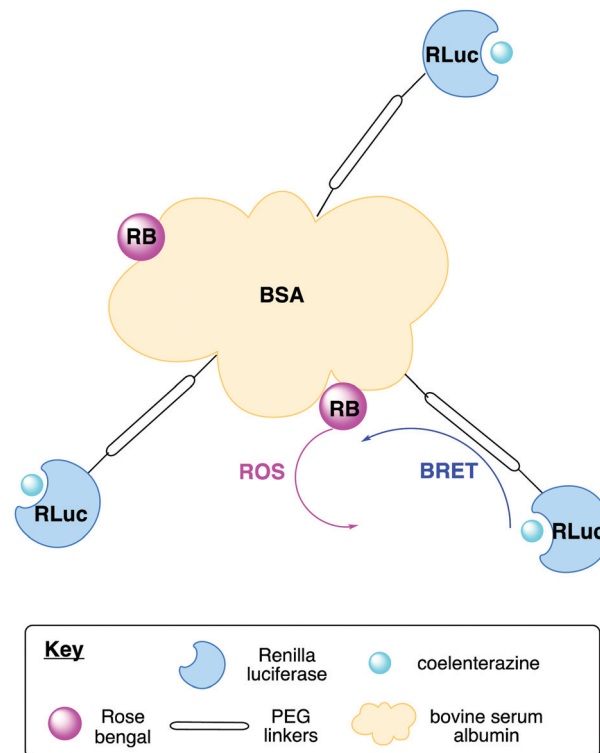


Fig. 19 Figure showing the Rose-Bengal-BSA-RLuc conjugate.

the brightness of the luciferin/luciferase reaction. As brighter luciferin/luciferase pairs are developed, it is hoped that this area will also expand into new territories.

#### 4.11 Effector applications

Whilst traditionally the light from bioluminescence assays was primarily used for sensing applications such as the ones discussed previously, more recently bioluminescence-based technology has found avenues in effector technologies, wherein the light from the bioluminescent reaction can be used to affect or control other processes.<sup>366</sup> This work was initially inspired by the relatively well-established field of optogenetics, where external light sources are used to control photoactive proteins and ion channels and hence cells such as neurones.<sup>367,368</sup> Light from a luciferin-luciferase reaction provides an attractive possibility of localised and controlled light output of a wavelength of choice, compared to external light sources that are often harsh and can indiscriminately excite other endogenous fluorophores causing damage and autoluminescence.

The earliest targets to be affected by bioluminescent light output were channelrhodopsins. Channelrhodopsins are light-sensitive ion channels that are naturally found in algae and are responsible for their movement in response to light *i.e.* phototaxis.<sup>369,370</sup> When expressed in neurons, rhodopsins allow light to control the state of the ion-channel by either opening it or closing it and hence the ability of the neuron to fire action potentials.<sup>371</sup> The channelrhodopsins absorb blue light (480 nm), so are ideal targets for *RLuc*, *Gluc* or *NLuc*.<sup>372</sup> The gene for channelrhodopsins can be encoded together with



the gene for luciferase leading to a fusion protein consisting of a channelrhodopsin with a luciferase. This led to the development of 'luminopsins' which are now a class of optogenetic reporters, in which the addition of coelenterazine luciferin and subsequent light output controls the state of the ion-channel, and hence the ability of neurone cells to fire action potentials.<sup>17,373–376</sup> The use of bioluminescent light to control gene expression has been discussed in Section 4.6.

Bioluminescent light has also been used for novel photo-uncaging reactions by Winssinger and co-workers. In 2018, they reported a photo-uncaging using BRET from Nluc to a ruthenium photocatalyst to release pyridinium species. Further developments by this group in 2019 saw the first true 'bioluminolysis' wherein no photocatalyst was needed to uncage drugs and molecules of interest using BRET from Nanoluc-Halotag chimera protein (Hluc) to a coumarin photocage (Fig. 20).<sup>15,16</sup>

Photopharmacology including photodynamic therapy, photouncaging and photoisomerism is an area of growing interest in medicinal chemistry to develop and harness new therapies.<sup>377</sup> Bioluminescence has potential to be of great use here as a light source *in vivo* in close proximity to species of interest. The fact that luciferases are usually genetically encoded makes this a challenging endeavour in humans and complex on several fronts. However, with the advent of luciferase conjugated nanoparticles, this challenge in the delivery of the enzyme to its desired site of action might soon be getting addressed.

## 5. Blue-sky research and new horizons

### 5.1 Glowing plants

Bioluminescence imaging has found limited use in the imaging of plant metabolites, proteins and physiology. The fact that plants have chlorophyll rather than haemoglobin means that they have a different and distinct optical window compared to small mammals.<sup>378</sup> The four types of chlorophyll each absorb light at two distinct wavelengths; the first  $\lambda \sim 450$  nm and the second  $\lambda \sim 650$  nm.<sup>379</sup> Moreover, the circulation of water and nutrients in plants is not as rapid as in small mammals, and so the delivery of luciferin to the cells of interest is a challenge. This limited the use of BLI to small seedlings or cell cultures

that could be grown in Petri dishes in the lab. Nonetheless, despite these limitations, noteworthy work was done to develop our understanding of the circadian clock using a fused, genetically encoded Fluc reporter in a pioneering study by Kay *et al.*<sup>380,381</sup> In their seminal work, Kay *et al.* fused the Fluc gene with a gene for the promoter of the chlorophyll a-b binding protein (*cab2*), which is a membrane protein in plant cells and plays an important role in photosynthesis. The *Arabidopsis* plants were grown on sterile culture plates and sprayed with a solution of luciferin. Bioluminescence imaging was used to visualise the organ localisation of *cab2* during the light and dark. In this study, based on the cyclical changes in *cab2* expression levels, the length of the circadian clock cycle of the plants could be determined.<sup>380</sup> After this work, the authors reported another study in which they used this methodology to identify *Arabidopsis* mutants which have aberrant circadian clock cycles, and tried to investigate which genes were responsible for these changes.<sup>381</sup>

To circumvent the problem of delivery of D-luciferin to the cells of interest, it was thought that an autoluminescent plant would be of more use. To this end, genetically modified plants were produced, in which the bacterial *lux* operon would be expressed in the plastids, but this failed to produce sufficient light, partly due to the fact that bioluminescent bacteria emit blue light, whilst chlorophyll absorbs strongly in that region. Moreover, the expression of the bacterial bioluminescent system was found to be toxic to the plant.<sup>115</sup> Since the recent discovery of the fully genetically encoded bioluminescence pathway of fungal bioluminescence in 2018,<sup>126</sup> this year two different groups reported successfully creating genetically modified plants with the fungal bioluminescence pathway genetically encoded into them, making them autoluminescent.<sup>128,382</sup> This opens up a new avenue for BLI in plant research as it has moved BLI in plants from the laboratory Petri-dish to more real life examples grown in soil. Moreover, it also opens the exciting avenue of using such plants for 'green' lighting purposes in the future. Notably, in their work Yampolsky and Sarkisyan *et al.* also reported an autoluminescent mammalian cell line using the genes responsible for fungal bioluminescence.<sup>128</sup> However, no attempt was made to compare the brightness of the light output with that obtained from the bacterial *lux* operon.

Apart from genetically encoded autoluminescent systems, a nanobionic light emitting plant has also been reported in the

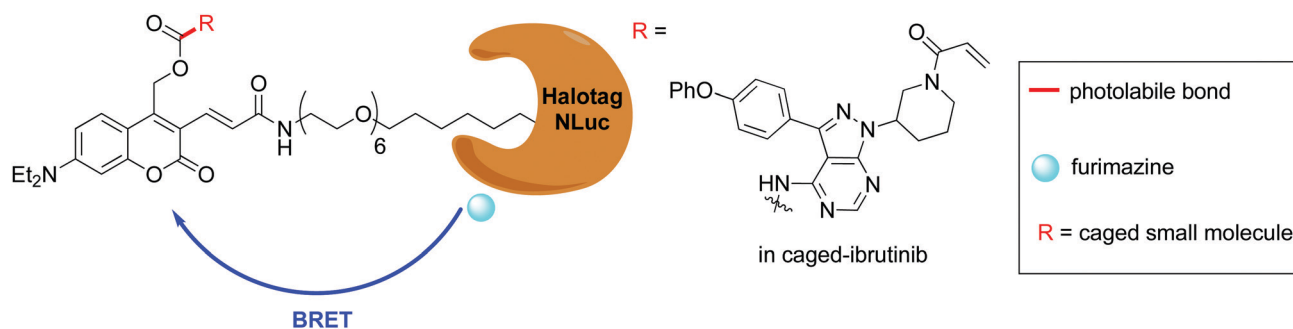


Fig. 20 The use of bioluminolysis for the release of the photocaged small-molecule kinase inhibitor ibrotinib by BRET.



literature. In this system, Fluc was conjugated into silica nanoparticles (SNP-Luc) and D-luciferin was conjugated into poly(lactic-co-glycolic acid) (PLGA-LH<sub>2</sub>) nanoparticles. Both types of nanoparticles were slowly able to release their cargo inside plant cells to allow the bioluminescence reaction to take place and to give the plant a yellow-green glow.<sup>18</sup> However, a pressurized bath infusion of nanoparticles was used to administer the mixture of nanoparticles to the plant, which makes this sort of a light emitting plant unsustainable.

## 5.2 Lifestyle

The natural phenomenon of bioluminescence has enthralled people for centuries and the advent of modern technology has allowed us to bring this natural beauty, from the wilderness to the lab and finally to our homes and places of recreation. Indeed, bioluminescent systems are now being considered as green alternatives to outdoor lighting in public spaces in architecture.<sup>383</sup> Moreover, a simple search online would lead one to lamps based on bioluminescent dinoflagellate to decorate the home. The French start-up company Glowee was founded in 2014 and has used bioluminescent bacteria to develop lamps as a form of sustainable lighting. Since its initiation, the company has managed to increase the lifespan of the bacteria, and hence the lamps from 3 days up to 1 month.

As the use of bioluminescent systems become more widespread, they have inspired both scientists and artists alike towards innovation and novel applications. There are a number of examples of artists that are inspired by and actively use bioluminescence in their work. Novel and rare art work known as 'living art' has been produced using some bioluminescent systems – namely bioluminescent bacteria and the bioluminescence from single-celled dinoflagellate.<sup>384</sup> The bacterial bioluminescence art work is done on Petri dishes and lasts up to 2 weeks, gradually dying off and depicting different aspects of the art as the light fades. Thus, these bioluminescent systems serve as tools for the artist's expression as well as starting points for science communication (Fig. 21).

## 5.3 Limitations of bioluminescent systems

Although the light from bioluminescence has quickly reached several uncharted territories, it is still limited from use in a wider-array of applications by the fact that most of the probes have poor quantum yields, with the quantum yield of D-luciferin/Fluc at 0.41, being one the highest photon outputs from a natural wild-type system. Although, engineered systems such as Nluc/coelenterazine have higher photon outputs, the wavelength of emission of these systems is not ideal for all potential applications and the more-redshifted variants of Nluc are not commercially available. Some of the natural and synthetic luciferins also suffer from issues arising due to poor stability, cell-compatibility and bioavailability. The development of complementary luciferin and luciferase pairs with improved properties is an active area of research, and with further advances, including the cloning and understanding of auto-luminescent systems such as that of the fungi, will assuredly lead to more novel applications.

A



B



Fig. 21 Art from bioluminescent creatures – (A) 'flow visualisation' by Iyvone Khoo made using bioluminescent dinoflagellate, [www.iyvonekhoo.co.uk](http://www.iyvonekhoo.co.uk). (B) 'Rabbit: stage 1' photograph of drawing created with bioluminescent bacteria, Hunter Cole, [www.HunterCole.org](http://www.HunterCole.org).

## 6. Conclusions

Research in bioluminescence and bioluminescent organisms has made phenomenal progress over time. From early discovery research into undiscovered luciferins and luciferases, to new



applications for known bioluminescent reporters, designer luciferins and luciferases, and other developing technology that assists these systems, a lot of great work has helped develop and progress the field. Moreover, enzyme engineering, biophotonics, computational chemistry and synthetic chemistry are rapidly evolving fields as well and it can be reasonably expected that developments in these areas will feed into the research and applications of bioluminescence in biotechnology. As bioluminescence has found utility in various fields including medicine, biology, physics and engineering and led to exciting multidisciplinary science across all of them, we hope this review, that briefly details the origins and mechanisms of bioluminescence, the currently available luciferin and luciferase systems and covers extensively the key and recent applications of bioluminescence in biotechnology across various fields and makes them accessible to chemists in particular will stimulate further exciting research and foster collaborations in the community.

## Conflicts of interest

There are no conflicts to declare.

## Acknowledgements

The authors would like to thank the artists Iyvette Khoo and Hunter Cole for sharing their work with us.

## Notes and references

- 1 S. H. D. Haddock, M. A. Moline and J. F. Case, *Ann. Rev. Mar. Sci.*, 2010, **2**, 443–493.
- 2 V. B. Meyer-Rochow, *Luminescence*, 2007, **22**, 251–265.
- 3 K. F. Stanger-Hall, J. E. Lloyd and D. M. Hillis, *Mol. Phylogenet. Evol.*, 2007, **45**, 33–49.
- 4 R. Boyle, *Philos. Trans. R. Soc.*, 1667, **2**, 605–612.
- 5 O. Shimomura, *J. Microsc.*, 2005, **217**, 3–15.
- 6 A. Chiesa, E. Rapizzi, V. Tosello, P. Pinton, M. De Virgilio, K. E. Fogarty and R. Rizzuto, *Biochem. J.*, 2001, **355**, 1–12.
- 7 E. S. Vysotski and J. Lee, *Acc. Chem. Res.*, 2004, **37**, 405–415.
- 8 L. P. Burakova and E. S. Vysotski, *Appl. Microbiol. Biotechnol.*, 2019, **103**, 5929–5946.
- 9 A. Fleiss and K. S. Sarkisyan, *Curr. Genet.*, 2019, **65**, 877–882.
- 10 Z. M. Kaskova, A. S. Tsarkova and I. V. Yampolsky, *Chem. Soc. Rev.*, 2016, **45**, 6048–6077.
- 11 A. A. Kotlobay, M. A. Dubinnyi, K. V. Purtov, E. B. Guglya, N. S. Rodionova, V. N. Petushkov, Y. V. Bolt, V. S. Kublitski, Z. M. Kaskova, R. H. Ziganshin, Y. V. Nelyubina, P. V. Dorovatovskii, I. E. Eliseev, B. R. Branchini, G. Bourenkov, I. A. Ivanov, Y. Oba, I. V. Yampolsky and A. S. Tsarkova, *Proc. Natl. Acad. Sci. U. S. A.*, 2019, **116**, 18911–18916.
- 12 E. H. White, F. McCapra, G. F. Field and W. D. McElroy, *J. Am. Chem. Soc.*, 1961, **83**, 2402–2403.
- 13 O. Shimomura, T. Masugi, F. H. Johnson and Y. Haneda, *Biochemistry*, 1978, **17**, 994–998.
- 14 S. Kim, H. Jo, M. Jeon, M. G. Choi, S. K. Hahn and S. H. Yun, *Chem. Commun.*, 2017, **53**, 4569–4572.
- 15 D. Chang, E. Lindberg, S. Feng, S. Angerani, H. Riezman and N. Winssinger, *Angew. Chem., Int. Ed.*, 2019, **58**, 16033–16037.
- 16 E. Lindberg, S. Angerani, M. Anzola and N. Winssinger, *Nat. Commun.*, 2018, **9**, 3539.
- 17 S. Y. Park, S. H. Song, B. Palmateer, A. Pal, E. D. Petersen, G. P. Shall, R. M. Welchko, K. Ibata, A. Miyawaki, G. J. Augustine and U. Hochgeschwender, *J. Neurosci. Res.*, 2020, **98**, 410–421.
- 18 S. Y. Kwak, J. P. Giraldo, M. H. Wong, V. B. Koman, T. T. S. Lew, J. Ell, M. C. Weidman, R. M. Sinclair, M. P. Landry, W. A. Tisdale and M. S. Strano, *Nano Lett.*, 2017, **17**, 7951–7961.
- 19 E. Conti, N. P. Franks and P. Brick, *Structure*, 1996, **4**, 287–298.
- 20 O. Shimomura, T. Goto and Y. Hirata, *Bull. Chem. Soc. Jpn.*, 1957, **30**, 929–933.
- 21 T. Kishi, T. Goto, Y. Hirata, O. Shimomura and F. H. Johnson, *Tetrahedron Lett.*, 1966, **7**, 3427–3436.
- 22 E. M. Thompson, S. Nagata and F. I. Tsuji, *Proc. Natl. Acad. Sci. U. S. A.*, 1989, **86**, 6567–6571.
- 23 K. Hori, H. Charbonneau, R. C. Hart and M. J. Cormier, *Proc. Natl. Acad. Sci. U. S. A.*, 1977, **74**, 4285–4287.
- 24 S. Inouye, K. Watanabe, H. Nakamura and O. Shimomura, *FEBS Lett.*, 2000, **481**, 19–25.
- 25 W. W. Lorenz, R. O. McCann, M. Longiaru and M. J. Cormier, *Proc. Natl. Acad. Sci. U. S. A.*, 1991, **88**, 4438–4442.
- 26 J. R. de Wet, K. V. Wood, D. R. Helinski and M. DeLuca, *Proc. Natl. Acad. Sci. U. S. A.*, 1985, **82**, 7870–7873.
- 27 K. V. Wood, Y. A. Lam, H. H. Seliger and W. D. McElroy, *Science*, 1989, **244**, 700–702.
- 28 J. H. Devine, G. D. Kutuzova, V. A. Green, N. N. Ugarova and T. O. Baldwin, *Biochim. Biophys. Acta, Gene Struct. Expression*, 1993, **1173**, 121–132.
- 29 M. Tsutomu, T. Hiroki and N. Eiichi, *Gene*, 1989, **77**, 265–270.
- 30 N. Kajiyama, T. Masuda, H. Tatsumi and E. Nakano, *Biochim. Biophys. Acta, Protein Struct. Mol. Enzymol.*, 1992, **1120**, 228–232.
- 31 H. Tatsumi, N. Kajiyama and E. Nakano, *Biochim. Biophys. Acta, Gene Struct. Expression*, 1992, **1131**, 161–165.
- 32 V. R. Viviani, A. C. R. Silva, G. L. O. Perez, R. V. Santelli, E. J. H. Bechara and F. C. Reinach, *Photochem. Photobiol.*, 1999, **70**, 254–260.
- 33 B. Said Alipour, S. Hosseinkhani, M. Nikkhah, H. Naderi-Manesh, M. J. Chaichi and S. K. Osaloo, *Biochem. Biophys. Res. Commun.*, 2004, **325**, 215–222.
- 34 P. S. F. McCapra, D. J. Gilfoyle, D. W. Young and N. J. Church, *Bioluminescence and Chemiluminescence Fundamentals and Applied Aspects*, Wiley-Blackwell, 1994.
- 35 B. R. Branchini, C. E. Behney, T. L. Southworth, D. M. Fontaine, A. M. Gulick, D. J. Vinyard and G. W. Brudvig, *J. Am. Chem. Soc.*, 2015, **137**, 7592–7595.



- 36 J. A. Koo, S. P. Schmidt and G. B. Schuster, *Proc. Natl. Acad. Sci. U. S. A.*, 1978, **75**, 30–33.
- 37 C. Ribeiro and J. C. G. Esteves da Silva, *Photochem. Photobiol. Sci.*, 2008, **7**, 1085–1090.
- 38 H. Fraga, D. Fernandes, J. Novotny, R. Fontes and J. C. G. Esteves da Silva, *ChemBioChem*, 2006, **7**, 929–935.
- 39 Y. Ando, K. Niwa, N. Yamada, T. Enomoto, T. Irie, H. Kubota, Y. Ohmiya and H. Akiyama, *Nat. Photonics*, 2008, **2**, 44–47.
- 40 D. K. Welsh and T. Noguchi, *Cold Spring Harb. Protoc.*, 2012, **7**, 852–866.
- 41 J. R. Knowles, *Annu. Rev. Biochem.*, 1980, **49**, 877–919.
- 42 A. Lundin, *Methods Enzymol.*, 2000, **305**, 346–370.
- 43 B. R. Branchini, T. L. Southworth, D. M. Fontaine, D. Kohrt, M. Talukder, E. Michelini, L. Cevenini, A. Roda and M. J. Grossel, *Anal. Biochem.*, 2015, **484**, 148–153.
- 44 A. Lundin, B. Jaderlund and T. Lovgren, *Clin. Chem.*, 1982, **28**, 609–614.
- 45 G. Scheuerbrandt, A. Lundin, T. Lövgren and W. Mortier, *Muscle Nerve*, 1986, **9**, 11–23.
- 46 A. Lundin, A. Rickardsson and A. Thore, *Anal. Biochem.*, 1976, **75**, 611–620.
- 47 A. Lundin, M. Hasenson, J. Persson and Å. Pousette, *Methods Enzymol.*, 1986, **133**, 27–42.
- 48 A. Lundin, *Adv. Biochem. Eng. Biotechnol.*, 2014, **145**, 31–62.
- 49 A. Lundin, P. Arner and J. Hellmér, *Anal. Biochem.*, 1989, **177**, 125–131.
- 50 J. Hellmér, P. Arner and A. Lundin, *Anal. Biochem.*, 1989, **177**, 132–137.
- 51 D. Morse and B. A. Tannous, *Mol. Ther.*, 2012, **20**, 692–693.
- 52 M. L. N. Dubuisson, B. De Wergifosse, A. Trouet, F. Baguet, J. Marchand-Brynaert and J. F. Rees, *Biochem. Pharmacol.*, 2000, **60**, 471–478.
- 53 A. Roda, M. Guardigli, E. Michelini and M. Mirasoli, *TrAC, Trends Anal. Chem.*, 2009, **28**, 307–322.
- 54 R. Weissleder and V. Ntziachristos, *Nat. Med.*, 2003, **9**, 123–128.
- 55 G. L. Andreason and G. A. Evans, *Anal. Biochem.*, 1989, **180**, 269–275.
- 56 C. H. Contag, S. D. Spilman, P. R. Contag, M. Oshiro, B. Eames, P. Dennerly, D. K. Stevenson and D. A. Benaron, *Photochem. Photobiol.*, 1997, **66**, 523–531.
- 57 C. H. Contag and M. H. Bachmann, *Annu. Rev. Biomed. Eng.*, 2002, **4**, 235–260.
- 58 D. C. McCutcheon, M. A. Paley, R. C. Steinhardt and J. A. Prescher, *J. Am. Chem. Soc.*, 2012, **134**, 7604–7607.
- 59 D. C. McCutcheon, W. B. Porterfield and J. A. Prescher, *Org. Biomol. Chem.*, 2015, **13**, 2117–2121.
- 60 T. Vo-Dinh, *Biomedical Photonics Handbook: Biomedical Diagnostics*, CRC Press, 2014, 2nd edn, 2014.
- 61 R. Shinde, J. Perkins and C. H. Contag, *Biochemistry*, 2006, **45**, 11103–11112.
- 62 M. S. Evans, J. P. Chaurette, S. T. Adams, G. R. Reddy, M. A. Paley, N. Aronin, J. A. Prescher and S. C. Miller, *Nat. Methods*, 2014, **11**, 393–395.
- 63 F. Berger, R. Paulmurugan, S. Bhaumik and S. S. Gambhir, *Eur. J. Nucl. Med. Mol. Imaging*, 2008, **35**, 2275–2285.
- 64 S. Iwano, M. Sugiyama, H. Hama, A. Watakabe, N. Hasegawa, T. Kuchimaru, K. Z. Tanaka, M. Takahashi, Y. Ishida, J. Hata, S. Shimozone, K. Namiki, T. Fukano, M. Kiyama, H. Okano, S. Kizaka-Kondoh, T. J. McHugh, T. Yamamori, H. Hioki, S. Maki and A. Miyawaki, *Science*, 2018, **359**, 935–939.
- 65 G. Zomer, J. W. Hastings, F. Berthold, A. Lundin, A. M. Garcia Campana, R. Niessner, T. K. Christopoulos, C. Lowik, B. Branchini, S. Daunert, L. Blum, L. J. Kricka and A. Roda, *Chemiluminescence and Bioluminescence*, The Royal Society of Chemistry, 2010.
- 66 A. P. Jathoul, H. Grounds, J. C. Anderson and M. A. Pule, *Angew. Chem., Int. Ed.*, 2014, **53**, 13059–13063.
- 67 L. Mezzanotte, I. Que, E. Kaijzel, B. Branchini, A. Roda and C. Löwik, *PLoS One*, 2011, **6**, 19277.
- 68 C. L. Stowe, T. A. Burley, H. Allan, M. Vinci, G. Kramer-Marek, D. M. Ciobota, G. N. Parkinson, T. L. Southworth, G. Agliardi, A. Hotblack, M. F. Lythgoe, B. R. Branchini, T. L. Kalber, J. C. Anderson and M. A. Pule, *eLife*, 2019, **8**, e45801.
- 69 R. Podsiadły, A. Grzelakowska, J. Modrzejewska, P. Siarkiewicz, D. Słowiński, M. Szala and M. Świerczyńska, *Dyes Pigm.*, 2019, 170.
- 70 W. D. McElroy and B. L. Strehler, *Arch. Biochem.*, 1949, **22**, 420–433.
- 71 J. P. Steghens, K. L. Min and J. C. Bernengo, *Biochem. J.*, 1998, **336**, 109–113.
- 72 H. Caysa, R. Jacob, N. Müther, B. Branchini, M. Messerle and A. Söling, *Photochem. Photobiol. Sci.*, 2009, **8**, 52–56.
- 73 A. Kitayama, H. Yoshizaki, Y. Ohmiya, H. Ueda and T. Nagamune, *Photochem. Photobiol.*, 2003, **77**, 333.
- 74 H. H. Seliger and W. D. McElroy, *Proc. Natl. Acad. Sci. U. S. A.*, 1964, **52**, 75–81.
- 75 B. R. Branchini, T. L. Southworth, D. M. Fontaine, M. H. Murtiashaw, A. McGurk, M. H. Talukder, R. Qureshi, D. Yetil, J. A. Sundlov and A. M. Gulick, *Photochem. Photobiol.*, 2017, **93**, 479–485.
- 76 G. Oliveira and V. R. Viviani, *Photochem. Photobiol. Sci.*, 2019, **18**, 2682–2687.
- 77 J. F. Thompson, L. S. Hayes and D. B. Lloyd, *Gene*, 1991, **103**, 171–177.
- 78 S. V. Markova, M. D. Larionova and E. S. Vysotski, *Photochem. Photobiol.*, 2019, **95**, 705–721.
- 79 G. A. Stepanyuk, Z. J. Liu, S. S. Markova, L. A. Frank, J. Lee, E. S. Vysotski and B. C. Wang, *Photochem. Photobiol. Sci.*, 2008, **7**, 442–447.
- 80 M. Verhaegent and T. K. Christopoulos, *Anal. Chem.*, 2002, **74**, 4378–4385.
- 81 M. S. Titushin, S. V. Markova, L. A. Frank, N. P. Malikova, G. A. Stepanyuk, J. Lee and E. S. Vysotski, *Photochem. Photobiol. Sci.*, 2008, **7**, 189–196.
- 82 S. V. Markova, S. Golz, L. A. Frank, B. Kalthof and E. S. Vysotski, *J. Biol. Chem.*, 2004, **279**, 3212–3217.
- 83 Y. Takenaka, H. Masuda, A. Yamaguchi, S. Nishikawa, Y. Shigeri, Y. Yoshida and H. Mizuno, *Gene*, 2008, **425**, 28–35.



- 84 Y. Takenaka, A. Yamaguchi, N. Tsuruoka, M. Torimura, T. Gojobori and Y. Shigeri, *Mol. Biol. Evol.*, 2012, **29**, 1669–1681.
- 85 T. B. Shrestha, D. L. Troyer and S. H. Bossmann, *Synthesis*, 2014, 646–652.
- 86 A. Pichler, J. L. Prior and D. Piwnica-Worms, *Proc. Natl. Acad. Sci. U. S. A.*, 2004, **101**, 1702–1707.
- 87 L. J. Kricka, *Encyclopedia of Analytical Science*, 2nd edn, 2005.
- 88 Y. Xu, D. W. Piston and C. H. Johnson, *Proc. Natl. Acad. Sci. U. S. A.*, 1999, **96**, 151–156.
- 89 M. D. Larionova, S. V. Markova and E. S. Vysotski, *Biochem. Biophys. Res. Commun.*, 2017, **483**, 772–778.
- 90 S. Knappskog, H. Ravneberg, C. Gjerdrum, C. Tröfse, B. Stern and I. F. Pryme, *J. Biotechnol.*, 2007, **128**, 705–715.
- 91 J. C. Matthews, K. Hori and M. J. Cormier, *Biochemistry*, 1977, **16**, 85–91.
- 92 M. D. Larionova, S. V. Markova and E. S. Vysotski, *J. Photochem. Photobiol., B*, 2018, **183**, 309–317.
- 93 A. M. Loening, T. D. Fenn, A. M. Wu and S. S. Gambhir, *Protein Eng., Des. Sel.*, 2006, **19**, 391–400.
- 94 E. A. Meighen, *Microbiol. Rev.*, 1991, **55**, 123–142.
- 95 J. Engebrecht, K. Nealson and M. Silverman, *Cell*, 1983, **32**, 773–781.
- 96 J. L. Bose, C. S. Rosenberg and E. V. Stabb, *Arch. Microbiol.*, 2008, **190**, 169–183.
- 97 N. E. Boemare, R. J. Akhurst and R. G. Mourant, *Int. J. Syst. Bacteriol.*, 1993, **43**, 249–255.
- 98 B. Austin and X. H. Zhang, *Lett. Appl. Microbiol.*, 2006, **43**, 119–124.
- 99 M. J. Jensen, B. M. Tebo, P. Baumann, M. Mandel and K. H. Nealson, *Curr. Microbiol.*, 1980, **3**, 311–315.
- 100 W. D. McElroy and A. A. Green, *Arch. Biochem. Biophys.*, 1955, **56**, 240–255.
- 101 E. P. C. Rocha, *Annu. Rev. Genet.*, 2008, **42**, 211–233.
- 102 H. Echols, *Operators and Promoters: The Story of Molecular Biology and Its Creators*, University of California Press, 2001.
- 103 S. Nijvipakul, J. Wongratana, C. Suadee, B. Entsch, D. P. Ballou and P. Chaiyen, *J. Bacteriol.*, 2008, **190**, 1531–1538.
- 104 E. Brodl, A. Winkler and P. Macheroux, *Comput. Struct. Biotechnol. J.*, 2018, **16**, 551–564.
- 105 T. O. Baldwin, M. Z. Nicoli, J. E. Becvar and J. W. Hastings, *J. Biol. Chem.*, 1975, **250**, 2763–2768.
- 106 M. Kurfurst, S. Ghisla and J. W. Hastings, *Proc. Natl. Acad. Sci. U. S. A.*, 1984, **81**, 2990–2994.
- 107 J. W. Hastings, C. Balny, C. L. Peuch and P. Douzou, *Proc. Natl. Acad. Sci. U. S. A.*, 1973, **70**, 3468–3472.
- 108 J. Vervoort, F. Muller, W. A. M. van den Berg, C. T. W. Moonen and J. Lee, *Biochemistry*, 1986, **25**, 8062–8067.
- 109 F. M. Raushel and T. O. Baldwin, *Biochem. Biophys. Res. Commun.*, 1989, **164**, 1137–1142.
- 110 G. Merényi, J. Lind, H. I. X. Mager and S. C. Tu, *J. Phys. Chem.*, 1992, **96**, 10528–10533.
- 111 J. W. Eckstein, J. W. Hastings and S. Ghisla, *Biochemistry*, 1993, **32**, 404–411.
- 112 L. F. Greer and A. A. Szalay, *Luminescence*, 2002, **17**, 43–74.
- 113 C. Koncz, W. H. R. Langridge, O. Olsson, J. Schell and A. A. Szalay, *Dev. Genet.*, 1990, **11**, 224–232.
- 114 C. Koncz, O. Olsson and W. H. R. Langridge, *Proc. Natl. Acad. Sci. U. S. A.*, 1987, **84**, 131–135.
- 115 A. Krichevsky, B. Meyers, A. Vainstein, P. Maliga and V. Citovsky, *PLoS One*, 2010, **5**, e15461.
- 116 D. M. Close, S. S. Patterson, S. Ripp, S. J. Baek, J. Sanseverino and G. S. Sayler, *PLoS One*, 2010, **5**, e12441.
- 117 C. Gregor, J. K. Pape, K. C. Gwosch, T. Gilat, S. J. Sahl and S. W. Hell, *Proc. Natl. Acad. Sci. U. S. A.*, 2019, **116**, 26491–26496.
- 118 L. Su, W. Jia, C. Hou and Y. Lei, *Biosens. Bioelectron.*, 2011, **26**, 1788–1799.
- 119 F. Fernández-piñas, I. Rodea-palomares, F. Leganés, M. González-pleiter and M. Angeles MuñOz-Martín, *Adv. Biochem. Eng. Biotechnol.*, 2014, **145**, 65–135.
- 120 T. Xu, D. Close, A. Smartt, S. Ripp and G. Sayler, *Adv. Biochem. Eng. Biotechnol.*, 2014, **144**, 111–151.
- 121 Y. Aleksandrov, *Bulg. J. Agric. Sci.*, 2020, **26**, 332–338.
- 122 J. W. Hastings, K. Weber, J. Friedland, A. Eberhard, G. W. Mitchell and A. Gunsalus, *Biochemistry*, 1969, **8**, 4681–4689.
- 123 J. G. Dorn, R. J. Frye and R. M. Maier, *Appl. Environ. Microbiol.*, 2003, **69**, 2209–2216.
- 124 J. W. Hastings and K. H. Nealson, *Annu. Rev. Microbiol.*, 1977, **31**, 549–595.
- 125 F. H. Johnson, O. Shimomura, Y. Saiga, L. C. Gershman, G. T. Reynolds and J. R. Waters, *J. Cell. Comp. Physiol.*, 1962, **60**, 85–103.
- 126 A. A. Kotlobay, K. S. Sarkisyan, Y. A. Mokrushina, M. Marcet-Houben, E. O. Serebrovskaya, N. M. Markina, L. G. Somermeyer, A. Y. Gorokhovatsky, A. Vvedensky, K. V. Purtov, V. N. Petushkov, N. S. Rodionova, T. V. Chepurnyh, L. I. Fakhranurova, E. B. Guglya, R. Ziganshin, A. S. Tsarkova, Z. M. Kaskova, V. Shender, M. Abakumov, T. O. Abakumova, I. S. Povolotskaya, F. M. Eroshkin, A. G. Zaraisky, A. S. Mishin, S. V. Dolgov, T. Y. Mitiouchkina, E. P. Kopantzev, H. E. Waldenmaier, A. G. Oliveira, Y. Oba, E. Barsova, E. A. Bogdanova, T. Gabaldón, C. V. Stevani, S. Lukyanov, I. V. Smirnov, J. I. Gitelson, F. A. Kondrashov and I. V. Yampolsky, *Proc. Natl. Acad. Sci. U. S. A.*, 2018, **115**, 12728–12732.
- 127 Z. M. Kaskova, F. A. Dörr, V. N. Petushkov, K. V. Purtov, A. S. Tsarkova, N. S. Rodionova, K. S. Mineev, E. B. Guglya, A. Kotlobay, N. S. Baleeva, M. S. Baranov, A. S. Arseniev, J. I. Gitelson, S. Lukyanov, Y. Suzuki, S. Kanie, E. Pinto, P. Di Mascio, H. E. Waldenmaier, T. A. Pereira, R. P. Carvalho, A. G. Oliveira, Y. Oba, E. L. Bastos, C. V. Stevani and I. V. Yampolsky, *Sci. Adv.*, 2017, **3**, e1602847.
- 128 T. Mitiouchkina, A. S. Mishin, L. G. Somermeyer, N. M. Markina, T. V. Chepurnyh, E. B. Guglya, T. A. Karataeva, K. A. Palkina, E. S. Shakhova,



- L. I. Fakhranurova, S. V. Chekova, A. S. Tsarkova, Y. V. Golubev, V. V. Negrebetsky, S. A. Dolgushin, P. V. Shalaev, D. Shlykov, O. A. Melnik, V. O. Shipunova, S. M. Deyev, A. I. Bubyrev, A. S. Pushin, V. V. Choob, S. V. Dolgov, F. A. Kondrashov, I. V. Yampolsky and K. S. Sarkisyan, *Nat. Biotechnol.*, 2020, **38**, 944–946.
- 129 L. Liu, T. Wilson and J. W. Hastings, *Proc. Natl. Acad. Sci. U. S. A.*, 2004, **101**, 16555–16560.
- 130 D. Morse, A. M. Pappenheimer and J. W. Hastings, *J. Biol. Chem.*, 1989, **264**, 11822–11826.
- 131 C. Suzuki, Y. Nakajima, H. Akimoto, C. Wu and Y. Ohmiya, *Gene*, 2005, **344**, 61–66.
- 132 M. Kato, T. Chiba, M. Li and Y. Hanyu, *Assay Drug Dev. Technol.*, 2011, **9**, 31–39.
- 133 M. Endoh, Y. Kobayashi, Y. Yamakami, R. Yonekura, M. Fujii and D. Ayusawa, *Biogerontology*, 2009, **10**, 213–221.
- 134 O. Shimomura, *J. Biolumin. Chemilumin.*, 1995, **10**, 91–101.
- 135 R. Kay, *Proc. R. Soc. London, Ser. B*, 1965, **162**, 365–386.
- 136 H. Nakamura, B. Musicki, Y. Kishi and O. Shimomura, *J. Am. Chem. Soc.*, 1988, **110**, 2683–2685.
- 137 O. Shimomura and F. H. Johnson, *Biochemistry*, 1968, **7**, 2574–2580.
- 138 O. Shimomura and F. H. Johnson, *Biochemistry*, 1968, **7**, 1734–1738.
- 139 M. Nakamura, M. Mamino, M. Masaki, S. Maki, R. Matsui, S. Kojima, T. Hirano, Y. Ohmiya and H. Niwa, *Tetrahedron Lett.*, 2005, **46**, 53–56.
- 140 M. Nakamura, M. Masaki, S. Maki, R. Matsui, M. Hieda, M. Mamino, T. Hirano, Y. Ohmiya and H. Niwa, *Tetrahedron Lett.*, 2004, **45**, 2203–2205.
- 141 S. Kojima, S. Maki, T. Hirano, Y. Ohmiya and H. Niwa, *Tetrahedron Lett.*, 2000, **41**, 4409–4413.
- 142 O. Shimomura, F. H. Johnson and Y. Kohama, *Proc. Natl. Acad. Sci. U. S. A.*, 1972, **69**, 2086–2089.
- 143 R. Bellisario, T. E. Spencer and M. J. Cormier, *Biochemistry*, 1972, **11**, 2256–2266.
- 144 J. E. Wampler and B. G. M. Jamieson, *Comp. Biochem. Physiol., Part B: Biochem. Mol. Biol.*, 1980, **66**, 43–50.
- 145 J. E. Wampler, M. G. Mulkerrin and E. S. Rich Jr, *Clin. Chem.*, 1979, **25**, 1628–1634.
- 146 N. G. Rudie, M. G. Mulkerrin and J. E. Wampler, *Biochemistry*, 1981, **20**, 344–350.
- 147 V. N. Petushkov and N. S. Rodionova, *J. Photochem. Photobiol., B*, 2007, **87**, 130–136.
- 148 V. N. Petushkov and N. S. Rodionova, *Dokl. Biochem. Biophys.*, 2005, **401**, 115–118.
- 149 V. N. Petushkov, M. A. Dubinnyi, A. S. Tsarkova, N. S. Rodionova, M. S. Baranov, V. S. Kublitski, O. Shimomura and I. V. Yampolsky, *Angew. Chem., Int. Ed.*, 2014, **53**, 5566–5568.
- 150 Y. Mitani, R. Yasuno, M. Isaka, N. Mitsuda, R. Futahashi, Y. Kamagata and Y. Ohmiya, *Sci. Rep.*, 2018, **8**, 12789.
- 151 O. C. Watkins, M. L. Sharpe, N. B. Perry and K. L. Krause, *Sci. Rep.*, 2018, **8**, 3278.
- 152 V. R. Viviani, J. R. Silva, D. T. Amaral, V. R. Bevilaqua, F. C. Abdalla, B. R. Branchini and C. H. Johnson, *Sci. Rep.*, 2020, **10**, 9608.
- 153 H. Zhao, T. C. Doyle, O. Coquoz, F. Kalish, B. W. Rice and C. H. Contag, *J. Biomed. Opt.*, 2005, **10**, 041210.
- 154 C. C. Woodrooffe, P. L. Meisenheimer, D. H. Klaubert, Y. Kovic, J. C. Rosenberg, C. E. Behney, T. L. Southworth and B. R. Branchini, *Biochemistry*, 2012, **51**, 9807–9813.
- 155 E. H. White, H. Worther, H. H. Seliger and W. D. McElroy, *J. Am. Chem. Soc.*, 1966, **88**, 2015–2019.
- 156 W. Wu, J. Su, C. Tang, H. Bai, Z. Ma, T. Zhang, Z. Yuan, Z. Li, W. Zhou, H. Zhang, Z. Liu, Y. Wang, Y. Zhou, L. Du, L. Gu and M. Li, *Anal. Chem.*, 2017, **89**, 4808–4816.
- 157 H. Simonyan, C. Hurr and C. N. Young, *Physiol. Genomics*, 2016, **48**, 762–770.
- 158 R. C. Steinhardt, C. M. Rathbun, B. T. Krull, J. M. Yu, Y. Yang, B. D. Nguyen, J. Kwon, D. C. McCutcheon, K. A. Jones, F. Furche and J. A. Prescher, *ChemBioChem*, 2017, **18**, 96–100.
- 159 S. Iwano, R. Obata, C. Miura, M. Kiyama, K. Hama, M. Nakamura, Y. Amano, S. Kojima, T. Hirano, S. Maki and H. Niwa, *Tetrahedron*, 2013, **69**, 3847–3856.
- 160 M. Kiyama, S. Iwano, S. Otsuka, S. W. Lu, R. Obata, A. Miyawaki, T. Hirano and S. A. Maki, *Tetrahedron*, 2018, **74**, 652–660.
- 161 R. Saito, T. Kuchimaru, S. Higashi, S. W. Lu, M. Kiyama, S. Iwano, R. Obata, T. Hirano, S. Kizaka-Kondoh and S. A. Maki, *Bull. Chem. Soc. Jpn.*, 2019, 608–618.
- 162 N. Kitada, R. Saito, R. Obata, S. Iwano, K. Karube, A. Miyawaki, T. Hirano and S. A. Maki, *Chirality*, 2020, **32**, 922–931.
- 163 J. C. Anderson, C. H. Chang, A. P. Jathoul and A. J. Syed, *Tetrahedron*, 2019, **75**, 347–356.
- 164 G. V. M. Gabriel and V. R. Viviani, *Photochem. Photobiol. Sci.*, 2014, **13**, 1661–1670.
- 165 M. P. Hall, C. C. Woodrooffe, M. G. Wood, I. Que, M. Van'T Root, Y. Ridwan, C. Shi, T. A. Kirkland, L. P. Encell, K. V. Wood, C. Löwik and L. Mezzanotte, *Nat. Commun.*, 2018, **9**, 132.
- 166 T. Kuchimaru, S. Iwano, M. Kiyama, S. Mitsumata, T. Kadonosono, H. Niwa, S. Maki and S. Kizaka-Kondoh, *Nat. Commun.*, 2016, **7**, 11856.
- 167 S. T. Adams, D. M. Mofford, G. S. K. K. Reddy and S. C. Miller, *Angew. Chem., Int. Ed.*, 2016, **55**, 4943–4946.
- 168 C. M. Rathbun, W. B. Porterfield, K. A. Jones, M. J. Sagoe, M. R. Reyes, C. T. Hua and J. A. Prescher, *ACS Cent. Sci.*, 2017, **3**, 1254–1261.
- 169 S. J. Williams and J. A. Prescher, *Acc. Chem. Res.*, 2019, **52**, 3039–3050.
- 170 K. Saito, Y. F. Chang, K. Horikawa, N. Hatsugai, Y. Higuchi, M. Hashida, Y. Yoshida, T. Matsuda, Y. Arai and T. Nagai, *Nat. Commun.*, 2012, **3**, 1262.
- 171 A. Takai, R. Haruno, T. Nagai and Y. Okada, *Mol. Biol. Cell*, 2014, **25**, 25.
- 172 A. Takai, M. Nakano, K. Saito, R. Haruno, T. M. Watanabe, T. Ohyanagi, T. Jin, Y. Okada and T. Nagai, *Proc. Natl. Acad. Sci. U. S. A.*, 2015, **112**, 4352–4356.
- 173 K. Suzuki, T. Kimura, H. Shinoda, G. Bai, M. J. Daniels, Y. Arai, M. Nakano and T. Nagai, *Nat. Commun.*, 2016, **7**, 13718.



- 174 M. P. Hall, J. Unch, B. F. Binkowski, M. P. Valley, B. L. Butler, M. G. Wood, P. Otto, K. Zimmerman, G. Vidugiris, T. MacHleidt, M. B. Robers, H. A. Benink, C. T. Eggers, M. R. Slater, P. L. Meisenheimer, D. H. Klaubert, F. Fan, L. P. Encell and K. V. Wood, *ACS Chem. Biol.*, 2012, **7**, 1848–1857.
- 175 C. G. England, E. B. Ehlerding and W. Cai, *Bioconjugate Chem.*, 2016, **27**, 1175–1187.
- 176 H. W. Yeh, T. Wu, M. Chen and H. W. Ai, *Biochemistry*, 2019, **58**, 1689–1697.
- 177 F. X. Schaub, M. S. Reza, C. A. Flaveny, W. Li, A. M. Musicant, S. Hoxha, M. Guo, J. L. Cleveland and A. L. Amelio, *Cancer Res.*, 2015, **75**, 5023–5033.
- 178 T. Machleidt, C. C. Woodrooffe, M. K. Schwinn, J. Méndez, M. B. Robers, K. Zimmerman, P. Otto, D. L. Daniels, T. A. Kirkland and K. V. Wood, *ACS Chem. Biol.*, 2015, **10**, 1797–1804.
- 179 J. Hiblot, Q. Yu, M. D. B. Sabbadini, L. Reymond, L. Xue, A. Schena, O. Sallin, N. Hill, R. Griss and K. Johnsson, *Angew. Chem., Int. Ed.*, 2017, **56**, 14556–14560.
- 180 S. Inouye and O. Shimomura, *Biochem. Biophys. Res. Commun.*, 1997, **233**, 349–353.
- 181 R. Paulmurugan, Y. Umezawa and S. S. Gambhir, *Proc. Natl. Acad. Sci. U. S. A.*, 2002, **99**, 15608–15613.
- 182 A. M. Loening, A. M. Wu and S. S. Gambhir, *Nat. Methods*, 2007, **4**, 641–643.
- 183 A. Shakhmin, M. P. Hall, T. Machleidt, J. R. Walker, K. V. Wood and T. A. Kirkland, *Org. Biomol. Chem.*, 2017, **15**, 8559–8567.
- 184 H. W. Yeh, O. Karmach, A. Ji, D. Carter, M. M. Martins-Green and H. W. Ai, *Nat. Methods*, 2017, **14**, 971–974.
- 185 J. Chu, Y. Oh, A. Sens, N. Ataie, H. Dana, J. J. Macklin, T. Laviv, E. S. Welf, K. M. Dean, F. Zhang, B. B. Kim, C. T. Tang, M. Hu, M. A. Baird, M. W. Davidson, M. A. Kay, R. Fiolka, R. Yasuda, D. S. Kim, H. L. Ng and M. Z. Lin, *Nat. Biotechnol.*, 2016, **34**, 760–767.
- 186 H. W. Yeh, Y. Xiong, T. Wu, M. Chen, A. Ji, X. Li and H. W. Ai, *ACS Chem. Biol.*, 2019, **14**, 959–965.
- 187 Y. Su, J. R. Walker, Y. Park, T. P. Smith, L. X. Liu, M. P. Hall, L. Labanieh, R. Hurst, D. C. Wang, L. P. Encell, N. Kim, F. Zhang, M. A. Kay, K. M. Casey, R. G. Majzner, J. R. Cochran, C. L. Mackall, T. A. Kirkland and M. Z. Lin, *Nat. Methods*, 2020, **17**, 852–860.
- 188 C. H. Li and S. C. Tu, *Biochemistry*, 2005, **44**, 13866–13873.
- 189 J. M. Sparks and T. O. Baldwin, *Biochemistry*, 2001, **40**, 15436–15443.
- 190 C. H. Li and S. C. Tu, *Biochemistry*, 2005, **44**, 12970–12977.
- 191 Z. T. Campbell, A. Weichsel, W. R. Montfort and T. O. Baldwin, *Biochemistry*, 2009, **48**, 6085–6094.
- 192 Z. T. Campbell and T. O. Baldwin, *J. Biol. Chem.*, 2009, **284**, 32827–32834.
- 193 S. Hosseinkhani, R. Szttnner and E. A. Meighen, *Biochem. J.*, 2005, **385**, 575–580.
- 194 L. Y. C. Lin, R. Szttnner, R. Friedman and E. A. Meighen, *Biochemistry*, 2004, **43**, 3183–3194.
- 195 C. Gregor, K. C. Gwosch, S. J. Sahl and S. W. Hell, *Proc. Natl. Acad. Sci. U. S. A.*, 2018, **115**, 962–967.
- 196 M. Easter, *Food Sci. Technol.*, 2009, **23**, 48–49.
- 197 M. DeLuca and W. D. McElroy, *Biochemistry*, 1974, **13**, 921–925.
- 198 A. Lundin and J. Eriksson, *Assay Drug Dev. Technol.*, 2008, **6**, 531–541.
- 199 A. Lundin and I. Styrélius, *Clin. Chim. Acta*, 1978, **87**, 199–209.
- 200 S. Lee, C. Zhang and X. Liu, *J. Biol. Chem.*, 2015, **290**, 904–917.
- 201 M. J. Bird, X. W. Wijeyeratne, J. C. Komen, A. Laskowski, M. T. Ryan, D. R. Thorburn and A. E. Frazier, *Biosci. Rep.*, 2014, **34**, 701–715.
- 202 N. Zhang, Z. Fu, S. Linke, J. Chicher, J. J. Gorman, D. Visk, G. G. Haddad, L. Poellinger, D. J. Peet, F. Powell and R. S. Johnson, *Cell Metab.*, 2010, **11**, 364–378.
- 203 K. Palikaras and N. Tavernarakis, *Bio-Protoc.*, 2016, **6**, e2048.
- 204 J. García-Bermúdez, C. Nuevo-Tapióles and J. M. Cuezva, *Bio-Protoc.*, 2016, **6**, e1905.
- 205 B. R. Branchini, T. L. Southworth, D. M. Fontaine, D. Kohrt, F. S. Welcome, C. M. Florentine, E. R. Henricks, D. B. DeBartolo, E. Michelini, L. Cevenini, A. Roda and M. J. Gossel, *Anal. Biochem.*, 2017, **534**, 36–39.
- 206 G. Morciano, A. C. Sarti, S. Marchi, S. Missiroli, S. Falzoni, L. Raffaghello, V. Pistoia, C. Giorgi, F. Di Virgilio and P. Pinton, *Nat. Protoc.*, 2017, **12**, 1542–1562.
- 207 G. F. Pelentir, V. R. Bevilacqua and V. R. Viviani, *Photochem. Photobiol. Sci.*, 2019, **18**, 2061–2070.
- 208 S. Kawabe and Y. Uchiho, *Luminescence*, 2020, 1–4, DOI: 10.1002/bio.3828.
- 209 M. F. Santangelo, S. Libertino, A. P. F. Turner, D. Filippini and W. C. Mak, *Biosens. Bioelectron.*, 2018, **99**, 464–470.
- 210 M. M. Calabretta, R. Álvarez-Diduk, E. Michelini, A. Roda and A. Merkoçi, *Biosens. Bioelectron.*, 2020, **150**, 1–8.
- 211 E. Amodio and C. Dino, *J. Infect. Public Health*, 2014, **7**, 92–98.
- 212 P. Dostálek and T. Brányik, *Czech J. Food Sci.*, 2005, **23**, 85–92.
- 213 A. A. Ali, A. B. Altemimi, N. Alhelfi and S. A. Ibrahim, *Biosensors*, 2020, **10**, 58.
- 214 R. Morrissey, C. Hill and M. Begley, *Trends Food Sci. Technol.*, 2013, **32**, 4–15.
- 215 R. A. Cooper, C. J. Griffith, R. E. Malik, P. Obee and N. Looker, *Am. J. Infect. Control*, 2007, **35**, 338–341.
- 216 T. Lewis, C. Griffith, M. Gallo and M. Weinbren, *J. Hosp. Infect.*, 2008, **69**, 156–163.
- 217 B. G. Mitchell, A. McGhie, G. Whiteley, A. Farrington, L. Hall, K. Halton and N. M. White, *Infect. Dis. Health*, 2020, **25**, 168–174.
- 218 J. A. Rodriguez and G. Hooper, *AORN J.*, 2019, **110**, 596–604.
- 219 Y. Baba, Y. Sato, G. Owada and S. Minakuchi, *J. Prosthodont. Res.*, 2018, **62**, 353–358.



- 220 P. Howgate, *Int. J. Food Sci. Technol.*, 2006, **41**, 341–353.
- 221 T. Møretro, M. A. Normann, H. R. Sæbø and S. Langsrud, *J. Appl. Microbiol.*, 2019, **127**, 186–195.
- 222 J. W. F. Law, N. S. A. Mutalib, K. G. Chan and L. H. Lee, *Front. Microbiol.*, 2015, **5**, 1–19.
- 223 S. N. A. Qazi, E. Counil, J. Morrissey, C. E. D. Rees, A. Cockayne, K. Winzer, W. C. Chan, P. Williams and P. J. Hill, *Infect. Immun.*, 2001, **69**, 7074–7082.
- 224 M. F. Jacobs, S. Tynkkynen and M. Sibakov, *Appl. Microbiol. Biotechnol.*, 1995, **44**, 405–412.
- 225 H. Ramsaran, J. Chen, B. Brunke, A. Hill and M. W. Griffiths, *J. Dairy Sci.*, 1998, **81**, 1810–1817.
- 226 K. J. Allen and M. W. Griffiths, *J. Food Prot.*, 2001, **64**, 2058–2062.
- 227 X. Xu, S. A. Miller, F. Baysal-Gurel, K. H. Gartemann, R. Eichenlaub and G. Rajashekar, *Appl. Environ. Microbiol.*, 2010, **76**, 3978–3988.
- 228 M. K. Dommel, E. Frenzel, B. Strasser, C. Blöching, S. Scherer and M. Ehling-Schulz, *Appl. Environ. Microbiol.*, 2010, **76**, 1232–1240.
- 229 J. Hardy, K. P. Francis, M. DeBoer, P. Chu, K. Gibbs and C. H. Contag, *Science*, 2004, **303**, 851–853.
- 230 H. Loessner, S. Leschner, A. Endmann, K. Westphal, K. Wolf, K. Kochruebe, T. Miloud, J. Altenbuchner and S. Weiss, *Microbes Infect.*, 2009, **11**, 1097–1105.
- 231 M. Cronin, R. D. Sleator, C. Hill, G. F. Fitzgerald and D. Van Sinderen, *BMC Microbiol.*, 2008, **8**, 1–12.
- 232 S. H. A. Hassan, S. W. Van Ginkel, M. A. M. Hussein, R. Abskharon and S. E. Oh, *Environ. Int.*, 2016, **92–93**, 106–118.
- 233 E. A. Widder and B. Falls, *IEEE J. Sel. Top. Quantum Electron.*, 2014, **20**, 232–241.
- 234 N. C. Casavant, D. Thompson, G. A. Beattie, G. J. Phillips and L. J. Halverson, *Environ. Microbiol.*, 2003, **5**, 238–249.
- 235 A. Date, P. Pasini and S. Daunert, *Anal. Chem.*, 2007, **79**, 9391–9397.
- 236 N. J. Hillson, P. Hu, G. L. Andersen and L. Shapiro, *Appl. Environ. Microbiol.*, 2007, **73**, 7615–7621.
- 237 T. J. H. Jonkers, M. Steenhuis, L. Schalkwijk, J. Luirink, D. Bald, C. J. Houtman, J. Kool, M. H. Lamoree and T. Hamers, *Sci. Total Environ.*, 2020, **729**, 139028.
- 238 A. Kassim, M. I. E. Halmi, S. S. A. Gani, U. H. Zaidan, R. Othman, K. Mahmud and M. Y. A. Shukor, *Ecotoxicol. Environ. Saf.*, 2020, **196**, 1–13.
- 239 M. Bhuvaneshwari, E. Eltzov, B. Veltman, O. Shapiro, G. Sadhasivam and M. Borisover, *Water Res.*, 2019, **164**, 1–12.
- 240 D. K. A. Kusumahastuti, M. Sihtmäe, I. V. Kapitanov, Y. Karpichev, N. Gathergood and A. Kahru, *Ecotoxicol. Environ. Saf.*, 2019, **172**, 556–565.
- 241 D. Harpaz, L. P. Yeo, F. Cecchini, T. H. P. Koon, A. Kushmaro, A. I. Y. Tok, R. S. Marks and E. Eltzov, *Molecules*, 2018, **23**, 2454.
- 242 E. L. M. Vermeirssen, S. Campiche, C. Dietschweiler, I. Werner and M. Burkhardt, *Environ. Toxicol. Chem.*, 2018, **37**, 2246–2256.
- 243 S. Prévéral, C. Brutesco, E. C. T. Descamps, C. Escoffier, D. Pignol, N. Ginot and D. Garcia, *Environ. Sci. Pollut. Res.*, 2017, **24**, 25–32.
- 244 T. Fukuba, Y. Aoki, N. Fukuzawa, T. Yamamoto, M. Kyo and T. Fujii, *Lab Chip*, 2011, **11**, 3508–3515.
- 245 C. B. Hansen, A. Kerrouche, K. Tatari, A. Rasmussen, T. Ryan, P. Summersgill, M. P. Y. Desmulliez, H. Bridle and H. J. Albrechtsen, *J. Microbiol. Methods*, 2019, **165**, 105713.
- 246 E. Kabir, A. Azzouz, N. Raza, S. K. Bhardwaj, K. H. Kim, M. Tabatabaei and D. Kukkar, *ACS Sens.*, 2020, **5**, 1254–1267.
- 247 D. T. Nguyen, H. R. Kim, J. H. Jung, K. B. Lee and B. C. Kim, *Sens. Actuators, B*, 2018, **260**, 274–281.
- 248 S. J. Lee, J. S. Park, H. T. Im and H. Il Jung, *Sens. Actuators, B*, 2008, **132**, 443–448.
- 249 T. Han, M. Wren, K. DuBois, J. Therkorn and G. Mainelis, *J. Aerosol Sci.*, 2015, **90**, 114–123.
- 250 C. W. Park, J. W. Park, S. H. Lee and J. Hwang, *Biosens. Bioelectron.*, 2014, **52**, 379–383.
- 251 J. W. Park, H. R. Kim and J. Hwang, *Anal. Chim. Acta*, 2016, **941**, 101–107.
- 252 P. Fernandes, *Appl. Microbiol. Biotechnol.*, 2006, **73**, 291–296.
- 253 G. Ranalli, P. Pasini and A. Roda, Proceedings of the 9th International Congress on Deterioration and Conservation of Stone, 2000.
- 254 G. Ranalli, E. Zanardini, P. Pasini and A. Roda, *Ann. Microbiol.*, 2003, **53**, 1.
- 255 N. Unković, M. Ljaljević Grbić, M. Stupar, J. Vukojević, G. Subakov-Simić, A. Jelikić and D. Stanojević, *Nat. Prod. Res.*, 2019, **33**, 1061–1069.
- 256 J. Li, L. Chen, L. Du and M. Li, *Chem. Soc. Rev.*, 2013, **42**, 662–676.
- 257 E. Lindberg, S. Mizukami, K. Ibata, A. Miyawaki and K. Kikuchi, *Chem. – Eur. J.*, 2013, **19**, 14970–14976.
- 258 M. Yuan, X. Ma, T. Jiang, C. Zhang, H. Chen, Y. Gao, X. Yang, L. Du and M. Li, *Org. Biomol. Chem.*, 2016, **14**, 10267–10274.
- 259 N. Nomura, R. Nishihara, T. Nakajima, S. B. Kim, N. Iwasawa, Y. Hiruta, S. Nishiyama, M. Sato, D. Citterio and K. Suzuki, *Anal. Chem.*, 2019, **91**, 9546–9553.
- 260 D. H. Klaubert, P. Meisenheimer, J. Unch and W. Zhou, *Eur. Pat.*, WO2012/061477, 2012.
- 261 M. A. Sellmyer, L. Bronsart, H. Imoto, C. H. Contag, T. J. Wandless and J. A. Prescher, *Proc. Natl. Acad. Sci. U. S. A.*, 2013, **110**, 8567–8572.
- 262 D. M. Mofford, S. T. Adams, G. S. K. K. Reddy, G. R. Reddy and S. C. Miller, *J. Am. Chem. Soc.*, 2015, **137**, 8684–8687.
- 263 R. Geigera, E. Schneider, K. Wallenfels and W. Miska, *Biol. Chem. Hoppe-Seyler*, 1992, **373**, 1187–1192.
- 264 A. Dragulescu-Andrasi, G. Liang and J. Rao, *Bioconjugate Chem.*, 2009, **20**, 1660–1666.
- 265 H. Yao, M. K. So and J. Rao, *Angew. Chem., Int. Ed.*, 2007, **46**, 7031–7034.
- 266 T. Monsees, W. Miska and R. Geiger, *Anal. Biochem.*, 1994, **221**, 329–334.



- 267 W. Zhou, J. W. Shultz, N. Murphy, E. M. Hawkins, L. Bernad, T. Good, L. Moothart, S. Frackman, D. H. Klaubert, R. F. Bulleit and K. V. Wood, *Chem. Commun.*, 2006, 4620–4622.
- 268 A. G. Vorobyeva, M. Stanton, A. Godinat, K. B. Lund, G. G. Karateev, K. P. Francis, E. Allen, J. G. Gelovani, E. McCormack, M. Tangney and E. A. Dubikovskaya, *PLoS One*, 2015, **10**, e0131037.
- 269 S. J. Duellman, M. P. Valley, V. Kotraiah, J. Vidugiriene, W. Zhou, L. Bernad, J. Osterman, J. J. Kimball, P. Meisenheimer and J. J. Cali, *Anal. Biochem.*, 2013, **434**, 226–232.
- 270 A. S. Cohen, E. A. Dubikovskaya, J. S. Rush and C. R. Bertozzi, *J. Am. Chem. Soc.*, 2010, **132**, 8563–8565.
- 271 X. Tian, Z. Li, C. Lau and J. Lu, *Anal. Chem.*, 2015, **87**, 11325–11331.
- 272 G. C. Van De Bittner, C. R. Bertozzi and C. J. Chang, *J. Am. Chem. Soc.*, 2013, **135**, 1783–1795.
- 273 X. Tian, X. Liu, A. Wang, C. Lau and J. Lu, *Anal. Chem.*, 2018, **90**, 5951–5958.
- 274 A. Wang, X. Li, Y. Ju, D. Chen and J. Lu, *Analyst*, 2020, **145**, 550–556.
- 275 G. C. Van de Bittner, E. A. Dubikovskaya, C. R. Bertozzi and C. J. Chang, *Proc. Natl. Acad. Sci. U. S. A.*, 2010, **107**, 21316–21321.
- 276 M. C. Heffern, H. M. Park, H. Y. Au-Yeung, G. C. Van De Bittner, C. M. Ackerman, A. Stahl and C. J. Chang, *Proc. Natl. Acad. Sci. U. S. A.*, 2016, **113**, 14219–14224.
- 277 A. T. Aron, M. C. Heffern, Z. R. Lonergan, M. N. Vander Wal, B. R. Blank, B. Spangler, Y. Zhang, H. M. Park, A. Stahl, A. R. Renslo, E. P. Skaar and C. J. Chang, *Proc. Natl. Acad. Sci. U. S. A.*, 2017, **114**, 12669–12674.
- 278 P. Feng, L. Ma, F. Xu, X. Gou, L. Du, B. Ke and M. Li, *Talanta*, 2019, **203**, 29–33.
- 279 B. Ke, L. Ma, T. Kang, W. He, X. Gou, D. Gong, L. Du and M. Li, *Anal. Chem.*, 2018, **90**, 4946–4950.
- 280 T. A. Su, K. J. Bruemmer and C. J. Chang, *Curr. Opin. Biotechnol.*, 2019, **60**, 198–204.
- 281 A. A. Bazhin, R. Sinisi, U. De Marchi, A. Hermant, N. Sambiagio, T. Maric, G. Budin and E. A. Goun, *Nat. Chem. Biol.*, 2020, **16**, 1385–1393.
- 282 A. P. De Silva, H. Q. N. Gunaratne, T. Gunnlaugsson, A. J. M. Huxley, C. P. McCoy, J. T. Rademacher and T. E. Rice, *Chem. Rev.*, 1997, **97**, 1515–1566.
- 283 H. Kobayashi, M. Ogawa, R. Alford, P. L. Choyke and Y. Urano, *Chem. Rev.*, 2010, **110**, 2620–2640.
- 284 H. Takakura, R. Kojima, M. Kamiya, E. Kobayashi, T. Komatsu, T. Ueno, T. Terai, K. Hanaoka, T. Nagano and Y. Urano, *J. Am. Chem. Soc.*, 2015, **137**, 4010–4013.
- 285 R. Kojima, H. Takakura, M. Kamiya, E. Kobayashi, T. Komatsu, T. Ueno, T. Terai, K. Hanaoka, T. Nagano and Y. Urano, *Angew. Chem., Int. Ed.*, 2015, **54**, 14768–14771.
- 286 T. T. Ong, Z. Ang, R. Verma, R. Koean, J. K. C. Tam and J. L. Ding, *Front. Bioeng. Biotechnol.*, 2020, **8**, 412.
- 287 Y. Qian, V. Rancic, J. Wu, K. Ballanyi and R. E. Campbell, *ChemBioChem*, 2019, **20**, 516–520.
- 288 R. Griss, A. Schena, L. Reymond, L. Patiny, D. Werner, C. E. Tinberg, D. Baker and K. Johnsson, *Nat. Chem. Biol.*, 2014, **10**, 598–603.
- 289 L. Xue, Q. Yu, R. Griss, A. Schena and K. Johnsson, *Angew. Chem., Int. Ed.*, 2017, **56**, 7112–7116.
- 290 R. Arts, I. Den Hartog, S. E. Zijlema, V. Thijssen, S. H. E. Van Der Beelen and M. Merckx, *Anal. Chem.*, 2016, **88**, 4525–4532.
- 291 R. Arts, S. K. J. Ludwig, B. C. B. Van Gerven, E. M. Estirado, L. G. Milroy and M. Merckx, *ACS Sens.*, 2017, **2**, 1730–1736.
- 292 K. Tenda, B. van Gerven, R. Arts, Y. Hiruta, M. Merckx and D. Citterio, *Angew. Chem., Int. Ed.*, 2018, **57**, 15369–15373.
- 293 K. Tomimuro, K. Tenda, Y. Ni, Y. Hiruta, M. Merckx and D. Citterio, *ACS Sens.*, 2020, **5**, 1786–1794.
- 294 I. Brányiková, S. Lucáková, G. Kuncová, J. Trögl, V. Synek, J. Rohovec and T. Navrátil, *Sensors*, 2020, **20**, 3138.
- 295 R. Hajimohammadi, M. Johari-Ahar and S. Ahmadpour, *Int. J. Environ. Anal. Chem.*, 2020, DOI: 10.1080/03067319.2020.1760858.
- 296 E. L. Sciuto, M. A. Coniglio, D. Corso, J. R. van der Meer, F. Acerbi, A. Gola and S. Libertino, *Water*, 2019, **11**, 1986.
- 297 S. R. White and T. K. Christopoulos, *Nucleic Acids Res.*, 1999, **27**, e25–32.
- 298 T. K. Christopoulos and N. H. L. Chiu, *Anal. Chem.*, 1995, **67**, 4290–4294.
- 299 J. Y. Byun, K. H. Lee, Y. B. Shin and D. M. Kim, *ACS Sens.*, 2019, **4**, 93–99.
- 300 N. H. L. Chiu and T. K. Christopoulos, *Anal. Chem.*, 1996, **68**, 2304–2308.
- 301 F. A. Iannotti, E. Pagano, O. Guardiola, S. Adinolfi, V. Saccone, S. Consalvi, F. Piscitelli, E. Gazzerri, G. Busetto, D. Carrella, R. Capasso, P. L. Puri, G. Minchiotti and V. Di Marzo, *Nat. Commun.*, 2018, **9**, 3950.
- 302 E. Rincón, T. Cejalvo, D. Kanojia, A. Alfranca, M. Á. Rodríguez-Milla, R. A. G. Hoyos, Y. Han, L. Zhang, R. Alemany, M. S. Lesniak and J. García-Castro, *Oncotarget*, 2017, **8**, 45415–45431.
- 303 A. Taminiua, A. Draime, J. Tys, B. Lambert, J. Vandeputte, N. Nguyen, P. Renard, D. Geerts and R. Rezsöhazy, *Nucleic Acids Res.*, 2016, **44**, 7331–7349.
- 304 S. Bhaumik and S. S. Gambhir, *Proc. Natl. Acad. Sci. U. S. A.*, 2002, **99**, 377–382.
- 305 G. Zhao, L. Du, C. Ma, Y. Li, L. Li, V. K. Poon, L. Wang, F. Yu, B. J. Zheng, S. Jiang and Y. Zhou, *Virology*, 2013, **10**, 266.
- 306 Y. Yang, L. Du, C. Liu, L. Wang, C. Ma, J. Tang, R. S. Baric, S. Jiang and F. Li, *Proc. Natl. Acad. Sci. U. S. A.*, 2014, **111**, 12516–12521.
- 307 J. Shang, G. Ye, K. Shi, Y. Wan, C. Luo, H. Aihara, Q. Geng, A. Auerbach and F. Li, *Nature*, 2020, **581**, 221–224.
- 308 J. Lan, J. Ge, J. Yu, S. Shan, H. Zhou, S. Fan, Q. Zhang, X. Shi, Q. Wang, L. Zhang and X. Wang, *Nature*, 2020, **581**, 215–220.
- 309 C. K. Kim, K. F. Cho, M. W. Kim and A. Y. Ting, *eLife*, 2019, **8**, e43826.



- 310 K. D. G. Pflieger and K. A. Eidne, *Nat. Methods*, 2006, **3**, 165–174.
- 311 N. C. Dale, E. K. M. Johnstone, C. W. White and K. D. G. Pflieger, *Front. Bioeng. Biotechnol.*, 2019, **7**, 56.
- 312 T. Azad, A. Tashakor and S. Hosseinkhani, *Anal. Bioanal. Chem.*, 2014, **406**, 5541–5560.
- 313 D. C. Harris, *Quantitative Chemical Analysis*, 8th edn, 2010, pp. 419–444.
- 314 J. Zheng, *Methods Mol. Biol.*, 2006, **337**, 65–77.
- 315 P. A. Johnston, D. D. Dudgeon, S. N. Shinde, T. Y. Shun, J. S. Lazo, C. J. Strock, K. A. Giuliano, D. L. Taylor and P. A. Johnston, *Assay Drug Dev. Technol.*, 2010, **8**, 437–458.
- 316 L. Comps-Agrar, D. Maurel, P. Rondard, J. P. Pin, E. Trinquet and L. Prézeau, *Methods Mol. Biol.*, 2011, **756**, 201–214.
- 317 N. S. Eyre, A. L. Aloia, M. A. Joyce, M. Chulanetra, D. L. Tyrrell and M. R. Beard, *Virology*, 2017, **507**, 20–31.
- 318 X. L. Mo, Y. Luo, A. A. Ivanov, R. Su, J. J. Havel, Z. Li, F. R. Khuri, Y. Du and H. Fu, *J. Mol. Cell Biol.*, 2016, **8**, 271–281.
- 319 E. Moreno, J. Canet, E. Gracia, C. Lluís, J. Mallol, E. I. Canela, A. Cortés and V. Casadó, *Front. Pharmacol.*, 2018, **9**, 106.
- 320 Q. Wan, N. Okashah, A. Inoue, R. Nehme, B. Carpenter, C. G. Tate and N. A. Lambert, *J. Biol. Chem.*, 2018, **293**, 7466–7473.
- 321 B. L. Hoare, S. Bruell, A. Sethi, P. R. Gooley, M. J. Lew, M. A. Hossain, A. Inoue, D. J. Scott and R. A. D. Bathgate, *iScience*, 2019, **11**, 93–113.
- 322 D. C. Alcobia, A. I. Ziegler, A. Kondrashov, E. Comeo, S. Mistry, B. Kellam, A. Chang, J. Woolard, S. J. Hill and E. K. Sloan, *iScience*, 2018, **6**, 280–288.
- 323 B. R. Branchini, D. M. Ablamsky and J. C. Rosenberg, *Bioconjugate Chem.*, 2010, **21**, 2023–2030.
- 324 A. Kamkaew, H. Sun, C. G. England, L. Cheng, Z. Liu and W. Cai, *Chem. Commun.*, 2016, **52**, 6997–7000.
- 325 A. M. Deraus, W. C. W. Chan and S. N. Bhatia, *Nano Lett.*, 2004, **4**, 11–18.
- 326 O. M. Thirukkumaran, C. Wang, N. J. Asouzu, E. Fron, S. Rocha, J. Hofkens, L. D. Lavis and H. Mizuno, *Front. Chem.*, 2020, **7**, 938.
- 327 M. C. Wehr and M. J. Rossner, *Drug Discovery Today*, 2016, **21**, 415–429.
- 328 K. E. Luker, M. C. P. Smith, G. D. Luker, S. T. Gammon, H. Piwnica-Worms and D. Piwnica-Worms, *Proc. Natl. Acad. Sci. U. S. A.*, 2004, **101**, 12288–12293.
- 329 E. Stefan, S. Aquin, N. Berger, C. R. Landry, B. Nyfeler, M. Bouvier and S. W. Michnick, *Proc. Natl. Acad. Sci. U. S. A.*, 2007, **104**, 16916–16921.
- 330 I. Remy and S. W. Michnick, *Nat. Methods*, 2006, **3**, 977–979.
- 331 B. K. Sung, M. Sato and H. Tao, *Anal. Chem.*, 2009, **81**, 67–74.
- 332 K. E. Luker and G. D. Luker, *Methods Mol. Biol.*, 2014, **1098**, 59–69.
- 333 F. Z. Wang, N. Zhang, Y. J. Guo, B. Q. Gong and J. F. Li, *J. Integr. Plant Biol.*, 2020, **62**, 1065–1079.
- 334 Y. Kanai, S. Komoto, T. Kawagishi, R. Nouda, N. Nagasawa, M. Onishi, Y. Matsuura, K. Taniguchi and T. Kobayashi, *Proc. Natl. Acad. Sci. U. S. A.*, 2017, **114**, 2343–2348.
- 335 B. Mistry, J. S. Long, J. Schreyer, E. Staller, R. Y. Sanchez-David and W. S. Barclay, *J. Virol.*, 2019, **94**, e01353–19.
- 336 J. Zhao, T. J. Nelson, Q. Vu, T. Truong and C. I. Stains, *ACS Chem. Biol.*, 2016, **11**, 132–138.
- 337 L. Shen, Y. Yang, F. Ye, G. Liu, M. Desforges, P. J. Talbot and W. Tan, *Antimicrob. Agents Chemother.*, 2016, **60**, 5492–5503.
- 338 L. Shen, J. Niu, C. Wang, B. Huang, W. Wang, N. Zhu, Y. Deng, H. Wang, F. Ye, S. Cen and W. Tan, *J. Virol.*, 2019, **93**, e00023–19.
- 339 F. L. Esteban Florez, R. D. Hiers, Y. Zhao, J. Merritt, A. J. Rondinone and S. S. Khajotia, *Dent. Mater.*, 2020, **36**, 353–365.
- 340 N. Sengupta, M. Jović, E. Barnaeva, D. W. Kim, X. Hu, N. Southall, M. Dejmek, I. Mejdova, R. Nencka, A. Baumlova, D. Chalupska, E. Boura, M. Ferrer, J. Marugan and T. Balla, *J. Lipid Res.*, 2019, **60**, 683–693.
- 341 H. Y. Jin, Y. Tudor, K. Choi, Z. Shao, B. A. Sparling, J. G. McGivern and A. Symons, *SLAS Discovery*, 2020, **25**, 215–222.
- 342 N. Thorne, D. S. Auld and J. Inglese, *Curr. Opin. Chem. Biol.*, 2010, **14**, 315–324.
- 343 N. Thorne, J. Inglese and D. S. Auld, *Chem. Biol.*, 2010, **17**, 646–657.
- 344 L. Mezzanotte, M. van't Root, H. Karatas, E. A. Goun and C. W. G. M. Löwik, *Trends Biotechnol.*, 2017, **35**, 640–652.
- 345 M. Endo and T. Ozawa, *Int. J. Mol. Sci.*, 2020, **21**, 1–19.
- 346 I. D. Jacobsen, A. Lüttich, O. Kurzai, B. Hube and M. Brock, *J. Antimicrob. Chemother.*, 2014, **69**, 2785–2796.
- 347 M. Hutchens and G. D. Luker, *Cell. Microbiol.*, 2007, **9**, 2315–2322.
- 348 E. A. Karlsson, V. A. Meliopoulos, C. Savage, B. Livingston, A. Mehle and S. Schultz-Cherry, *Nat. Commun.*, 2015, **6**, 6738.
- 349 J. Niu, L. Shen, B. Huang, F. Ye, L. Zhao, H. Wang, Y. Deng and W. Tan, *Antiviral Res.*, 2020, **173**, 104646.
- 350 A. T. Phillips, A. B. Rico, C. B. Stauff, S. L. Hammond, T. A. Aboellail, R. B. Tjalkens and K. E. Olson, *J. Virol.*, 2016, **90**, 5785–5796.
- 351 S. Dorsaz, A. T. Coste and D. Sanglard, *Front. Microbiol.*, 2017, **8**, 1478.
- 352 J. P. J. Saeij, J. P. Boyle, M. E. Grigg, G. Arrizabalaga and J. C. Boothroyd, *Infect. Immun.*, 2005, **73**, 695–702.
- 353 M. D. Lewis, A. Fortes Francisco, M. C. Taylor, H. Burrell-Saward, A. P. Mclatchie, M. A. Miles and J. M. Kelly, *Cell. Microbiol.*, 2014, **16**, 1285–1300.
- 354 A. F. Francisco, M. D. Lewis, S. Jayawardhana, M. C. Taylor, E. Chatelain and J. M. Kelly, *Antimicrob. Agents Chemother.*, 2015, **59**, 4653–4661.
- 355 J. Q. Reimão, C. T. Trinconi, J. K. Yokoyama-Yasunaka, D. C. Miguel, S. P. Kalil and S. R. B. Uliana, *J. Microbiol. Methods*, 2013, **93**, 95–101.
- 356 E. Calvo-Alvarez, C. Cren-Travaillé, A. Crouzols and B. Rotureau, *Infect., Genet. Evol.*, 2018, **63**, 391–403.



- 357 J. L. C. Wong, M. Romano, L. E. Kerry, H. S. Kwong, W. W. Low, S. J. Brett, A. Clements, K. Beis and G. Frankel, *Nat. Commun.*, 2019, **10**, 3957.
- 358 C. N. Berger, V. F. Crepin, T. I. Roumeliotis, J. C. Wright, D. Carson, M. Pevsner-Fischer, R. C. D. Furniss, G. Dougan, M. Dori-Bachash, L. Yu, A. Clements, J. W. Collins, E. Elinav, G. J. Larrouy-Maumus, J. S. Choudhary and G. Frankel, *Cell Metab.*, 2017, **26**, 738–752.e6.
- 359 D. Vecchio, T. Dai, L. Huang, L. Fantetti, G. Roncucci and M. R. Hamblin, *J. Biophotonics*, 2013, **6**, 733–742.
- 360 L. Lu, B. Li, S. Ding, Y. Fan, S. Wang, C. Sun, M. Zhao, C. X. Zhao and F. Zhang, *Nat. Commun.*, 2020, **11**, 4192.
- 361 T. Theodossiou, J. S. Hothersall, E. A. Woods, K. Okkenhaug, J. Jacobson and A. J. MacRobert, *Cancer Res.*, 2003, **63**, 1818–1821.
- 362 M. L. Schipper, M. R. Patel and S. S. Gambhir, *Mol. Imaging Biol.*, 2006, **8**, 218–225.
- 363 C. Y. Hsu, C. W. Chen, H. P. Yu, Y. F. Lin and P. S. Lai, *Biomaterials*, 2013, **34**, 1204–1212.
- 364 C. M. Magalhães, J. C. G. Esteves da Silva and L. Pinto da Silva, *ChemPhysChem*, 2016, 2286–2294.
- 365 Y. Yang, W. Hou, S. Liu, K. Sun, M. Li and C. Wu, *Biomacromolecules*, 2018, **19**, 201–208.
- 366 A. C. Love and J. A. Prescher, *Cell Chem. Biol.*, 2020, **27**, 904–920.
- 367 L. Fenno, O. Yizhar and K. Deisseroth, *Annu. Rev. Neurosci.*, 2011, **34**, 389–412.
- 368 C. Brieke, F. Rohrbach, A. Gottschalk, G. Mayer and A. Heckel, *Angew. Chem., Int. Ed.*, 2012, **51**, 8446–8476.
- 369 G. Nagel, D. Ollig, M. Fuhrmann, S. Kateriya, A. M. Musti, E. Bamberg and P. Hegemann, *Science*, 2002, **296**, 2395–2398.
- 370 O. A. Sineshchekov, K. H. Jung and J. L. Spudich, *Proc. Natl. Acad. Sci. U. S. A.*, 2002, **99**, 8689–8694.
- 371 E. S. Boyden, F. Zhang, E. Bamberg, G. Nagel and K. Deisseroth, *Nat. Neurosci.*, 2005, **8**, 1263–1268.
- 372 C. Bamann, T. Kirsch, G. Nagel and E. Bamberg, *J. Mol. Biol.*, 2008, **375**, 686–694.
- 373 K. Berglund, E. Birkner, G. J. Augustine and U. Hochgeschwender, *PLoS One*, 2013, **8**, e59759.
- 374 K. Berglund, K. Clissold, H. E. Li, L. Wen, S. Y. Park, J. Gleixner, M. E. Klein, D. Lu, J. W. Barter, M. A. Rossi, G. J. Augustine, H. H. Yin and U. Hochgeschwender, *Proc. Natl. Acad. Sci. U. S. A.*, 2016, **113**, E358–E367.
- 375 K. Berglund, A. M. Fernandez, C. A. N. Gutekunst, U. Hochgeschwender and R. E. Gross, *J. Neurosci. Res.*, 2020, **98**, 422–436.
- 376 J. R. Zenchak, B. Palmateer, N. Dorka, T. M. Brown, L. M. Wagner, W. E. Medendorp, E. D. Petersen, M. Prakash and U. Hochgeschwender, *J. Neurosci. Res.*, 2020, **98**, 458–468.
- 377 M. J. Fuchter, *J. Med. Chem.*, 2020, **63**, 11436–11447.
- 378 Y. Furuhashi, A. Sakai, T. Murakami, A. Nagasaki and Y. Kato, *PLoS One*, 2020, **15**, e0227477.
- 379 R. J. Porra, W. A. Thompson and P. E. Kriedemann, *Biochim. Biophys. Acta, Bioenerg.*, 1989, **975**, 384–394.
- 380 A. J. Millar, S. R. Short, N. H. Chua and S. A. Kay, *Plant Cell*, 1992, **4**, 1075–1087.
- 381 A. J. Millar, I. A. Carré, C. A. Strayer, N. H. Chua and S. A. Kay, *Science*, 1995, **267**, 1161–1163.
- 382 A. Khakhar, C. G. Starker, J. C. Chamness, N. Lee, S. Stokke, C. Wang, R. Swanson, F. Rizvi, T. Imaizumi and D. F. Voytas, *eLife*, 2020, **9**, e52786.
- 383 R. Narboni, *Light Eng.*, 2020, **28**, 4–16.
- 384 M. I. Latz, *Mater. Today: Proc.*, 2017, **4**, 4959–4968.

